The Pressuremeter Test for Highway Applications

Publication No. FHWA-IP-89-008

July 1989

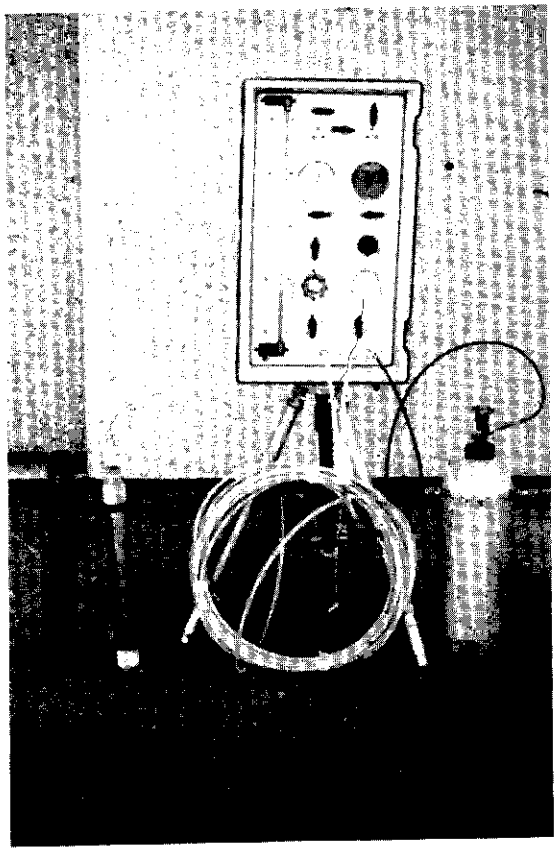

U.S. Department of Transportation
Federal Highway Administration

Research, Development, and Technology
Turner-Fairbank Highway Research Center
6300 Georgetown Pike
McLean, Virginia 22101-2296

Technical Report Documentation Page

1. Report No.	2. Government Accession No.	3. Recipient's Catalog No.
FHWA-IP-89-008		

4. Title and Subtitle	5. Report Date
The Pressuremeter Test for Highway Applications	July 1989
	6. Performing Organization Code
	8. Performing Organization Report No.
7. Author(s)	Research Report 7068
Jean-Louis Briaud	
9. Performing Organization Name and Address	10. Work Unit No. (TRAIS)
Texas Transportation Institute Texas A&M University System College Station, TX, 77843-3136, USA	NCP Code: 3E9C
	11. Contract or Grant No.
	DTFH61-86-C-00-93
	13. Type of Report and Period Covered
12. Sponsoring Agency Name and Address	Final Report 9-1-86 to 8-31-88
Federal Highway Administration Office of Implementation 6300 Georgetown Pike McLean, Virginia 22101-2296, USA	14. Sponsoring Agency Code TTI

15. Supplementary Notes

FHWA Contract Manager (COTR): Mr. Chien-Tan Chang, HRT-10
Technical Assistance: Jerry DiMaggio, HNG-31

16. Abstract

The design applications of the preboring pressuremeter (PBPMT) test include: shallow foundations under vertical loads, deep foundations under vertical and horizontal loads, ground anchors, cantilever drilled shaft walls and anchored bulkheads, pavements, ground improvement and compaction control. The preboring pressuremeter (PBPMT) test is of little use in slope stability analysis and in conventional active and passive earth pressure problems although there is potential for future development in the earth pressure problem area.

17. Key Words	18. Distribution Statement
Pressuremeter, Foundations, In Situ Test.	No restrictions. This document is available to the public through the National Technical Information Service, Springfield, Virginia, 22161.

19. Security Classif. (of this report)	20. Security Classif. (of this page)	21. No. of Pages	22. Price
Unclassified	Unclassified	156	

UNIT CONVERSIONS

Acceleration	9.81 m/s^2 = 386.22 $in./s^2$ = 32.185 ft/s^2, Paris: g = 9.80665 m/s^2 London : g = 3.2174×10^1 ft/s^2
Area	1 m^2 = 1.5500×10^3 $in.^2$ = 1.0764×10^1 ft^2 = 8.3610×10^{-1} yd^2 = 10^6 mm^2 = 10^4 cm^2
Coefficient of Consolidation	1 m^2/s = 10^4 cm^2/s = 6×10^5 cm^2/min = 3.6×10^7 cm^2/h = 8.64×10^8 cm^2/day = 2.628×10^{10} $cm^2/month$ = 3.1536×10^{11} $cm^2/year$ = 1.550×10^3 $in.^2/s$ = 4.0734×10^9 $in.^2/month$ = 1.3392×10^8 $in.^2/day$ = 4.8881×10^{10} $in.^2$ year = 9.4783×10^5 ft^2/day = 2.8830×10^7 $ft^2/month$ = 3.3945×10^8 $ft^2/year$
Flow	1 m^3/s = 10^6 cm^3/s = 8.64×10^4 m^3/day = 8.64×10^{10} cm^3/day = 3.5314×10^1 ft^3/s = 3.0511×10^6 ft^3/day
Force	10 kN = 2.2482×10^3 lb = 2.2482 kip = 1.1241 t (short ton = 2000 lb) = 1.0194×10^3 kg = 1.0194×10^6 g = 1.0194 T (metric ton = 1000 kg) = 10^9 dynes = 3.5971×10^4 ounces = 1.022 tl (long ton = 2200 lb)
Force per Unit Length	1 kN/m = 6.8526×10^1 lb/ft = 6.8526×10^{-2} kip/ft = 3.4263×10^{-2} t/ft = 1.0194×10^2 kg/m = 1.0194×10^{-1} T/m
Length	1 m = 3.9370×10^1 in. = 3.2808 ft = 9.1440×10^{-1} yd = 10^{10} Angstrom = 10^6 microns = 10^3 mm = 10^2 cm = 10^{-3} km = $6.2137\ 10^{-4}$ mile = $5.3996\ 10^{-4}$ nautical mile
Moment or Energy	1 kN.m = 7.3759×10^2 lb.ft = 7.3759×10^{-1} kip.ft = 3.6879×10^{-1} t.ft = 1.0194×10^3 g.cm = 1.0194×10^2 kg.m = 1.0194×10^{-1} T.m = 10^3 N.m = 10^3 Joule
Moment of Inertia	1 m^4 = 2.4025×10^6 $in.^4$ = 1.1586×10^2 ft^4 = 6.9911×10^{-1} yd^4 = 10^8 cm^4 = 10^{12} mm^4
Moment per Unit Length	1 kN.m/m = 2.2482×10^2 lb.ft/ft = 2.2482×10^{-1} kip.ft/ft = 1.1241×10^{-1} t.ft/ft = 1.0194×10^2 kg.m/m = 1.0194×10^{-1} T.m/m
Pressure	100 kPa = 10^2 kN/m^2 = 1.4503×10^1 $lb/in.^2$ = 2.0885×10^3 lb/ft^2 = 1.4503×10^{-2} $kip/in.^2$ = 2.0885 kip/ft^2 = 1.0442 t/ft^2 = 7.5003×10^1 cm of Hg (0°C) = 1.0197 kg/cm^2 = 1.0197×10^1 T/m^2 = 9.8689×10^{-1} Atm = 3.3455×10^1 ft of H_2O (4°C) = 1.0000 bar = 10^6 $dynes/cm^2$

Temperature	°C = 5/9 (°F - 32), °K = °C + 273.15
Time	1 year = 12 month = 365 day = 8760 h = 5.256×10^5 min = 3.1536×10^7 s
Unit Weight, Coefficient of Subgrade Reaction	10 kN/m^3 = 6.3654×10^1 lb/ft^3 = 3.6837×10^{-2} lb/$in.^3$ = 1.0196 g/cm^3 = 1.0196 T/m^3 = 1.0196×10^3 kg/m^3
Velocity or Permeability	1 m/s = 3.6 km/h = 2.2369 mile/h = 6×10^1 m/min = 10^2 cm/s = 1.9685×10^2 ft/min = 3.2808 ft/s = 1.0346×10^8 ft/year = 2.8346×10^5 ft/day
Volume	1 m^3 = 6.1024×10^4 $in.^3$ = 3.5315×10^1 ft^3 = $7.6455\ 10^{-1}$ yd^3 = 10^9 mm^3 = 10^6 cm^3 = 10^3 dm^3 = 10^3 liter = 2.1998×10^2 gallon (U.K.) = 2.6417×10^2 gallon (U.S.)
Volume Loss in a Tubing	1 cm^3/m/kPa = 8.91×10^{-4} $in.^3$/ft/psf

TABLE OF CONTENTS

LIST OF TABLES

LIST OF FIGURES

1. INTRODUCTION

The purpose of this report and the accompanying videotape is to provide guidelines for the proper use of the pressuremeter. This includes the proper way to perform a pressuremeter test, to reduce the data and to use the data in design. The pressuremeter test consists of placing a cylindrical probe in the ground and expanding the cylinder to pressurize the soil horizontally (figure 1). The pressure, p, on the soil (radial stress, σ_{rr} at the cavity wall) and the relative increase in cavity radius, $\Delta R_c / R_c$ (hoop strain, $\epsilon_{\theta\theta}$ at the cavity wall) are obtained; therefore the pressuremeter test gives an in-situ stress strain curve of the soil. The pressuremeter test is repeated at various depths in order to obtain profiles of soil parameters. There are several different kinds of pressuremeters (figure 2). They are the preboring pressuremeter (PBPMT), the selfboring pressuremeter (SBPMT), the cone pressuremeter either pushed (PCPMT) or driven (DCPMT) in place, and the pushed shelby tube pressuremeter (PSPMT). These various pressuremeters are different mainly because of the way the probe is placed in the ground. The scope of this report is limited to the preboring pressuremeter; the preboring pressuremeter is the one which is used most commonly in practice. The scope is not limited to soils, but does include some aspects of testing and design in rock.

The design applications of the preboring pressuremeter (PBPMT) test include: shallow foundation under vertical loads, deep foundations under vertical and horizontal loads, ground anchors, cantilever drilled shaft walls and anchored bulkheads, pavements, ground improvement and compaction control. The preboring pressuremeter (PBPMT) test is of little use in slope stability analysis and in conventional active and passive earth pressure problems although there is potential for future development in the earth pressure problem area.

Kogler, in 1933 in Germany, is credited with having developed the first preboring pressuremeter; however Kogler did not pursue his idea. Menard, in 1955, in France, developed a preboring pressuremeter to measure the in-situ soil deformation properties and started his own company. Fukuoka, in 1959 in Japan, developed the "Public Works Research Type K-Value Tester," a preboring pressuremeter, to obtain lateral soil moduli values. That same year Menard built the "slotted tube" where the probe protected inside a slotted casing was inserted by driving it into the ground. In 1963, Menard, from the experience gathered, published the first equations and charts relating pressuremeter results directly to foundation settlement and bearing capacity. In an effort to improve the procedure, Jezequel, in 1965 in France, developed the first selfboring pressuremeter at

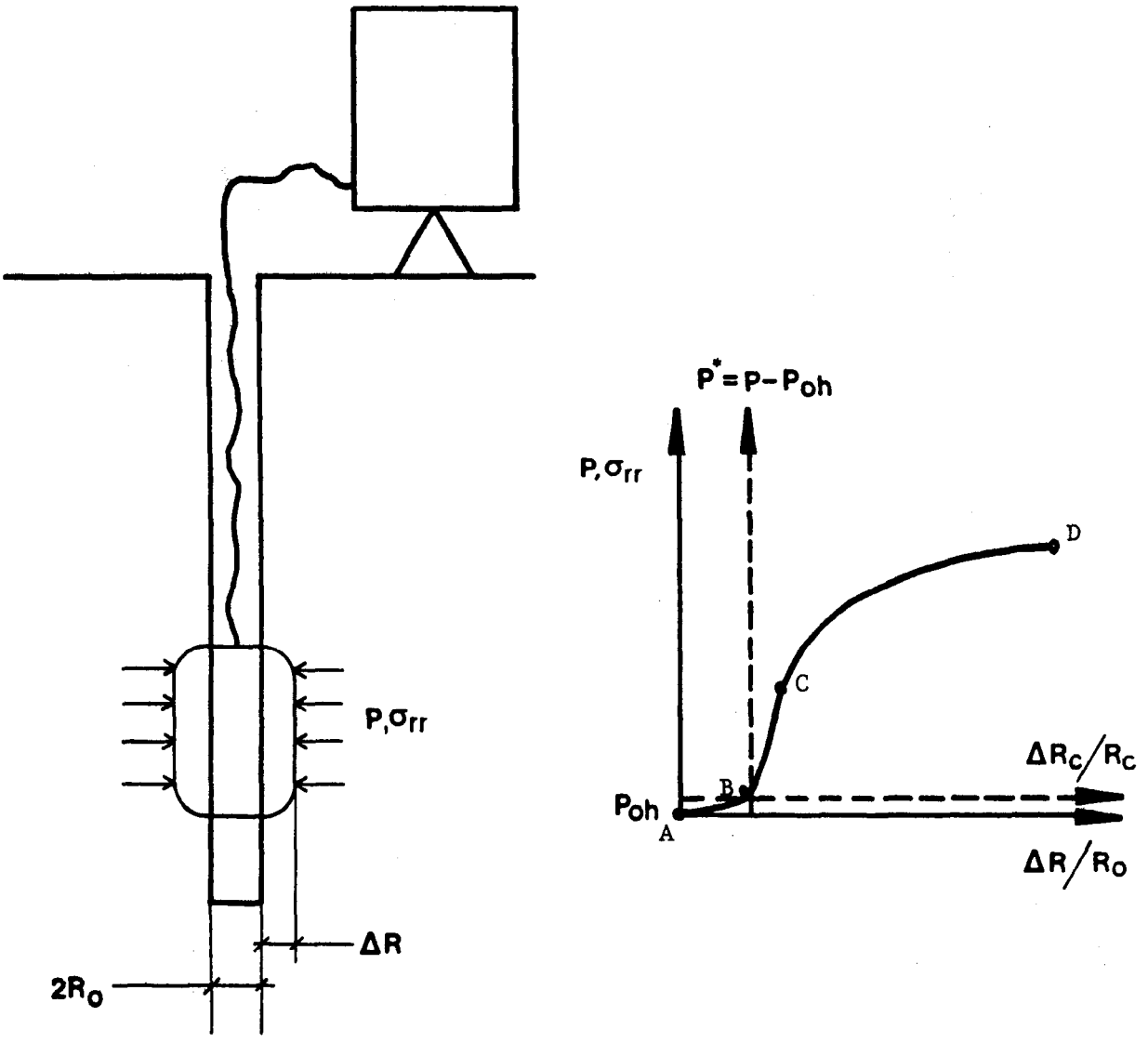

Figure 1. The preboring pressuremeter test.

PBPMT

1. Drill tight fitting hole
2. Remove drilling tool
3. Lower probe to testing depth

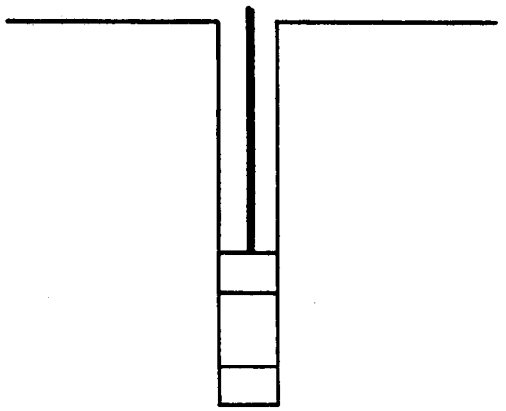

(a)

SBPMT

1. Probe selfbores its way into the soil down to the testing depth starting at the surface or from the bottom of a predrilled borehole.

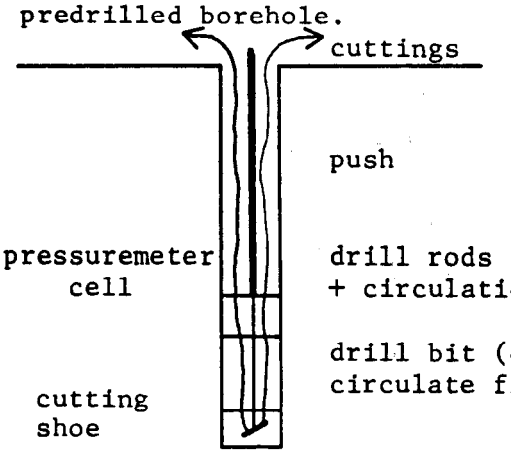

(b)

PCPMT
DCPMT

1. Push or drive the probe into place from the surface.

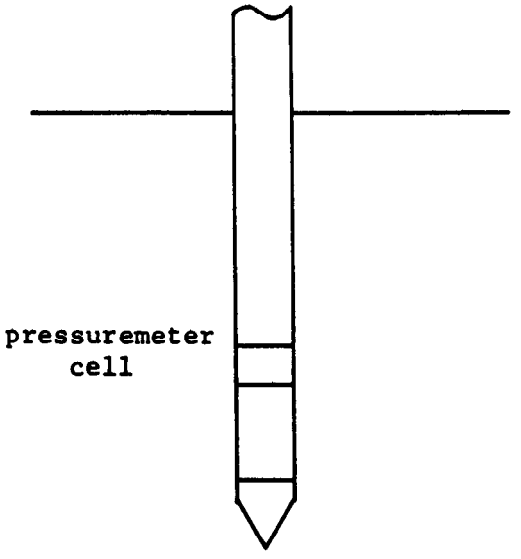

(c)

PSPMT

1. Push the "shelby tube shaped" pressuremeter from the bottom of a predrilled borehole.

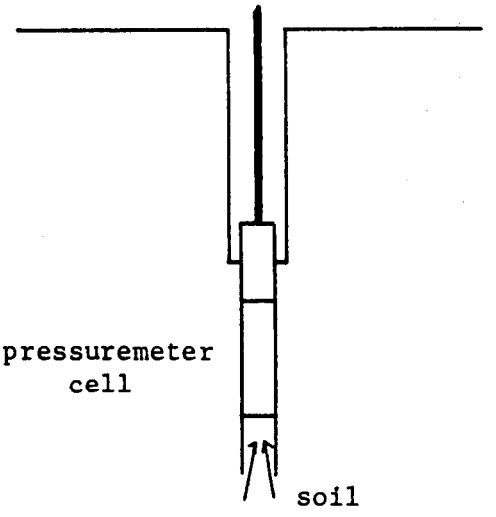

(d)

Figure 2. Different pressuremeters and insertion procedures.

the Laboratoire des Ponts et Chaussees. Jezequel's SBPMT called the PAF has been upgraded over the years. In 1966, Suyama, Imai and Ohya, of the OYO Corporation, developed the Lateral Load Tester and later on the Elastmeter 100; both are preboring pressuremeters.

Wroth and Hughes, in 1971 in England, developed a selfboring pressuremeter at the University of Cambridge which they called the Camkometer; this unit is now sold commercially by Cambridge In Situ. In 1975 the Building Research Establishment in the UK built a pushed shelby tube pressuremeter (PSPMT) for offshore applications; this pressuremeter is now operated by Stressprobe. In 1978, Briaud and Shields in Canada, developed a small pressuremeter for pavement design now known as the Pencell and sold by Roctest. In 1978 the Russian Research Institute of Foundations and Underground Bases (NIIOSP) developed an automatic pressuremeter called the PA108. Also in 1978, the French Petroleum Institute (IFP) developed a selfboring pressuremeter for offshore investigation called the PAM. The book by Baguelin, Jezequel and Shields on the Pressuremeter and Foundation Engineering was published in 1978.

In 1981, Hergheleglu and Unchesel reported that a prototype pressuremeter was manufactured in Romania. In 1982, Briaud and his co-workers developed the TEXAM, a preboring and selfboring pressuremeter now sold by Roctest. In 1982 the Laboratoire des Ponts et Chaussees in conjunction with the Techniques Louis Menard developed the LPC-TLM pressio-penetrometer for shallow offshore penetrations; this probe is a cone pressuremeter inserted by vibrations. The symposium on the Pressuremeter and Its Marine Applications took place in Paris in 1982. From 1982 to 1986 efforts have been made by various groups to develop cone pressuremeters; these groups include Cambridge InSitu, Fugro B.V., Hogentogler, Roctest, the University of British Columbia, and Texas A&M University. In 1984, Bonne Esperance in France introduced the PAC, an automated version of the Menard pressuremeter. In 1984, both Roctest and Cambridge InSitu developed high pressure pressuremeters for testing in rock. In 1986, the Second International Symposium on the Pressuremeter and Its Marine Applications took place at Texas A&M University. In 1988 an ASTM standard was published for Pressuremeter Testing in Soils (ASTM D4719-87).

In parallel with this equipment development, progress has been made in the interpretation and use of the pressuremeter data in France, England, Japan, Canada and more recently in Italy, Norway and the United States.

2. CALIBRATION OF THE EQUIPMENT

The following three chapters will deal with the proper way to perform a preboring pressuremeter test and will emphasize the key issues in pressuremeter testing. An ASTM standard exists (ASTM D4719-87) and is entitled "Standard Test Method for Pressuremeter Testing in Soils".

2.1 Checking for Saturation and Leaks

Preboring pressuremeters for testing soils are usually filled with water. For these types of systems, the first step is to saturate the complete apparatus: probe, tubing, pressure/volume control unit. This is done by purging water through the system. Then the system must be checked for leaks. This is done by sliding the deflated probe in a tight fitting calibration tube. The inside diameter of the calibration tube should be equal to about 1.005 times the outside diameter of the probe, the wall of this steel tube should be thick enough to ensure that, at full pressure, the deformation of the tube is negligible. Once the probe is in the steel tube the pressure is increased and a curve such as the one shown on figure 3 is obtained. From A to B the probe comes in contact with the steel tube. At 5 tsf of pressure (point C), a good contact is considered to exist and the pressure is increased to 25 tsf of pressure (point D). The tangent to the curve at C is extended back to zero pressure (point E). The pressuremeter system is considered to be properly de-aired and leakproof if the volume v_1 on figure 3 is smaller than 0.1 percent of the nominal volume of the measuring portion of the deflated probe v_o per 1 tsf (100 kPa) of pressure. This corresponds, for example, to having v_1 smaller than 50 cm^3 for a probe having a V_o of 2000 cm^3, and for 25 tsf (2500 kPa) of pressure. If this tolerance is not met, a better saturation must be achieved, or if the system is well saturated, a less deformable tubing needs to be used.

2.2 Establishing the Zero Volume of the Probe

A zero volume of the probe must be defined so that all tests start with the probe having the same deflated volume. This can be done as follows: at the end of the check for saturation and leaks, the probe is in the calibration steel tube under 25 tsf of pressure. The probe is then deflated, the pressure decreases, and the zero volume of the probe is defined as the volume reached when it first becomes possible to withdraw the probe from the tube by hand. This procedure is simple and quick but it is only valid if the calibration

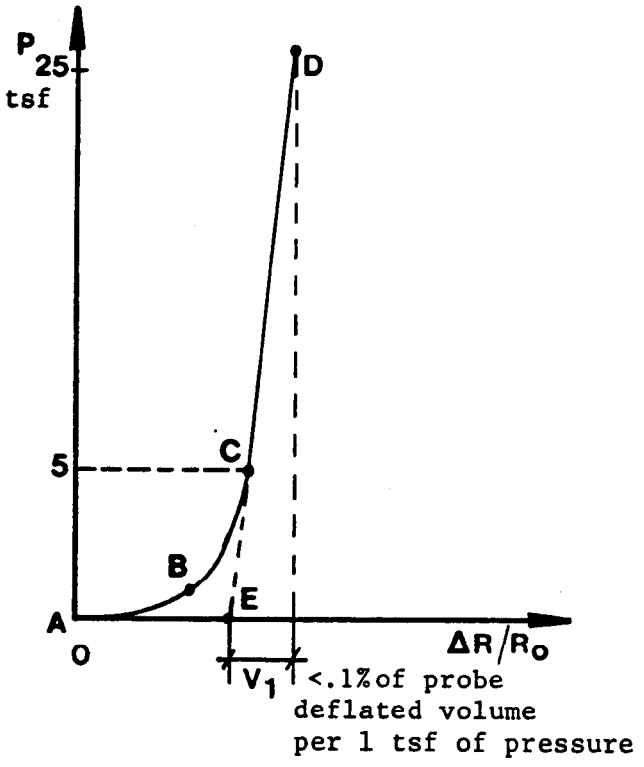

Figure 3. Checking saturation and leaks.

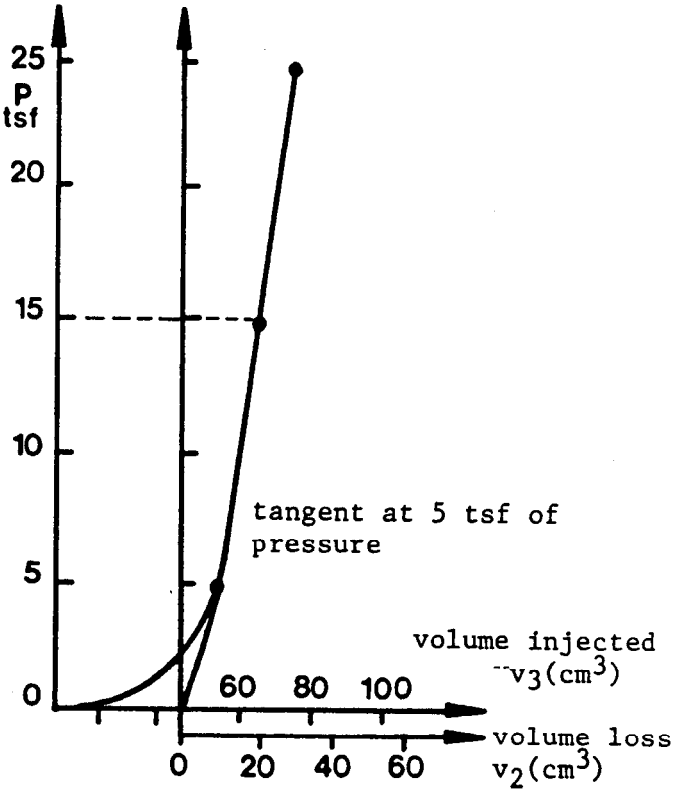

Figure 4. Correction curve for system compressibility.

steel tube meets the specifications described in section 2.1. Once the probe is at the zero volume, the volume reading scale is brought to zero by adding or wasting the necessary amount of water.

2.3 Calibration for System Compressibility

In order to measure the system compressibility and correct for it during the data reduction process, the probe is inserted in the calibration steel tube. The pressure is increased in steps to 5 tsf, 15 tsf, and 25 tsf. Each pressure step is held for 30 seconds. Readings of volume are taken at the end of each pressure step and a curve such as the one on figure 4 is obtained. The volume loss curve is obtained as shown on figure 4. For a given pressure, p, the volume v_2 is the volume lost in the expansion of the pressuremeter system. The volume v_2 is injected into the pressuremeter system, but does not correspond to any increase in volume of the probe (since the probe was held inside the rigid steel tube). Therefore the volume v_2 would not correspond to an increase in volume of the soil cavity during the test. As a result, the volume v_2 will be subtracted from the volume reading v_3 taken during the pressuremeter test in the soil.

As can be seen, the calibration for volume losses is very similar to the check for saturation and leaks. The tolerance which applied to the saturation and leaks, and described in section 2.1 (0.1 percent) of the nominal volume of the measuring portion of the deflated probe, v_o per 1 tsf of pressure) also applies to the calibration for volume losses.

2.4 Calibration for Membrane Resistance

At the end of the calibration for volume losses, the probe is deflated back to the zero volume v_o and removed from the steel tube. The probe is then fully inflated and deflated a minimum of three times to work the rubber. Then with the probe in the air and at the level of the pressure gauge, a calibration for membrane resistance is performed. This consists of inflating the probe to its maximum volume in equal increments of pressure (Method A) or of volume (Method B). For Method B, volume increments equal to 10 percent of the probe deflated volume v_o are used. Each pressure or volume step lasts 1 minute and readings of pressure and volume are taken at the end of each step. A curve such as the one shown on figure 5 is obtained. On figure 5, for a volume v_4 the pressure is p_4. This pressure exists inside the probe, but does not exist outside the probe (since the probe is in the air). This pressure p_4 would therefore not be exerted on the wall of the soil cavity during the test. As a result, the pressure p_4 will be subtracted from the pressure reading p_3 taken during the pressuremeter test in the soil. The preboring pressuremeters have the ability to expand up to approximately twice their deflated volume,

i.e. it is usually possible to inject approximately 2000 cm^3 in a probe which has a deflated zero volume of 2000 cm^3 in a probe which has a deflated zero volume of 2000 cm^3. At full inflation preboring probes typically have a membrane resistance of approximately 1 tsf (100 kPa).

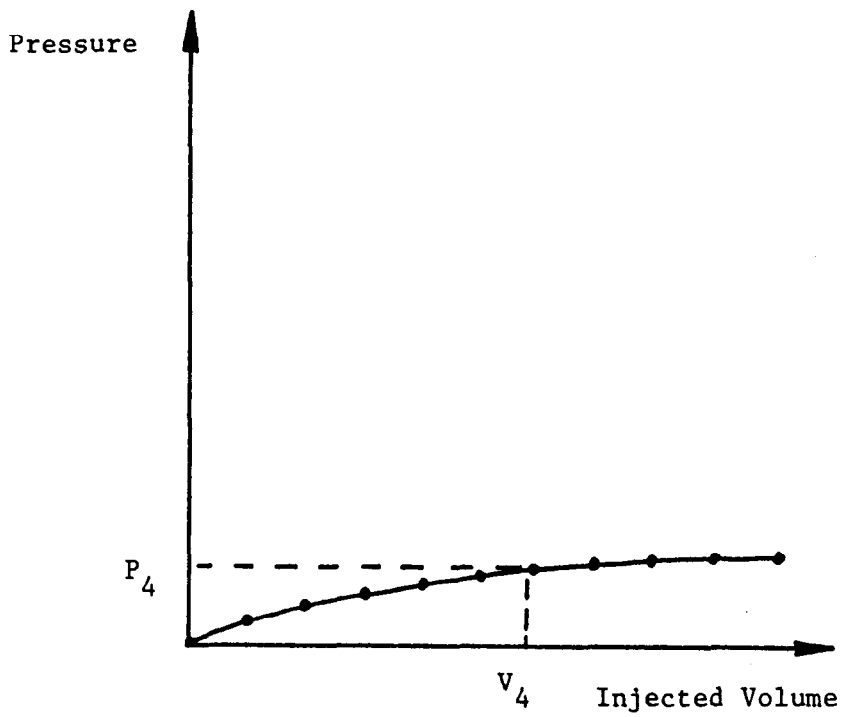

Figure 5. Calibration for membrane resistance.

3. PREPARING THE BOREHOLE

3.1 General Requirements

The preparation of a quality borehole is the single most important step in obtaining a satisfactory pressuremeter test. Two conditions are required to obtain a quality borehole: the diameter of the borehole must be within certain tolerances, the equipment and the method used to prepare the borehole should cause the least possible disturbance to the soil and the wall of the borehole. The diameter of the drilling tool is D_1 the diameter of the deflated probe is D_2 and the initial diameter of the borehole is D_3. The tolerances on the diameters are:

$$D_2 \leq D_1 \leq 1.03 D_2 \qquad (1)$$

$$1.03 D_2 \leq D_3 \leq 1.20 D_2 \qquad (2)$$

Those tolerances exist to help ensure that the borehole will not be too small, nor too large. If the borehole is too small it will be difficult to lower the probe in the hole, a curve like Curve A on figure 6 will be obtained and the net results will only be partially useful. If the borehole is too large a curve like Curve B on figure 6 will be obtained; indeed the probe inflates to a maximum of twice its zero volume and therefore the maximum probe diameter D_4 at full inflation is 1.41 D_2.

The equipment and the methods used to prepare the borehole are presented in table 1 with ranking as 1 = first choice, 2 = second choice, NR = not recommended, NA = not applicable. These methods have been selected for each type of soil from a wide range of field practices with the objective of recommending methods which create the least possible disturbance to the soil and the wall of the borehole. As can be seen from the table, rotary drilling with axial injection of prepared mud is by far the most versatile method. This method is discussed in detail in the following section.

3.2 Rotary Drilling with Axial Injection of Prepared Drilling Mud

For the proper preparation of a pressuremeter borehole with this method the following is recommended. The drill bit is a three wing bit for clays, silts and fine sands, and a roller bit for gravelly soils. The bit must allow the drilling mud to discharge axially against the bottom of the borehole. Any side discharge will lead to poor quality holes

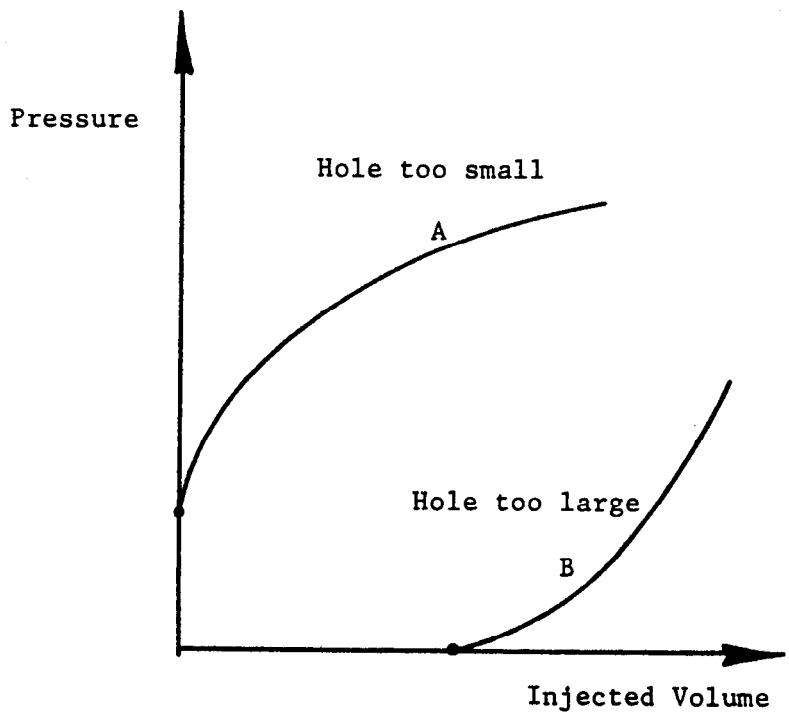

Figure 6. Influence of borehole diameter on pressuremeter curves.

Table 1. Guidelines for selection of borehole preparation method. (ASTM Standard D4719-87)

Soil	Type	Rotary Drilling with Bottom Discharge of Prepared Mud	Pushed Thin Wall Sampler	Pilot Hole Drilling and Subsequent Sampler Pushing	Pilot Hole Drilling and Simultaneous Shaving	Continuous Flight Auger	Hand Auger in the Dry	Hand Auger with Bottom Discharge of Prepared Mud	Driven or Vibrodriven Sampler	Core Barrel Drilling	Rotary Percussion	Driven, Vibrodriven or Pushed Slotted Tube
Clayey Soils	Soft	2[B]	2[B]	2	2	NR	NR	1	NR	NR	NR	NR
	Firm to Stiff	1[B]	1	2	2	1[B]	1	1	NR	NR	NR	NR
	Stiff to Hard	1	2	1	1	1[B]	NA	NA	NA	1[B]	2[B]	NR
Silty Soils	Above GWL[C]	1[B]	2[B]	2	2[B]	1	1	2	2	NR	NR	NR
	Under GWL[C]	1[B]	NR	NR	2[B]	NR	NR	1	NR	NR	NR	NR
Sandy Soils	Loose and Above GWL[C]	1[B]	NR	NR	2	2	2	1	2	NA	NR	NR
	Loose and Below GWL[C]	1[B]	NR	NR	2	NR	NR	1	NR	NA	NR	NR
	Medium to Dense	1[B]	NR	NR	2	1	1	1	2	NR	2[B]	NR
Sandy Gravel or Gravely Sands Below GWL	Loose	2	NA	NA	NA	NA	NA	NA	NR	NA	2	2
	Dense	NR	NA	NA	NA	NR	NA	NA	NR	NA	2	1[D]
Weathered Rock		1	NA	2[B]	NA	1	NA	NA	1	2	2	NR

[A] 1 is first choice, 2 is second choice, NR is not recommended and NA is nonapplicable.
[B] Method applicable only under certain conditions (see text for details).
[C] GWL is ground water level.
[D] Pilot hole drilling required beforehand.

especially in erodible soils. The diameter of the rods must be small enough compared to the diameter of the bit so as to allow good flow of the cuttings up the hole (say AW rods for a 3-in bit).

Prepared drilling mud with a thick consistency is necessary for sands, gravels, silts and soft clays. For clays, water circulation is often sufficient as the water-clay interaction will lead to a suitable mud. For the most difficult case of loose sand below the water table very thick mud is necessary. In all cases, rotation of the drill bit should be very slow (less than 60 rpm). The circulation of the drilling mud should also be very slow (no bubbles or big ripples on the return to the mud pit). Because of this slow mud flow some of the cuttings will not come back up all the way to the mud pit and will settle back at the bottom of the borehole once the mud flow is stopped. This is why it is recommended to drill 2 or 3 ft past the selected depth of testing; this allows the cuttings to settle at the bottom of the hole without filling the portion of the hole where the test is to be performed.

The borehole should be prepared in one downward passage of the bit followed by an immediate retrieval of the bit. Never should the borehole be "cleaned" by ramming the bit up and down the hole while circulating the mud at high flow; this leads to oversized boreholes. The penetration rate varies greatly from slow rates in stiff clays (say 1 ft in several minutes) to fast rates in clean sands (say 1 ft in 10 seconds). The borehole should always be advanced only deep enough to perform one pressuremeter test at a time. A sequence might be: drill to 8 ft, perform a test at 5 ft (middle of the probe at 5 ft), then drill to 13 ft, perform a test at 10 ft, and so on. The apparently more efficient technique which would consist of drilling to the bottom of the borehole and then performing all the pressuremeter tests in that hole usually leads to poor quality tests and ultimately to lost efficiency.

As can be seen, drilling a quality pressuremeter borehole is much different from drilling to obtain samples. For samples one cares about minimizing the disturbance to the soil below the drill bit while for pressuremeter tests one cares about minimizing disturbance to the borehole walls above the drill bit. As a result a period of adjustment should be allowed for any drilling crew to prepare quality pressuremeter boreholes.

4. RUNNING THE TEST

4.1 Inflating the Probe: The Standard Test

As in the membrane calibration, the probe can be inflated in a series of equal pressure increments (Method A) or a series of equal volume increments (Method B). For pressure increment tests (Method A), the anticipated limit pressure of the soil (pressure corresponding approximately to Point D on figure 1) is estimated using table 2. The pressure increment is then chosen as one tenth of the anticipated limit pressure. Each pressure step Δp lasts 1 minute including the time necessary to increase the pressure by Δp. For each pressure increment a reading of injected volume is taken after 30 seconds, v_{30} and 60 seconds, v_{60}. Ideally a test is brought to the limit pressure of the soil in 10 pressure increments for a ten minute test. Practically a good test is brought to the limit pressure of the soil after between 7 and 14 pressure increments. A typical raw data curve is shown in figure 7a. It is a plot of the pressure readings p versus the 60 second volume readings v_{60}. Figure 7b shows the evolution of $v_{60} - v_{30}$ a measure of the soil creep, as a function of the pressure level. The soil starts to yield when the value of $v_{60} - v_{30}$ starts to increase significantly (point A on figure 7a and b).

For volume increment tests (Method B), the volume of the inflatable part of the probe is increased in increments equal to $v_o/40$. Each volume step lasts 15 seconds including the time necessary to increase the volume by Δv. For each volume increment, a pressure reading p_{15} is taken at the end of the 15 second increment. The probe reaches twice its initial volume v_o after 40 volume increments for a 10 minute test. A typical raw data curve is shown in figure 8. It is a plot of the 15 second pressure readings p_{15} versus the increase in probe volume v_3. The soil starts to yield at the end of the straight portion of the curve (point B on figure 8).

Figure 9 and 10 are example data sheets for the pressure increments and volume increments test method respectively. It is useful, for reasons to be discussed later, to perform an unload-reload cycle at the end of the linear portion of the pressuremeter curve (figure 7a and 8). The end of the linear portion of the curve is found during the test by keeping track of the successive increases in volume Δv_{60} (figure 7a) for the pressure increment tests and of the successive increases in pressure Δp_{15} (figure 8) for the volume increment tests. The value of Δv_{60} or Δp_{15} will be relatively constant during the linear portion of the curve and then will increase or decrease, respectively, as the soil starts

Table 2. Guidelines for estimating the limit pressure of the soil.

SOILS	PRESSUREMETER P_L (tsf)	SPT BLOW COUNT N (bpf)	UNDRAINED SHEAR STRENGTH S_U (tsf)
Sand - Loose	0 - 5	0 - 10	
Medium	5 - 15	10 - 30	
Dense	15 - 25	30 - 50	
Very Dense	> 25	> 50	
Clay - Soft	0 - 2		0 - 0.25
Firm	2 - 4		0.25 - 0.5
Stiff	4 - 8		0.5 - 1
Very Stiff	8 - 16		1 - 2
Hard	> 16		> 2

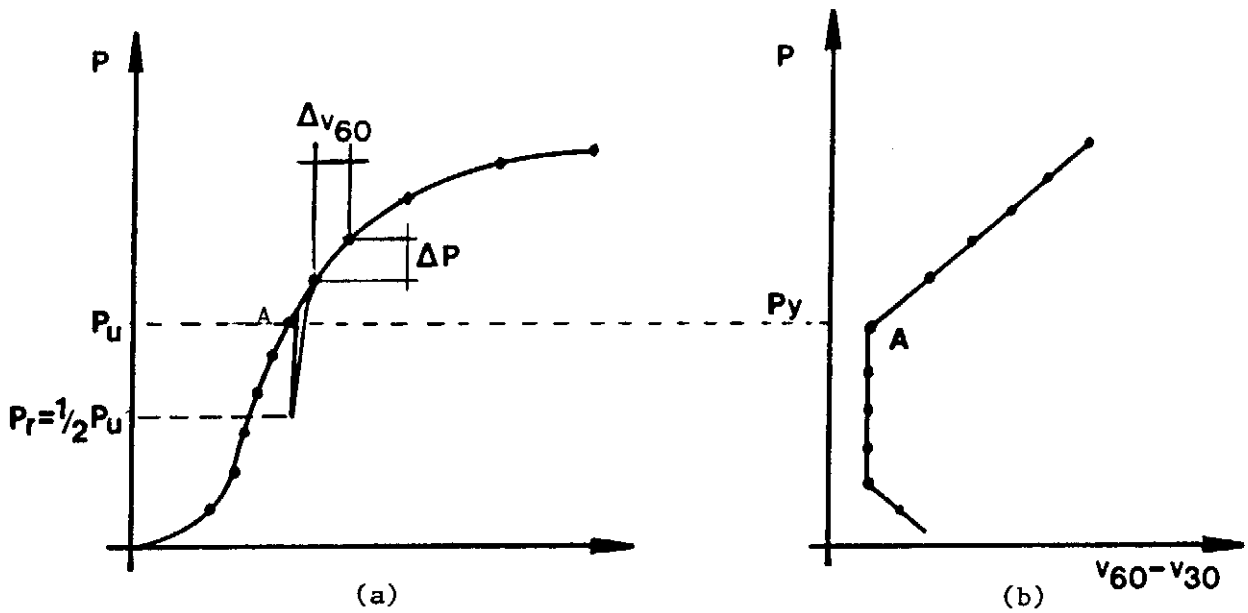

Figure 7. Pressure increment procedure.

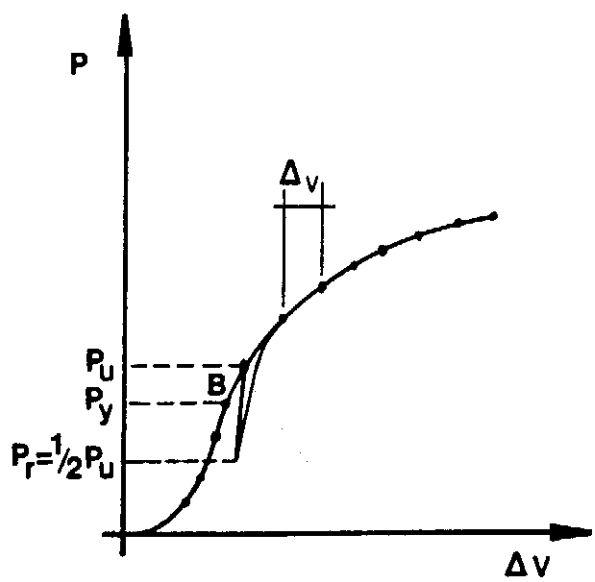

Figure 8. Volume increment procedure.

PRESSURE INCREMENT TEST - METHOD A

TEST NO. =	PROBE V_o =
BORING NO. =	PROBE R_o =
DEPTH =	HEIGHT OF GAGE ABOVE G.S. =

Pressure	Volume		Volume Increment	Pressure	Volume		Volume Increment
p	v_{30}	v_{60}	Δv	p	v_{30}	v_{60}	Δv
units=	units=		units=	units=	units=		units=

Figure 9. Data sheet for pressure increment test, method A.

VOLUME INCREMENT TEST - METHOD B

TEST NO. =	PROBE V_o =
BORING NO. =	PROBE R_o =
DEPTH =	HEIGHT OF GAGE ABOVE G.S. =

Pressure P_{15}	Volume v	Pressure Increment ΔP_{15}	Pressure P_{15}	Volume v	Pressure Increment ΔP_{15}
units=	units=	units=	units=	units=	units=

Figure 10. Data sheet for volume increment test, method B.

yielding. At that time the pressure is reduced to one-half of its value in one increment and then increased again in one increment as shown on figures 7a and 8. These increments last as long as those used before the unload-reload cycle.

4.2 Testing Sequence

The borehole must be advanced only far enough to perform one test. If tests are required at 10, 20, 30 and 40 ft, then the hole is drilled to approximately 13 ft (to have space for the cuttings to settle), the drill bit and rods are withdrawn and, immediately after, the probe is lowered in the borehole until the middle of the expandable part of the probe is 10 ft deep. After the test, the probe is withdrawn and the hole is advanced to 23 ft. The bit is withdrawn, the probe is lowered for the 20-ft test, and so on. This sequence is slower than drilling a 45-ft hole and then testing at 10-, 20-, 30, and 40-ft depth. However most of the time, only the 40-ft test will be good; the borehole diameter for the other tests is likely to be too large.

In an 8-hour day, 8 pressuremeter tests can be performed on the average. This number can vary from 5 to 12 tests. Sometimes the membrane will burst during the test. This is very rare in clays, silts and fine sands. It can happen in gravelly soils where the large gravel particles are sliced by the bit; the pieces of particles lodge themselves between the overlapping steel strips of the probe sheath and end up puncturing the rubber. This risk can be minimized by a thorough cleaning of the probe after each test. The probe can burst also in hard soils when the borehole diameter is too large; this is due to the fact that when the inflating probe finally comes in contact with the soil, the pressure quickly reaches high values while the probe is unsupported at each end of the probe. This problem can be minimized by not letting the pressure go over 25 tsf when the borehole diameter is found to be large (borehole diameter > 1.20 probe diameter).

5. DATA REDUCTION

5.1 Correcting the Raw Data

A microcomputer program PRESRED exists to perform data reduction and plotting automatically.(102).

The raw data collected during the test consists of the pressure read on the gauge of the control unit p_r and the volume read on the volume measuring device of the control until v_r. This raw data must be corrected to obtain the corrected pressure p_c acting against the wall of the soil cavity and the increase in volume of the probe v_c. The corrections include the corrections for membrane resistance, for hydrostatic pressure, for initial reading, for system compressibility.

The correction for membrane resistance consists of subtracting the pressure p_m read at a certain volume during the calibration for membrane resistance (section 2.4) from the raw pressure p_r is necessary to overcome the resistance of the membrane alone and is not exerted on the wall of the soil cavity.

The correction for hydrostatic pressure consists of adding to the raw pressure p_r the hydrostatic pressure p_h due to the column of water which exists between the control unit and the probe located at the testing depth in the borehole (figure 11). Indeed this pressure p_h exists in the probe but is not included in the raw pressure p_r read on the gauge of the control unit.

The correction for initial reading consists of subtracting the initial pressure p_i and/or initial volume v_i from the raw readings p_r and v_r. The initial readings p_i and v_i are taken with the probe at zero volume at the height of the gauge on the control unit immediately before lowering the probe in the borehole. The values of p_i and v_i should be zero; however sometimes due to temperature or other effects they are not and, if they are small, it may be more convenient to correct the data than to rezero the system.

The correction for system compressibility consists of subtracting the volume v_s read at a certain pressure during the calibration for system compressibility (section 2.3) from the raw volume v_r read at the same pressure (figure 11). Indeed this volume v_s is due to the compressibility of the system; it does not correspond to an increase in volume of the probe since it was measured with the probe fitting tightly inside the thick wall steel tube.

The corrected pressure p_c and the corrected volume v_c are therefore obtained as follows:

$$p_c = p_r - p_m + p_h - p_i \tag{3}$$

$$v_c = v_r - v_s - v_i \tag{4}$$

The parameters p_c and v_c represent the pressure on the wall of the cavity and the increase in volume of the probe. The plot of p_c versus v_c is the corrected pressuremeter curve (figure 11). This corrected curve is the one used for all parameter calculations.

5.2 Coefficient of Earth Pressure at Rest, K_O

A value of the coefficient of earth pressure at rest K_O can be obtained from the beginning of the pressuremeter curve. Prior to drilling the borehole, the horizontal stress is the horizontal stress at rest σ_{OH}. As the borehole is drilled, the borehole wall yields inward and the horizontal stress decreases. After drilling the borehole and prior to insertion of the probe, the horizontal stress decreases to about zero. After insertion of the probe and as the probe is inflated in small increments, the borehole wall is pushed back to its original position and then past that position. As this occurs the horizontal stress increases and passes through the special threshold of pressure corresponding to the horizontal pressure at rest σ_{OH}. It is argued that σ_{OH} is found on the early part of the pressuremeter curve at the point of maximum curvature (point A on figure 2). Before point A the soil is recompressing, after point A the soil is stressed in the virgin behavior.

The determination of point A is relatively easy if the borehole is properly prepared and is difficult if the borehole walls are disturbed by the drilling process. With a properly prepared borehole the transition between recompression and virgin behavior is sharp; with the disturbed borehole this transition is progressive and leads to a well rounded beginning of the curve from which it is difficult to get a point of maximum curvature.

The pressure corresponding to point A is σ_{OH}, the horizontal total stress at rest. The coefficient of earth pressure at rest K_O is obtained from:

$$K_o = \frac{\sigma_{OH} - u_o}{\sigma_{OV} - u_o} \tag{5}$$

where σ_{ov} is the total vertical stress at rest and u_0 is the hydrostatic porewater pressure. The values of σ_{ov} and u_0 are calculated from data on depth, total unit weight and ground water level. Values of K_0 obtained in this fashion have been found to be reasonable and consistent with other measurement such as SBPMT.(45)

Marsland and Randolph have proposed a different method to obtain σ_{OH} from PMT results.(68)

5.3 Plotting the Pressuremeter Curve

The corrected pressuremeter curve of figure 11 is presented in terms of correct ed pressure p_c versus corrected increase in probe volume v_c. This presents a problem in that large probes lead to large v_c, small probes to small v_c and therefore it is not possible to compare PMT results obtained from various size pressuremeters. In an effort to normalize the PMT curve, it is recommended that the curve be plotted as pressure versus relative increase in probe radius $\Delta R / R_o$ (figure 12); then the curves obtained with any pressurmeter can be compared directly. The p_c versus $\Delta R / R_o$ curve could be transformed into a p_c versus $\Delta R_c / R_c$ curve by using the construction of figure 12 and rezeroing the horizontal axis at $(\Delta R / R_o)_c$ which corresponds to the initial position of the cavity wall (figure 13). The plot of figure 13 is the stress strain curve σ_{rr} versus $\epsilon_{\theta\theta}$ where σ_{rr} is the radial stress at the wall of the cavity and $\epsilon_{\theta\theta}$ is the circumferential strain at the wall of the cavity.

5.4 Pressuremeter Modulus E_0 and Reload Modulus E_r

The pressuremeter modulus E_o is calculated by using the slope of the straight line portion of the pressuremeter curve. Referring to figure 14a for definition, the modulus E_o is calculated as:

$$E_o = (1+\upsilon)(p_2 - p_1)\frac{\left[1+\left(\frac{\Delta R}{R_o}\right)_2\right]^2 + \left[1+\left(\frac{\Delta R}{R_o}\right)_1\right]^2}{\left[1+\left(\frac{\Delta R}{R_o}\right)_2\right]^2 - \left[1+\left(\frac{\Delta R}{R_o}\right)_1\right]^2} \qquad (6)$$

It is general practice to assume a Poisson's ratio of 0.33 for all soils in the calculations of this modulus. Whatever value of Poisson's ratio is used, it should be stated next to the modulus value. Note that no assumption on υ is necessary if only the shear modulus G is required:

$$G = \frac{E}{2(1+\upsilon)} \qquad (7)$$

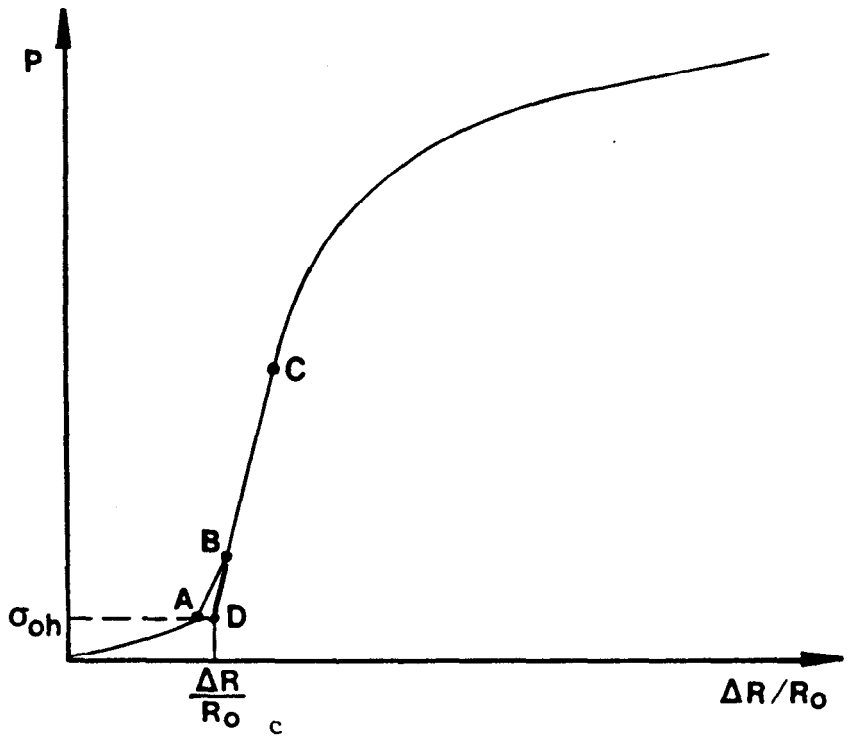

Figure 12. Obtaining the horizontal pressure at rest.

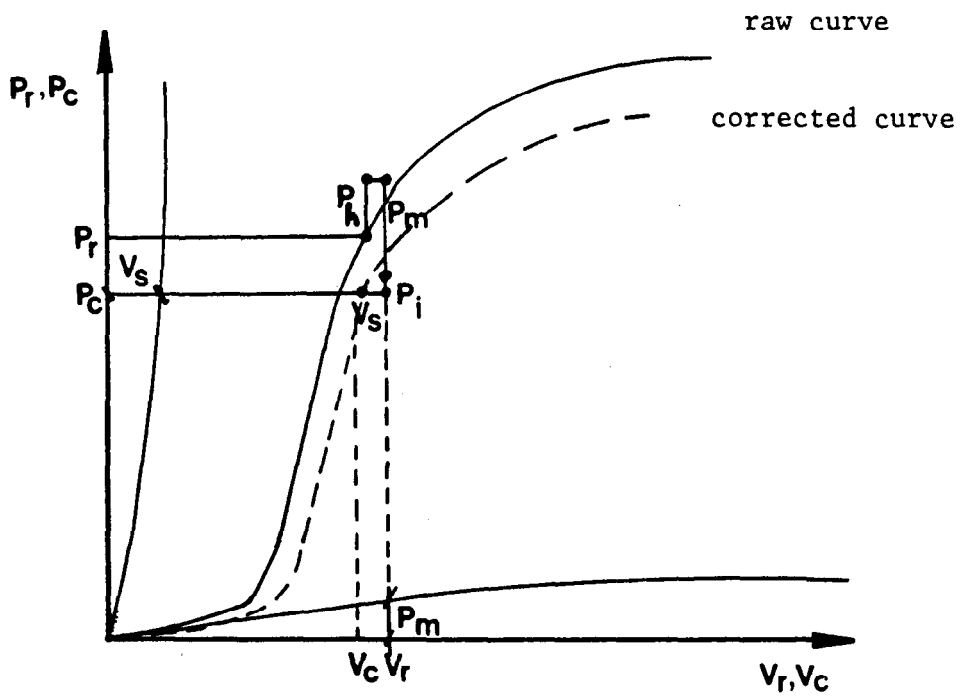

Figure 11. Correcting the raw data.

The pressuremeter reload modulus E_r is calculated in the same manner (figure 14a):

$$E_R = (1+\upsilon)(p_3 - p_4)\frac{\left[1+\left(\frac{\Delta R}{R_o}\right)_3\right]^2 + \left[1+\left(\frac{\Delta R}{R_o}\right)_4\right]^2}{\left[1+\left(\frac{\Delta R}{R_o}\right)_3\right]^2 - \left[1+\left(\frac{\Delta R}{R_o}\right)_4\right]^2} \qquad (8)$$

Note that the modulus E_r is measured in such a way that $p_4 = 1/2\ p_3$. Note that the unload-reload loop must be such that the pressure at the bottom of the cycle p_4 and the pressure at the top of the cycle p_3 (figure 14) satisfy the following condition:(107)

$$\text{in clays} \qquad p_4 - p_3 \leq 2S_u \qquad (9)$$

$$\text{in sands} \qquad \frac{p'_4}{p'_3} \geq K_a \qquad (10)$$

where p_4 and p_3 are the reload and unload total radial pressures respectively, as measured during the PMT test (figure 14), p'_4 and p'_3 are the corresponding effective radial pressures obtained by subtracting from p_4 and p_3 the hydrostatic pore pressure, S_U is the undrained shear strength and k_a the coefficient of active earth pressure. Equations 9 and 10 ensure that the elastic limit of the clay is not exceeded during the unload reload loop.(107) The aforementioned recommendation of taking p_3 close to the yield pressure p_y (section 4.1) and p_4 equal to $1/2\ p_3$ satisfies equations 9 and 10.

The pressuremeter modulus E_o is a relatively low modulus for one or more of the following reasons. First, E_o is measured over a large strain range; this strain range varies from 2 to 5 percent as given by the difference $(\Delta R/R_o)_2 - (\Delta R/R_o)_1$ in figure 14a. Second, the elasticity equation which is the basis for equation 6 assumes that the elastic soil has the same modulus in compression and in tension; since soils are very weak in tension and since tension may occur in the circumferential direction during the pressuremeter expansion, E_o represents an average between the compression and tension moduli of the soil.(36) Third, E_o is influenced by the disturbance of the wall of the borehole; for example if the disturbed zone extends to 1.41 times the radius of the cavity R_c (disturbed zone is 0.41 R_c thick) and if the disturbed soil modulus within the disturbed zone is 0.10 times the undisturbed soil modulus, the measured E_o will be 25 percent lower than the undisturbed modulus; therefore it is important to follow the recommended procedure to prepare the borehole (section 3). Fourth, E_o is influenced somewhat by the length to

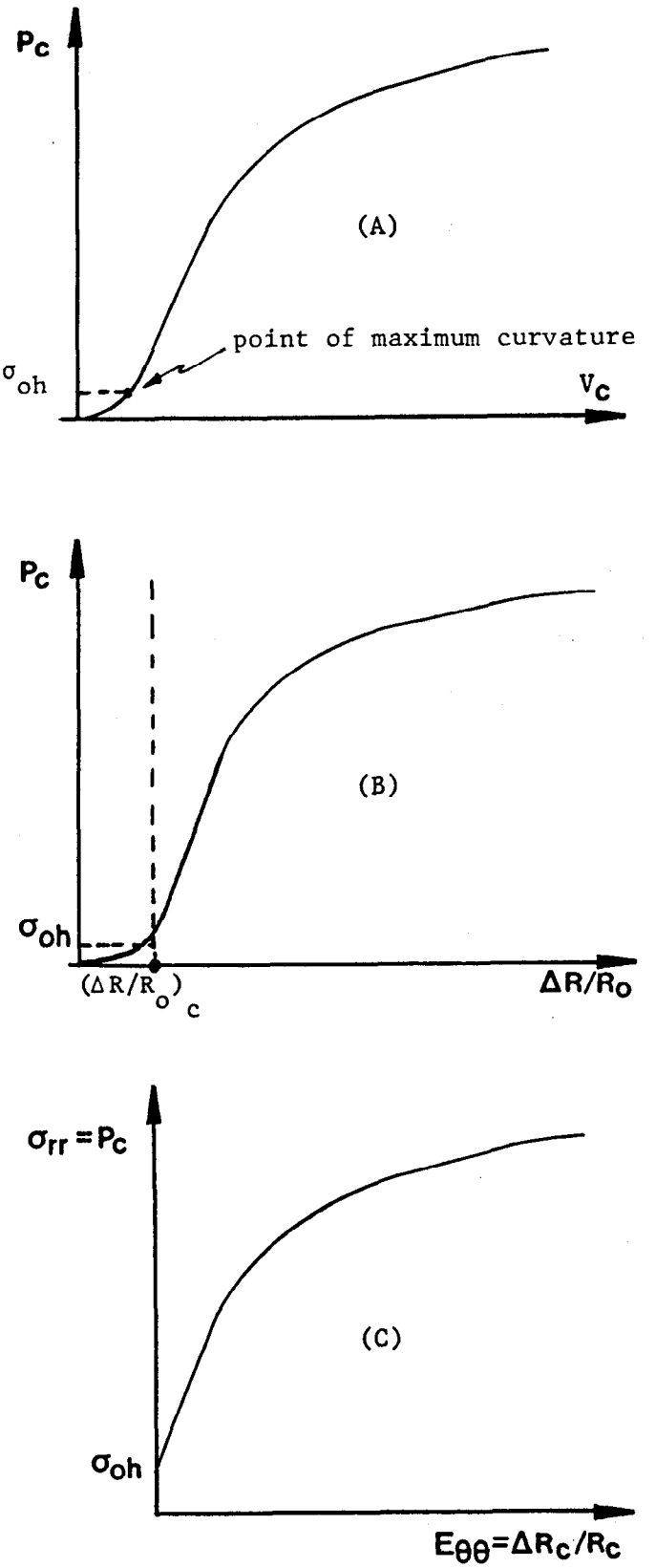

Figure 13. Obtaining the stress strain curve from the pressuremeter curve.

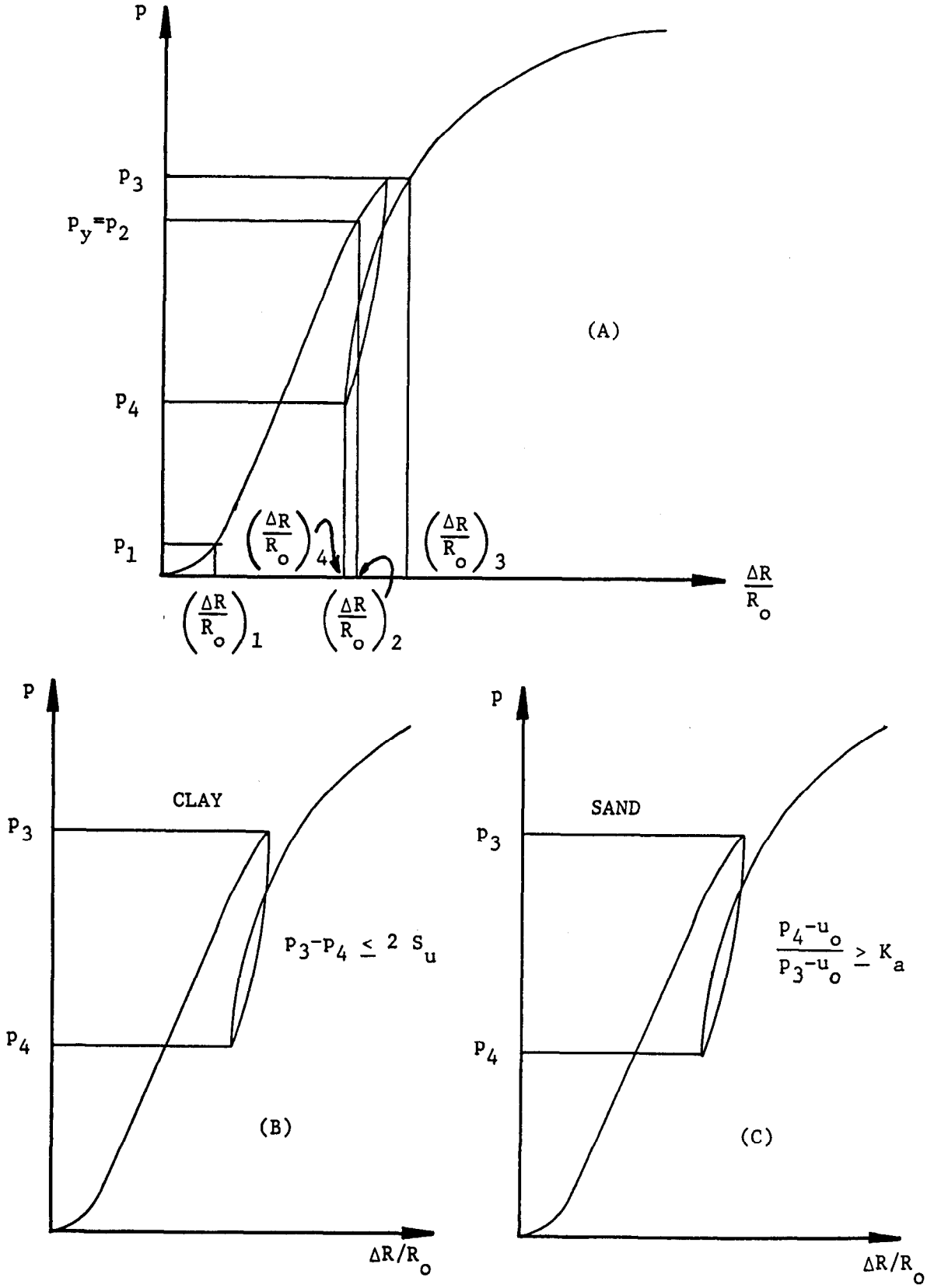

Figure 14. Unload-reload loop during a pressuremeter test.

diameter L/D ratio of the pressuremeter probe; equation 6 is based on the assumption of an infinitely long cylinder; Hartman showed that for an L/D ratio of 6.5, the modulus calculated using equation 56 is 5 percent larger than the modulus of the soil (modulus which would be calculated if the pressuremeter was infinitely long); shorter probes lead to larger errors and an L/D ratio of 6.5 is recommended.(48,36) Fifth, E_o is measured in about 2 minutes while the foundation for the structure will load the soil for say 50 years; Briaud used a model which tends to indicate that the modulus at 50 years may be 4 times smaller than the modulus at 2 minutes for soft clays and 1.4 times smaller for very stiff clays and sands. Sixth, the pressuremeter measures a horizontal modulus E_H and not a vertical modulus E_V; this concern about anisotropy is not as crucial as it might seem because both E_H and E_V are involved in the response of a foundation to vertical loading and because several investigators testing with a pressuremeter in the vertical and then horizontal direction found at most 5 percent difference between E_H and E_V in a wide variety of soils.(63,53,92)

All the above factors led Menard to propose a correction factor α (see table 8, page 53) in his settlement equation in order to better match predicted settlement with measured settlements.(79) The use of E_o in an elasticity settlement equation for a given foundation shape will generally overpredict the settlement observed at working loads during the load test on that foundation element. It has been suggested that E_o/α is equivalent to the Young's modulus for the soil.(62) Others have had success in predicting settlement when using the reload modulus E_r together with elasticity settlement equations.(55,58)

5.5 Yield, Limit and Net Limit Pressure

The yield pressure p_y is found at the end of the linear portion of the pressuremeter curve (figure 14a). This pressure p_y can be determined by simple inspection of the curve or by making use of the creep curve as shown in figure 7 (section 4.1). The yield pressure is useful in indicating beyond which pressure significant long term creep of the soil will occur.

The limit pressure is defined theoretically as the pressure reached for an infinite expansion of the cylinder. Such infinite expansion cannot be reached during the test; instead the limit pressure is defined practically as the pressure reached when the soil cavity has been inflated to twice its initial size; p_L is the pressure at $\Delta V_c / V_c = 1$. This corresponds to a relative increase in probe radius $(\Delta R / R_o)_L = 0.41 + 1.41 (\Delta R / R_o)_c$ where $(\Delta R / R_o)_c$ is the relative increase in probe radius corresponding to the initial size of the cavity (figure 13)

The value $(\Delta R/R_o)_L$ may not have been reached during the test, and some extrapolation technique may be necessary to obtain p_L. Several extrapolation techniques have been suggested.(10) The recommended procedure is to extend the curve manually to $(\Delta R/R_o)_L$ and read p_L on the extrapolated curve; the other techniques are not as consistently correct.

The net limit pressure p_L^* is defined as:

$$p_L^* = p_L - \sigma_{OH} \tag{11}$$

where σ_{OH} is the horizontal total stress at rest obtained either from the pressuremeter curve (section 5.2) or by calculation while making the necessary assumptions. The parameter p_L^* is a measure of the strength of the soil.

The value of p_L^* is relatively insensitive to the disturbance of the borehole wall which may occur during drilling.(10) However p_L^* is relatively sensitive, in theory, to the length to diameter ratio L/D of the pressuremeter probe; this is especially true in sands where p_L^* increases by 20 percent when L/D decreases from 10 to 5; in clays the variation is not as significant.(36) A length to diameter ratio of 6.5 is recommended.

In cohesionless soils the effective stress values of the yield pressure p_y and of the limit pressure p_L are obtained by subtracting the hydrostatic pore pressure u_o from p_y and p_L respectively.

$$p_y' = p_y - u_o \tag{12}$$

$$p_L' = p_L - u_o \tag{13}$$

The hydrostatic pore pressure u_0 is used because it is assumed that no excess pore pressures will develop during a 10 minute PMT test in cohesionless soils. The value of u_o is calculated as $\gamma_w h$ where γ_w is the unit weight of water and h is the distance from the PMT test to the water table.

5.6 Common Values and Soil Identification

Common values of the net limit pressure for various soils and for depth up to 100 ft are shown on table 4. Common values of the modulus E_o are also shown on the table. The yield pressure p_y is usually about one-half of the limit pressure in clays and one-third in sands. The ratio E_r / E_o is about 1.5 to 5 in clays and 3 to 10 in sands.

The ratio E_o / p_L can serve as an indication of the soil type. The following ratios can serve as general guidelines for soil identification:

$$\text{in clays} \quad 12 < E_o / p_L^* \tag{14}$$

$$\text{in sands} \quad 7 < E_o / p_L^* < 12 \tag{15}$$

This difference in behavior between clays and sands is also apparent in the shape of the curve. Clays will generally exhibit a relatively sharp bend in the curve and a relatively obvious limit pressure (figure 15); the more overconsolidated the clay, the more obvious those two features will be. On the contrary, sands will not exhibit a sharp bend but rather a smooth continuous curvature without clear evidence of reaching a limit pressure (figure 15). The reason for this difference is that sands are frictional materials which derive their shear strength from the normal stress on the failure plane. The pressuremeter, by expanding, is shearing the sand but also increases the normal stress level in the soil mass thereby increasing the strength of the sand; the more the pressuremeter expands the stronger the sand gets. As a result, no clear failure appears on a pressuremeter curve in sand. In clay, on the other hand, the undrained shear strength (PMT tests lasting 10 minutes are considered to be undrained tests in clays) is independent of the normal total stress increase imposed by the expanding pressuremeter and a clear failure is apparent towards the end of the test.

In summary a combination of the shape of the pressuremeter curve, the values of p_L^*, E_o, E_o / p_L^*, and inspection of the cuttings during drilling allows proper identification of the soil.

Table 3. Approximate common values for the pressuremeter parameters in clay.

SOIL TYPE	SOFT	MEDIUM	STIFF	VERY STIFF	HARD
p_L^* (tsf)	0 - 2	2 - 4	4 - 8	8 - 16	> 16
E_o (tsf)	0 - 25	25 - 50	50 - 120	120 - 250	> 250

Table 4. Approximate common values for the pressuremeter parameters in sand.

SOIL TYPE	LOOSE	COMPACT	DENSE	VERY DENSE
p_L^* (tsf)	0 - 5	5 - 15	15 - 25	> 25
E_o (tsf)	0 - 35	35 - 120	120 - 225	> 225

5.7 Judging the Quality of the Test

The quality of the test can be judged by inspecting the pressuremeter curve. Figure 16 shows the results of a test performed in a hole which is too large (curve A). The hole is considered to be too large when the radius of the cavity is larger than 1.20 times the radius of the deflated probe. Sometimes, even when the hole is too large the modulus E_o can still be obtained. Figure 16 also shows the results of a test performed in a hole which is too small (curve B). In this case the probe has to be forced into the soil and an initial horizontal pressure exists on the probe before the start of the expansion; in this case the modulus E_o cannot be obtained but the limit pressure p_L which is relatively insensitive to minor disturbance, can still be obtained. Curve C on figure 16 shows the results of a test where the soil was badly remolded by the drilling process; the results of this test cannot be used.

The quality of the test can also be judged by the value of the E_o / p_L^* ratio. Because the modulus E_o is more sensitive to disturbance than the limit pressure, values of E_o / p_L^* which are much lower than those mentioned in section 5.5 may be indicative of excessive disturbance.

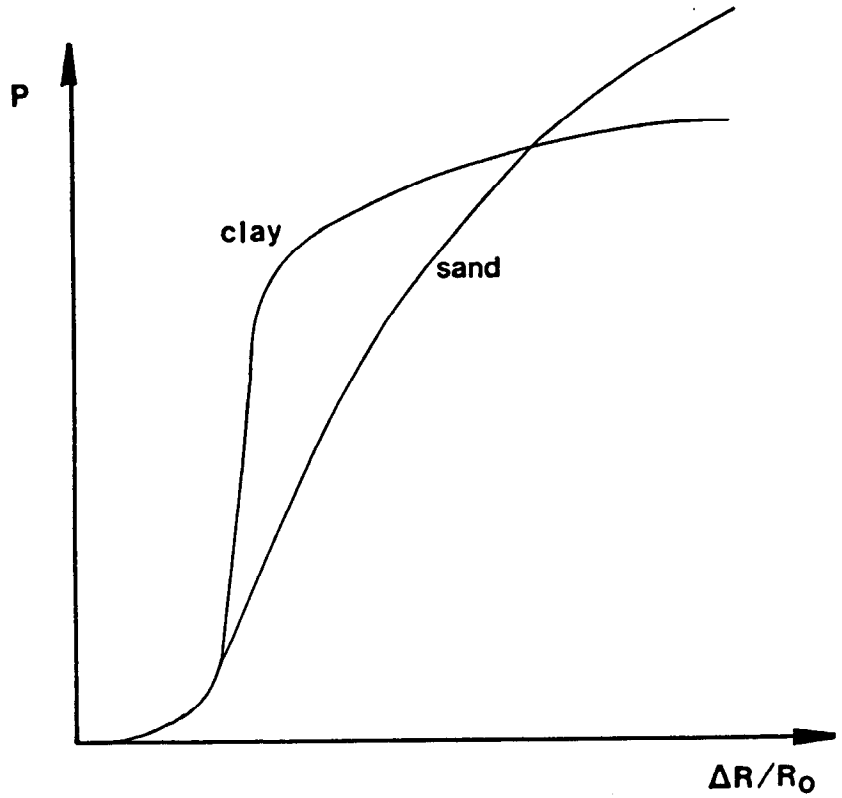

Figure 15. Difference in pressuremeter curve for clay and sand.

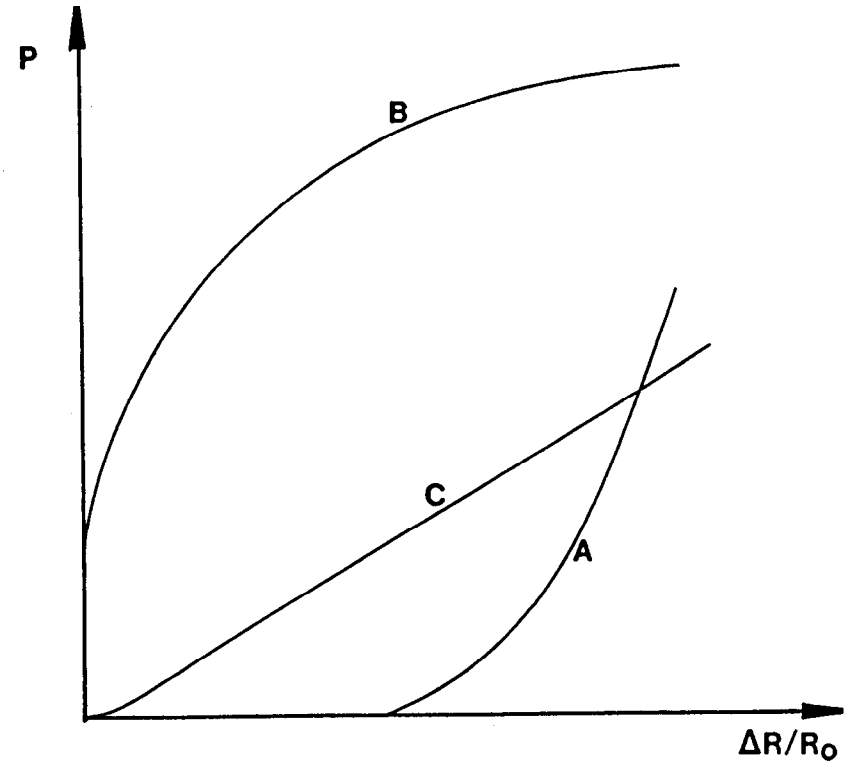

Figure 16. Examples of poor quality pressuremeter curves.

6. SOIL PARAMETERS AND COMPARISON WITH OTHER TESTS

6.1 Undrained Shear Strength of Cohesive Soils

There are various ways of obtaining the undrained shear strength of a cohesive soil from a pressuremeter test. They include the limit pressure method, empirical correlations, the yield pressure method, the Gibson-Anderson method, and the shear curve method.

The limit pressure method makes use of the theoretical expression of the limit pressure (plasticity theory with Tresca criterion):

$$p_L = \sigma_{OH} + S_u\left(1 + \mathrm{Ln}\frac{G}{S_u}\right) \qquad (16)$$

where p_L is the limit pressure, σ_{OH} is the total horizontal stress at rest, S_u is the undrained shear strength of the cohesive soil. Equation 36 can be rewritten:

$$S_u = \frac{p_L^*}{\beta} \qquad (17)$$

Menard in 1970 proposed that β be taken as 5.5. In fact the parameter β depends on the ratio of the shear modulus G over the undrained shear strength S_u. The ratio G/S_u varies from one clay to another depending mainly on the overconsolidation ratio. Some reasonable limits for G/S_u are 100 to 600. This leads to values of β between 5.6 and 7.4 for an average β of 6.5. Equation 16 is based on the assumption that the pressuremeter is infinitely long. It has been shown that the limit pressure for a sphere is equal to 1.33 times the limit pressure for an infinitely long cylinder.(36) Therefore the limit pressure for conventional pressuremeters is expected to be higher than the limit pressure in equation 16. As a result the average value of β needs to be higher than 6.5.

Baguelin et al. present an extensive comparison of undrained shear strength S_u and p_L^*.(10) The plot (figure 17) shows that the ratio p_L^*/S_u varies from about 5.5 for clays with S_u values less than 0.5 tsf to 10 for clays with S_u values of about 1.5 tsf. This suggests a nonlinear relationship between s_u and p_L^*. A log-log regression on figure 17 leads to:

$$S_u = 0.67\, p_L^{*0.75} \quad \ldots \text{ with } S_u \text{ and } p_L^* \text{ in } kPa \qquad (18)$$

or

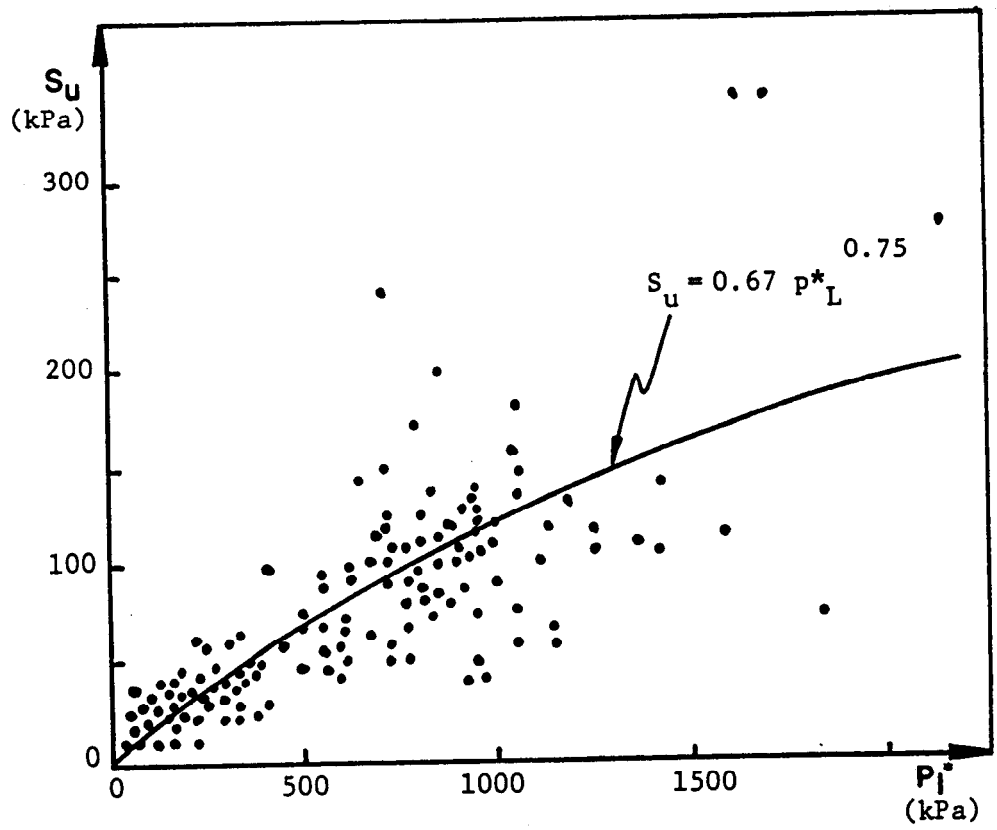

Figure 17. Correlation between S_u and p^*_L.(10)

$$S_u = 0.21\, p_L^{*0.75} \quad \ldots \quad \text{with} \quad S_u \quad \text{and} \quad p_L^* \quad \text{in} \quad \text{tsf} \qquad (19)$$

Baguelin et al. mentions the following reasons for the scatter in the data: different sample disturbance between soft and stiff clay, inaccuracies in evaluating σ_{oH} nonhomogeneity of the soil, sensitivity of the clay, length to diameter ratio of the PMT probe, anisotropy, borehole disturbance and unloading.(10) Others have compared S_u and p_L^* they include Cassan, Komornik et Al., Meigh and Greenland, Higgins, Amar and Jezequel, Lukas and LeClerc de Bussy, Roy et al.(39,57,72,49,2,67,91)

The above comments have led to the recommendation of the expression:

$$S_u = 0.21\, p_L^{*0.75} \quad \ldots \quad \text{with} \quad S_u \quad \text{and} \quad p_L^* \quad \text{in} \quad \text{tsf} \qquad (19)$$

Obtaining s_u from PMT tests is particularly useful in very fissured clays where triaxial test results may be widely scattered.

6.2 Friction Angle of Cohesionless Soils

There are several ways of obtaining the friction angle ϕ of a cohesionless soil from a pressuremeter test, none of which are very satisfactory. They include the yield pressure method, the limit pressure method, the Hughes-Wroth-Windle method, and empirical correlations. Of all those methods the Hughes-Wroth-Windle method is the one which is the most theoretically sound.(51) All in all however it is not recommended that the preboring pressuremeter be used solely t a site for obtaining the effective stress friction angle.

6.3 Comparison with Other Test Results

A data base of preboring pressuremeter test data and other test data was formed.(25) The pressuremeter data were collected over the last 10 years on various research and consulting projects. The pressuremeters used were the Menard pressuremeter, the TEXAM pressuremeter and the pavement pressuremeter all inserted in a prebored hole. The 82 pressuremeter borings were located in the south, southwest, west and central United States with 36 sand sites, 44 clay sites and 2 silt sites. Next to the PMT borings other borings were performed leading to data on undrained shear strength S_u effective stress friction angle ϕ' SPT blow count N, cone point and friction resistance q_c and f_s. At each depth in a boring a record was created which consisted of E_o, E_r, p_L, S_u, ϕ', N, q_c and f_s. A total of 426 records were accumulated. The data are described in detail.(25)

Table 5. Correlation results for sand. (Column A = Number in Table x Row B.)

A \ B	E_o tsf	E_R tsf	p^*_L tsf	q_c tsf	f_s tsf	N bl/ft
E_o tsf	1	0.125	8	1.15	57.5	4
E_R tsf	8	1	64	6.25	312.5	22.7
p^*_L tsf	0.125	0.0156	1	0.11	5.5	0.5
q_c tsf	0.87	0.16	9	1	50	5
f_s tsf	0.0174	0.0032	0.182	0.02	1	0.1
N bl/ft	0.25	0.044	2	0.2	10	1

Table 6. Correlation results for clay. (Column A = Number in Table x Row B.)

A \ B	E_o tsf	E_R tsf	p^*_L tsf	q_c tsf	f_s tsf	S_u tsf
E_o tsf	1	0.278	14	2.5	56	100
E_R tsf	3.6	1	50	13	260	300
p^*_L tsf	0.071	0.02	1	0.2	4	7.5
q_c tsf	0.40	0.077	5	1	20	27
f_s tsf	0.079	0.0038	0.25	0.05	1	1.6
S_u tsf	0.010	0.0033	0.133	0.037	0.625	1

The clay deposits had undrained shear strengths as low as 0.1 tsf (9.6 kPa), as high as 26 tsf (2490 kPa), and averaged 1.5 tsf. The sand deposits had blow counts as low as 1, as high as 100 and averaged 43. Best fit regressions were performed for the entire data base and for combinations of any two parameters. The results are shown in tables 5 and 6. The scatter in the correlations was very large as exemplified by figures 18 and 19. This drastic scatter makes these correlations essentially useless in design.

The value of the data base is to give a relative idea of the magnitude of the pressuremeter parameters. Among the relationships are:

In clay

$$p_L = 7.5 S_u \quad (20)$$

$$p_L = 0.2 q_c \quad (21)$$

$$p_L = 0.071 E_o \quad (22)$$

$$E_o = 100 S_u \quad (23)$$

$$E_o = 2.5 q_c \quad (24)$$

$$E_o = 0.278 E_R \quad (25)$$

In sand

$$p_L(tsf) = 0.5 N(\text{blows/ft}) \quad (26)$$

$$p_L = 0.11 q_c \quad (27)$$

$$p_L = 0.125 E_o \quad (28)$$

$$E_o(tsf) = 4 N(\text{blows/ft}) \quad (29)$$

$$E_0 = 1.15 q_c \quad (30)$$

$$E_o = 0.125 E_R \quad (31)$$

Equation 20 indicates that the pressuremeter limit pressure is somewhat larger than the ultimate bearing pressure of a shallow footing and somewhat smaller than the ultimate bearing pressure under the point of a pile. Equation 23 gives an idea of the magnitude of the preboring pressuremeter modulus; the scatter of the data on figure 18 tends to indicate that obtaining elastic moduli from undrained shear strength is unreliable. Comparison of equations 22 and 28 shows that the stiffness to strength ratio is much higher for clays than it is for sand and that the E_o / p_L ratio can serve as a soil classification index (section 5.5). Comparison of equations 25 and 31 shows that the reload to first load modulus ratio is much higher for sand than it is for clay and that the E_R / E_o ratio can also serve as a soil

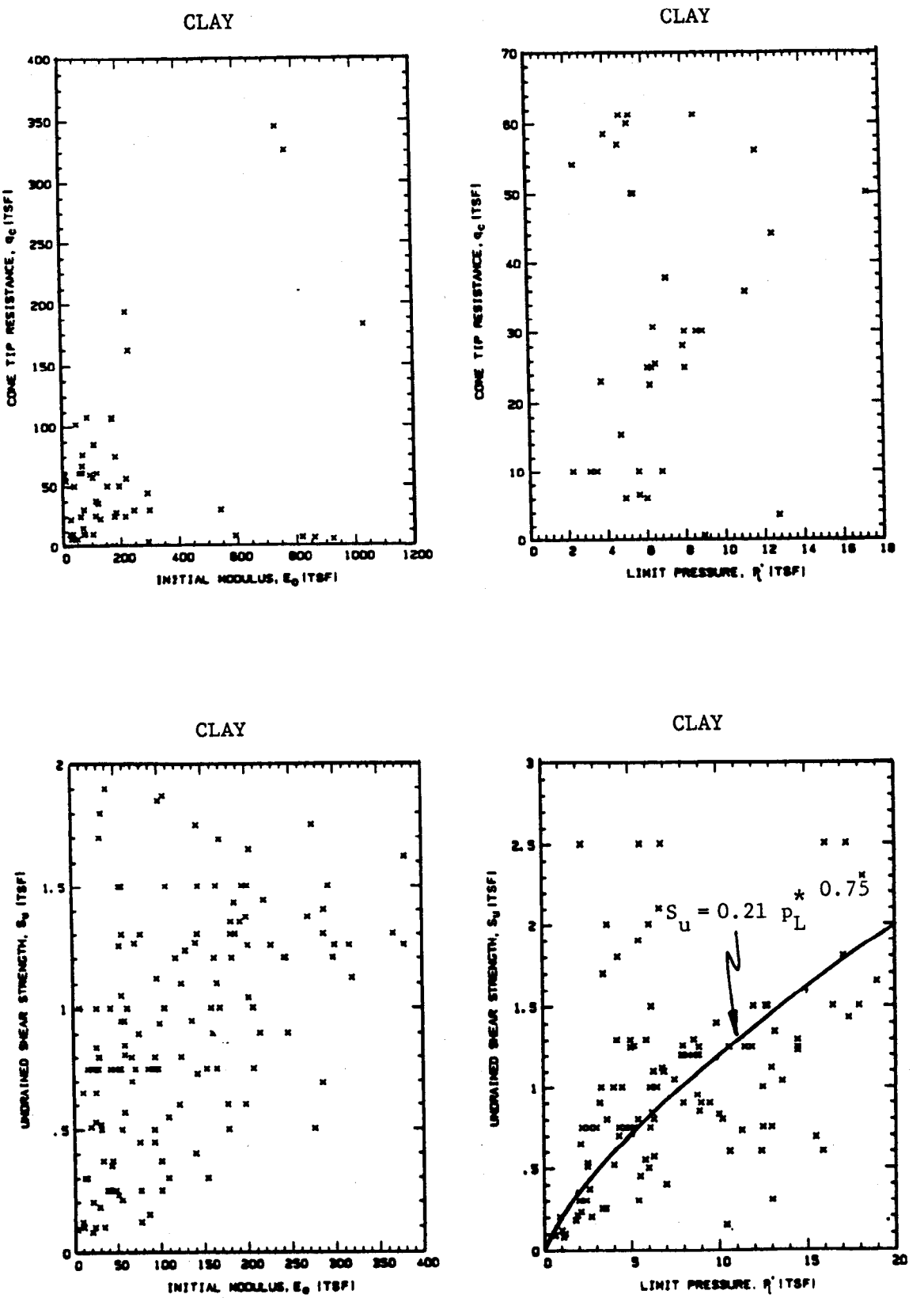

Figure 18. Examples of correlations in clay from PMT data base.

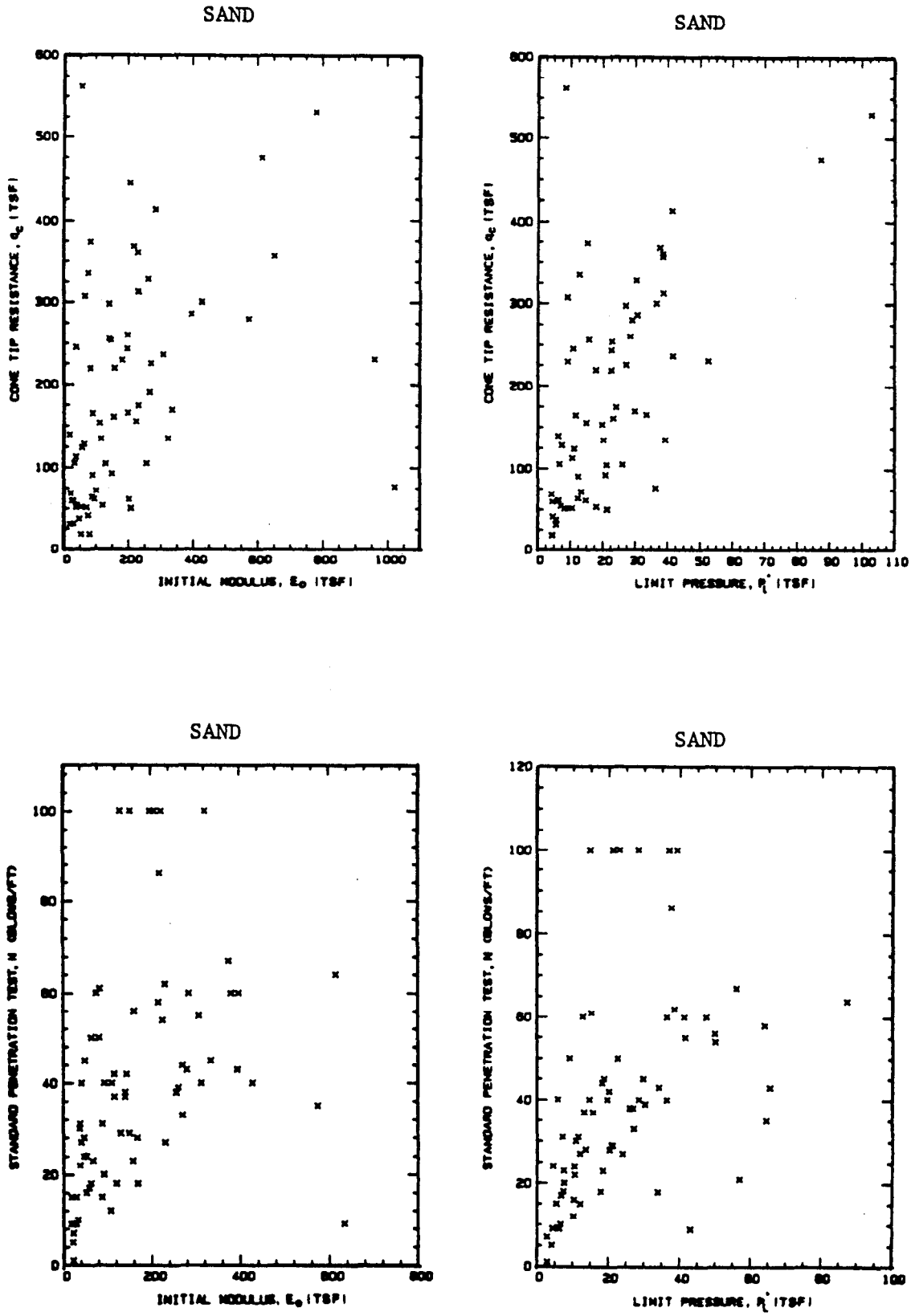

Figure 19. Examples of correlations in sand from PMT data base.

classification index (section 5.5). Equation 30 can be compared to the relationship proposed by Schmertmann in 1978 for calculating the settlement of spread footings on sands using elasticity:

$$E = 2.5 \quad to \quad 3.5 \quad q_c \tag{32}$$

This would indicate that the pressuremeter modulus E_o is 2 to 3 times too low for use in elasticity settlement formulas in sand.

Other comparisons have been made. Merritt et Al. compared K_o from PMT tests with K_o from oedometer tests and from Ladd's relationship at a site in Houston.(80,60) Although there was some scatter, all values of K_o were reasonable and showed general agreement. Gan and Briaud compared K_o from preboring PMT and selfboring PMT at three sites in stiff clay and in medium dense to loose sand.(45) The results showed very good agreement.

Davidson and Perez compared preboring PMT (PBPMT) moduli with those obtained from selfboring PMT (SBPMT) tests and from UU triaxial compression tests in the Seattle stiff clay.(42) Some of their conclusions were that the PBPMT moduli E_o are lower than the SBPMT moduli, the UU triaxial tests initial tangent moduli values are even lower than the PBPMT moduli, the unload-reload moduli of the PBPMT tests E_r are comparable to the SBPMT moduli; this finding is also mentioned by Baguelin et Al.(10) Shields and Bauer compared PBPMT moduli E_o with laboratory tests moduli, and plate tests moduli in a sensitive clay.(92) Some of their conclusions are that the PBPMT moduli E_o and the UU triaxial tests moduli are comparable, and are about two times smaller than the plate moduli. Closer agreement between E_o and the plate modulus was found by Greenland in a stiff varved clay.(46) Tavenas et Al. testing in a sensitive clay found that the PBPMT modulus E_o was drastically lower than the modulus measured on reconsolidated triaxial specimens.(98) On the other hand, Burgess and Eisenstein testing in a hard silty clay till found that the PBPMT modulus E_O was about twice the modulus from consolidated, undrained triaxial tests.(37) Briaud and Shields found very good agreement between the PBPMT reload modulus and the plate modulus; the plate modulus was a secant modulus at a plate deflection of 0.5 in, and the PBPMT reload modulus was obtained from an unload-reload cycle as described in equation 8 and figure 14 except that the bottom of the cycle was near zero pressure.(28) Briaud et Al. found good agreement between predicted deflections using the proper PBPMT modulus and measured deflections with the Falling

Weight Deflectometer; the deflections were very small (only a few thousandths of an inch) and the PBPMT moduli were chosen at the right strain level and stress level in order to properly predict the deflections.(17)

7. DESIGN OF SHALLOW FOUNDATIONS

7.1 Bearing Capacity: Step-by-Step Procedure

A microcomputer program, SHALPMT, exists to perform this procedure automatically.(100)

* Bearing capacity equation

The ultimate bearing capacity, q_p is:

$$q_p = k\, p^*_{Le} + q_o \qquad (33)$$

where

k = pressuremeter bearing capacity factor (figure 20),
p^*_L = net limit pressure = p_L - POH,
POH = total horizontal stress at rest, p_i = limite pressure (from test),
p^*_{Le} = equivalent net limit pressure near the foundation level, and
q_o = total stress overburden pressure at foundation level.

* Calculating p^*_{Le} the equivalent net limit pressure

$$p^*_{Le} = \sqrt[n]{p^*_{L1} \times p^*_{L2} \ldots x\, p^*_{Ln}} \qquad (34)$$

* Calculating H_e the equivalent depth of embedment

$$H_e = \frac{1}{p^*_{Le}} \sum_{1}^{n} \Delta z_i\, p^*_{Li} \qquad (35)$$

where p^*_{Li} are the net limit pressures obtained from tests between the ground surface and the foundation level, and Δz is the thickness of each elementary layer corresponding to the pressuremeter tests.

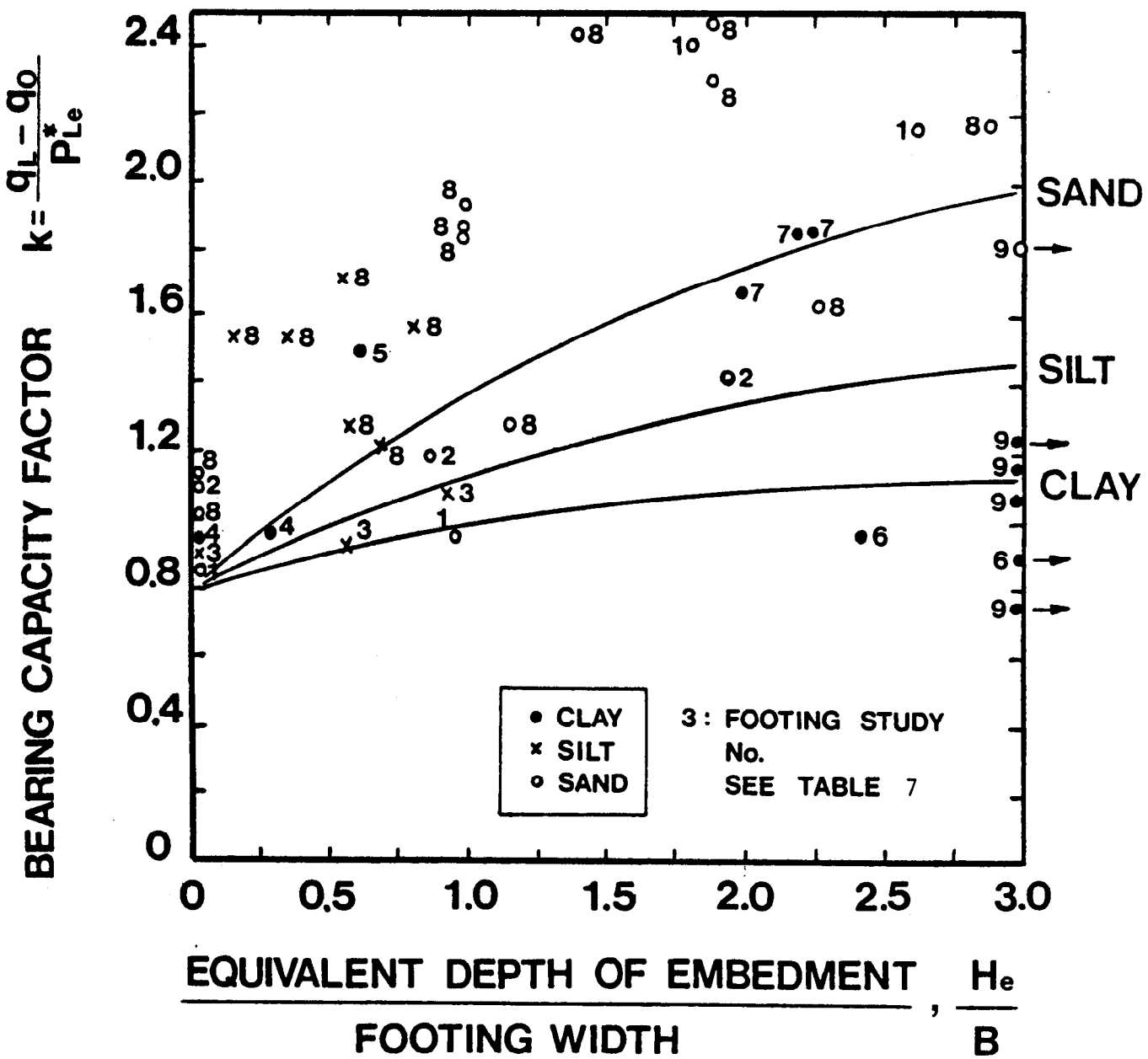

Figure 20. Recommended design curves for shallow foundations.

* Obtaining k, the pressuremeter bearing capacity factor

The relative embedment depth is H_e / B. The bearing capacity factor k is read on figure 20. This k value is for a square or circular footing. For a strip footing use k/1.2. If the footing is rectangular, linear interpolation is performed between the case of a square footing and the case of a strip footing; the interpolating parameter is B/L. For special cases such as inclined, eccentric loads and footings on slope, see section 7.3.

* Calculating q_p, q_{safe}, and q_{net}

$$q_p = k p^*_{Le} + q_o \tag{36}$$

$$q_{safe} = \frac{k p^*_{Le}}{3} + q_o, \quad \text{and} \tag{37}$$

$$q_{net} = q_{safe} - q_o = \frac{k p^*_{Le}}{3} \tag{38}$$

Examples are provided in section 7.7.

7.2 Bearing Capacity: Precision of the Design Rules

The data base for figure 20 is shown in table 3 and described in Briaud et al.(30) The data points used to select the recommended design curves are shown on figure 20. These curves correspond approximately to the curve which would split the data points in half (mean) minus one standard deviation of the scatter around the mean. It is emphasized that these curves are proposed to calculate the ultimate bearing pressure defined as the pressure necessary to generate a short term settlement equal to 1/10th of the footing width. It is also emphasized that one must follow rigorously the rules for obtaining p^*_{Le} and H_e.

The ratio of the ultimate bearing pressure predicted by these design curves to the measured ultimate bearing pressure varied between the extreme values of 0.65 to 1.65 for the data base (figure 20). For comparison purposes, the precision of the method which consists of using the general bearing capacity equations to predict the ultimate bearing pressure is shown on figure 21 for clay and figure 22 for sand. These figures come from a data base study performed by Amar, Baguelin and Canepa.(1) As can be seen, the ratio of predicted over measured ultimate bearing pressure varies from 0.51 to 1.67 in clay and from 0.12 to 12 in sand. Therefore the pressuremeter may not improve significantly the bearing capacity predictions in clay but may improve dramatically the predictions in sand.

Table 7. Data base for shallow footings.

Study No.	Footing I.D. No.	Reference	Soil	Footing Width (m)	Footing Depth (m)	Footing Type
1	1	Deschenes (1978)	Medium	0.30	0	Strip
	2	Briaud (1979)	Dense	0.30	0.30	Strip
	3		Sand	0.30	0.60	Strip
	4			0.30	0.90	Strip
2	5	Deschenes (1978)	Dense	0.30	0	Strip
	6	Briaud (1979)	Sand	0.30	0.30	Strip
	7			0.30	0.60	Strip
3	8	Amar-Baguelin-Canepa	Silt	1.0	0	Square
	9	(1984)		1.0	0.60	Square
	10			1.0	1.0	Square
4	11	Shields-Bauer (1975)	Clay	0.46	2.6	Circular
	12			3.1	0.70	Square
5	13	O'Neill-Sheikh (1985) Briaud-Riner (1984)	Clay	2.41	2.36	Circular
6	14	O'Neill-Reese (1970)	Clay	0.76	7.0	Circular
	15	WCC (1981)		2.29	7.0	Circular
7	16	Tand et al. (1986)	Clay	0.60	1.50	Circular
	17	Briaud Engineers (1984)		0.60	1.50	Circular
	18			0.60	1.50	Circular
8	19	Menard (1963)	Sand/ Silt	0.25-0.6	0.5-1.7	Circular Circular
9	20	Marsland-Randolph	Clay	0.865	6.1	Circular
	21	(1977)		0.865	12.2	Circular
	22			0.865	18.3	Circular
	23			0.865	24.0	Circular
10	24	Johnson (1986)	Clay	0.762	0.0	Circular

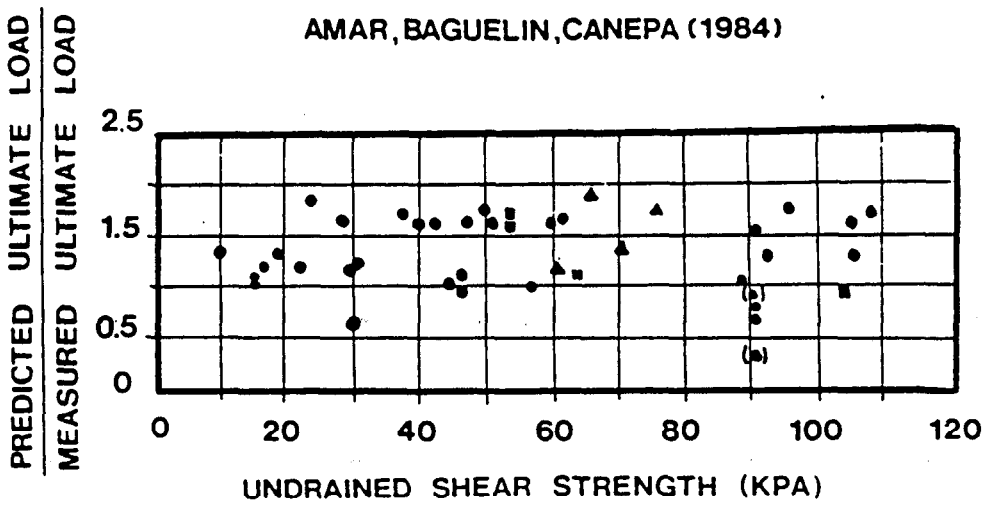

Figure 21. Measured vs predicted capacity by $q_u = N_c S_u + \gamma D$ for clay.

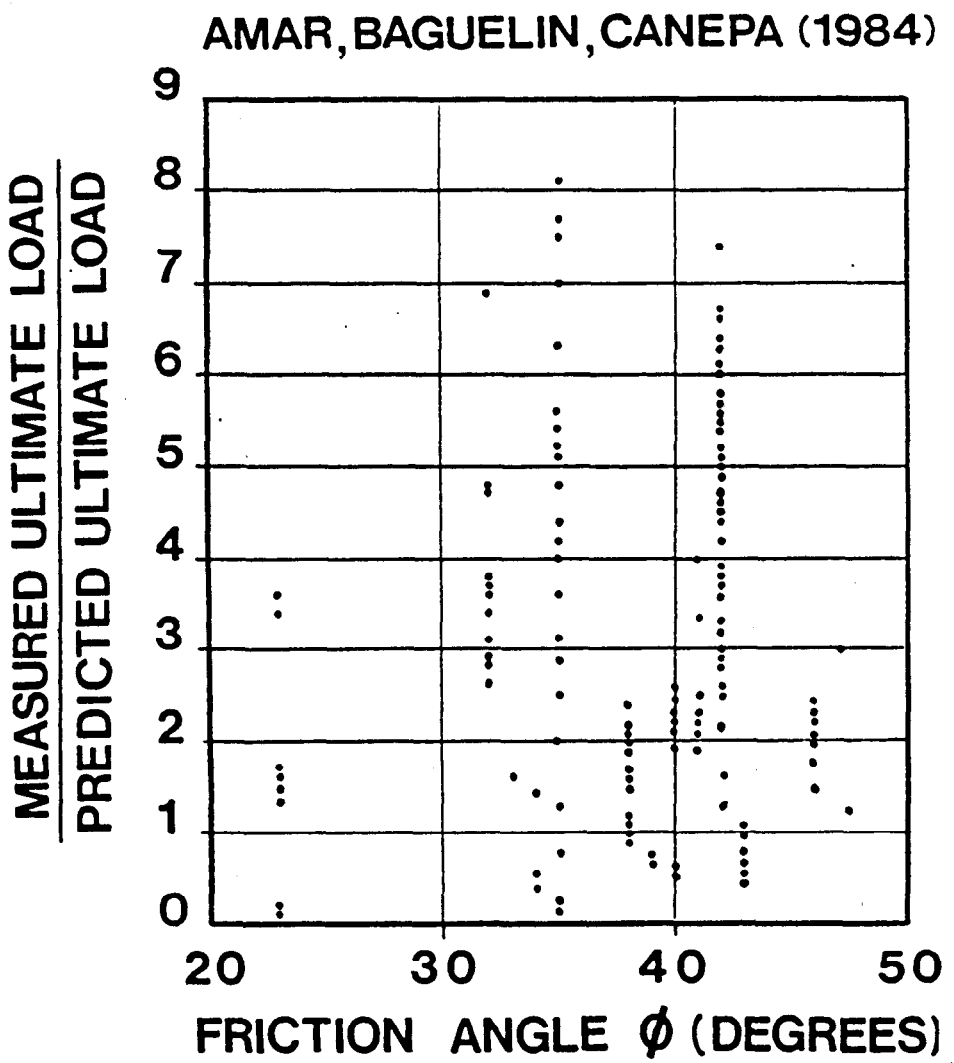

Figure 22. Measured vs predicted capacity by $q_u = 0.5\gamma B N_\gamma + \gamma D N_q$ for sand.

7.3 Bearing Capacity: Eccentric Load, Inclined Load, Slopes

The previous design rules refer to the case of a vertical load applied at the center of a shallow footing around which the ground surface is horizontal. The number of load tests which address the special problems of eccentric load, inclined load and footings near slopes are almost nonexistent. Some recent studies are: one study of footings near slopes reported by Shields et al. and an ongoing study by the Laboratoire Centrale des Ponts et Chaussees.(93) Baguelin, Jezequel and Shields list a few other studies and, after emphasizing the scarcity of the experimental data, propose to apply Meyerhof reduction coefficients to the pressuremeter rules.(10,81,82) These Meyerhof rules adapted to the pressuremeter approach by Baguelin, Jezequel and Shields are described below.

The ultimate load which can be carried by a footing loaded vertically, concentrically and on horizontal ground is called Q_u. The ultimate loads Q_{ue}, Q_{ui}, and Q_{us} refer to eccentric loading, inclined loading, and loading near a slope, respectively. The ultimate load Q_{uis} would refer to an inclined loading near a slope, Q_{uei} to an eccentric inclined loading, and Q_{ueis} to an eccentric inclined loading near a slope.

For eccentric loading (figure 23) a reduced width B' is used ($B' = B - 2e$) and the pressuremeter rules are applied to the B' wide concentrically loaded footing. The ultimate load is reduced and the reduction factor is:

$$i_e = \frac{Q_{ue}}{Q_u} \tag{39}$$

For inclined loading (figure 24) a reduction factor i_i is applied to Q_u. This factor is given by (see figure 24 for the definition of δ):

$$i_i = \left(1 - \frac{\delta}{90}\right)^2 (1 - \lambda) + \left(1 - \frac{\delta}{20}\right)\lambda \tag{40}$$

with

$$\lambda = \lambda_d \lambda_m \tag{41}$$

$$\lambda_d = 1 - D/B \quad \text{for} \quad 0 < D/B < 1 \tag{42}$$

$$\lambda_d = 0 \quad \text{for} \quad D/B > 1 \tag{43}$$

$$\lambda_m = 1 - m \quad \text{for} \quad 0 < m < 1 \tag{44}$$

$$\lambda_m = 0 \quad \text{for} \quad m > 1 \tag{45}$$

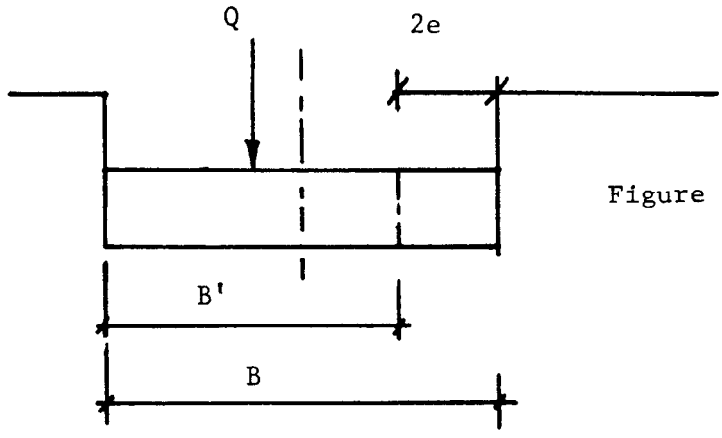

Figure 23. Eccentrically loaded shallow footing.

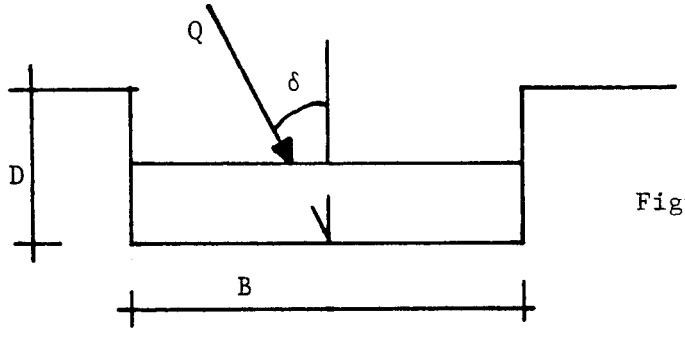

Figure 24. Shallow footing subjected to an inclined load.

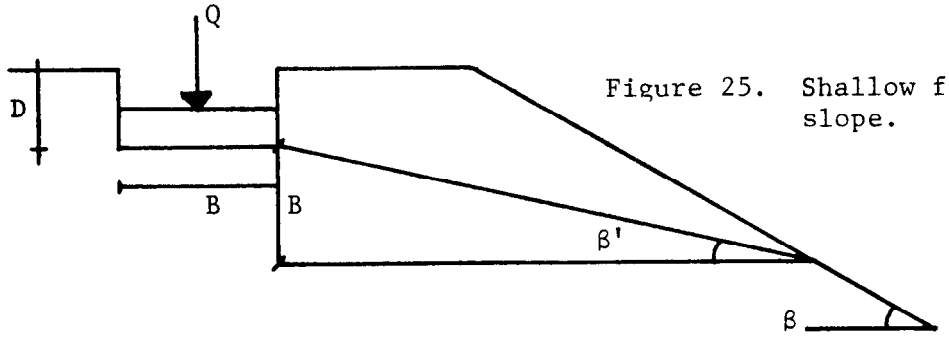

Figure 25. Shallow footing near a slope.

$$m = (p_L^* \quad \text{at} \quad z = D)/(p_L^* \quad at \quad z = D + B) \tag{46}$$

Then:
$$Q_{ui} = i_i Q_u \tag{47}$$

If i_i is negative, Q_{ui} is zero and the footing must be embedded deeper in order to gain capacity.

For footings near slopes (figure 25), the first step is to ensure that the slope with the footing load is sufficiently safe. If this is the case, the reduction factor i_s is calculated by using equations 40 to 47 in which δ is replaced by β', an angle defined on figure 25.

$$Q_{us} = i_s Q_u \tag{48}$$

For concentric inclined loading near a slope, two cases can occur; the inclined load is directed towards the slope (figure 26) or away from the slope (figure 27). If the inclined load is directed towards the slope the reduction factor i_{is} is calculated by using equations 40 to 46 after replacing δ by $\delta + \beta'$.

$$Q_{uis} = i_{is} Q_u \tag{49}$$

If the calculated load is directed away from the slope, the failure can occur towards the slope or away from the slope; the two cases are considered separately. For the failure towards the slope the reduction factor i_{is} is calculated by using equations 40 to 46 after replacing δ by $\beta' - \delta$. For the failure away from the slope the reduction factor is the same as the one for an inclined loading on horizontal ground (equations 40 to 46). The lower of the two loads obtained is the failure load for the case of an inclined load directed away from the slopes.

For eccentric inclined loading, two cases can occur; the case of figure 28 or the case of figure 29. In the case of figure 28, the reduction due to eccentricity is calculated first. This leads to the reduction factor i_e. Then the reduction due to the inclined load is applied to a footing of reduced width B' is B - 2e (figure 28). This leads to the reduction factor i_i. The ultimate load is:

$$Q_{uei} = i_e i_i Q_u \tag{50}$$

In the case of figure 29, the failure can occur to the left or to the right. For failure to the left, the reduction due to eccentricity is calculated; this leads to i_e. Then the reduction due to inclined loading is calculated (equations. 40 to 46) by using the real width B to calculate m and λ_d; this leads to i_i. The ultimate load is:

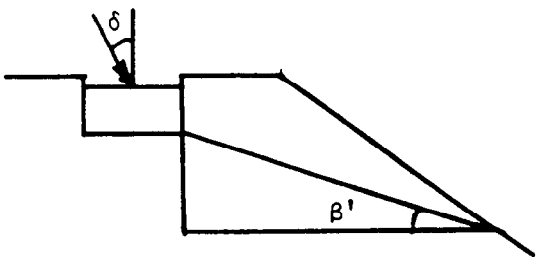

Figure 26. Shallow footing near a slope with a load inclined towards the slope.

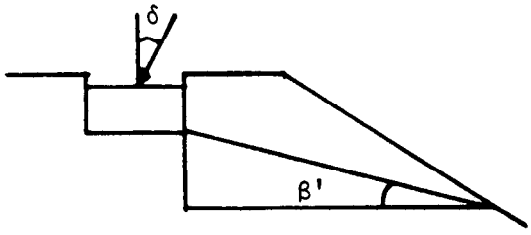

Figure 27. Shallow footing near a slope with a load inclined away from the slope.

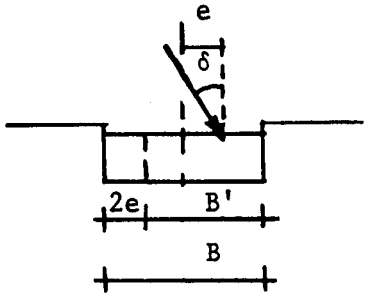

Figure 28. Shallow footing eccentrically loaded with a load inclined towards the edge.

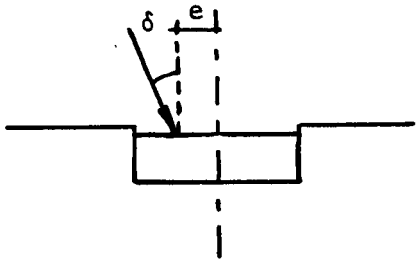

Figure 29. Shallow footing eccentrically loaded with a load inclined towards the center.

$$Q_{nei} = \frac{i_e}{i_i} Q_n \quad \text{if} \quad \frac{i_e}{i_i} < 1 \tag{51}$$

$$Q_{uei} = Q_u \quad \text{if} \quad \frac{i_e}{i_i} < 1 \tag{52}$$

For failure to the right, the footing is considered to have a width $B' = B + 2e$. The ultimate load Q_u for the $B + 2e$ wide footing subjected to concentric, vertical loading on horizontal ground is calculated. The reduction due to inclined loading is calculated (equations. 40 to 46) by using the real width B to calculate m and λ_d; this leads to i_i. The ultimate load is:

$$Q_{uei} = i_i Q_{u(B+2e)} \tag{53}$$

An example is given in section 7.7.

7.4 Settlement: Step-by-Step Procedure

A microcomputer program, SHALPMT, exists to perform this procedure automatically.(100)

* Settlement equation

The pressuremeter equation for settlement is:(79)

$$s = \frac{2}{9E_d} q B_o \left(\lambda_d \frac{B}{B_o} \right)^{\alpha} + \frac{\alpha}{E_c} q \lambda_c B \tag{54}$$

deviatoric settlement — spherical settlement

* Calculating the layer moduli

The soil below the foundation level is divided into a series of elementary layers B/2 thick (figure 30). In each layer the average pressuremeter modulus is calculated using the PMT results within that layer and the harmonic mean technique.

$$\frac{n}{E_k} = \frac{1}{E_1} + \frac{1}{E_2} + \ldots + \frac{1}{E_n} \tag{55}$$

where

Ei = PMT moduli within the k^{th} layer, and

Ek = average PMT modulus of the k^{th} layer.

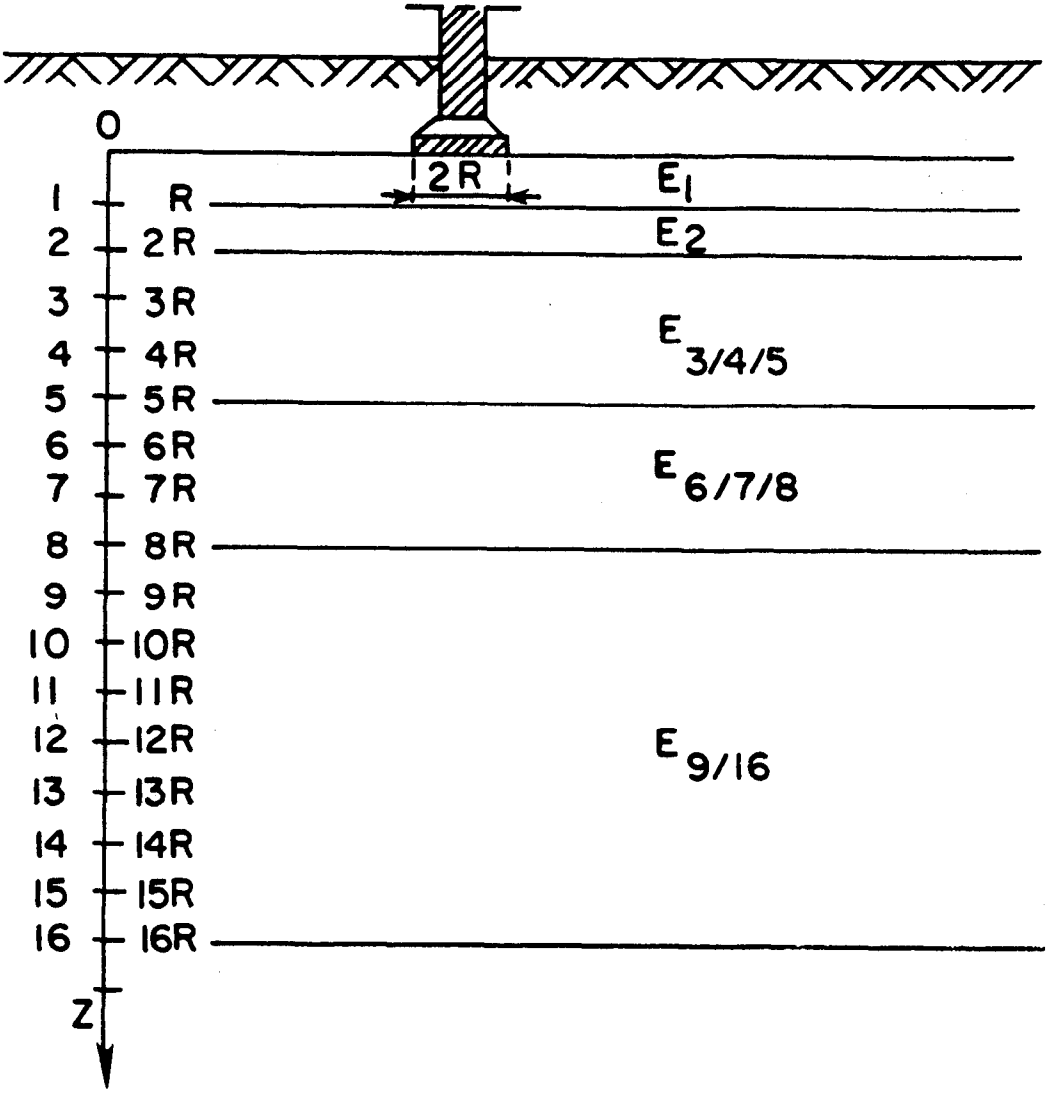

Figure 30. Decomposition of the soil into layers for settlement analysis.

This process is repeated for all layers (1 through 16); if no data is available beyond a certain depth z the moduli of the layers deeper than z are estimated based on other data available at the site.

* Calculating E_c and E_d

According to the theory of elasticity the spherical part of the strain tensor decreases rapidly with depth. However, the magnitude of the deviatoric part of the strain tensor is significant even at large depth. As a result, E_c is taken as the modulus of the first layer under the footing.

$$E_c = E_1 \tag{56}$$

On the other hand, E_d is taken as an equivalent modulus within 16 layers, B/2 thick, under the footing; the formula which gives the equivalent distortion modulus E_d is based on an assumed reasonable ϵ_d strain distribution:(75)

$$\frac{1}{E_d} = \frac{1}{4}\left(\frac{1}{E_1} + \frac{1}{0.85E_2} + \frac{1}{E_{3/4/5}} + \frac{1}{2.5E_{6/7/8}} + \frac{1}{2.5E_{9/16}} \right) \tag{57}$$

where $E_{p/q}$ is the harmonic mean of the moduli of layers p to q. For example,

$$\frac{3}{E_{3/4/5}} = \frac{1}{E_3} + \frac{1}{E_4} + \frac{1}{E_5} \tag{58}$$

* Obtaining α and λ

The parameters $\alpha, \lambda_d,$ and λ_c are obtained from table 8 and figure 31. The determination of α is made by assessing the soil type and estimating the state of consolidation through the use of the ratio, E/p_L. The shape factors λ_c and λ_d depend on the length to width ratio, L/B.

* Calculating the settlement

The settlement is calculated using equation 54 mentioned above; the bearing pressure is taken to be the net safe pressure:

$$q_{net} = q_{safe} - q_o \tag{59}$$

Note that the settlement is linearly proportional to q_{net}.

Table 8. Menard's α factors.

Soil Type	Peat		Clay		Silt		Sand		Sand and Gravel	
	E/p_L^*	α	E/p_L^*	α	E/p_L^*	α	E/p_L^*	α	E/p_L^*	α
Over-consolidated			>16	1	>14	2/3	>12	1/2	>10	1/3
Normally consolidated	For all Values	1	9-16	2/3	8-14	1/2	7-12	1/3	6-10	1/4
Weathered and/or remoulded			7-9	1/2		1/2		1/3		1/4

Rock	Extremely Fractured	Other	Slightly Fractured or Extremely Weathered
	α = 1/3	α = 1/2	α = 2/3

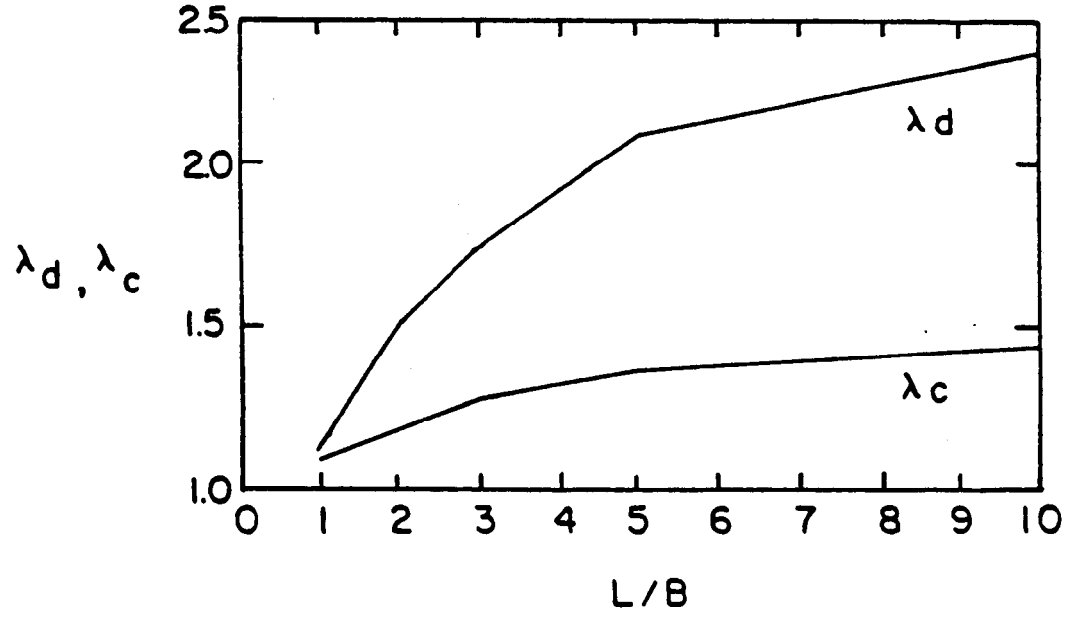

Figure 31. Menard's shape factors.

7.5 Settlement: Special Cases Involving a Thin Soft Layer

* Thin soft layer at depth

In this case the settlement is:(10)

$$s = s' + s'' \tag{60}$$

where s' is the settlement of the footing when considering that the modulus of the soft layer (E_{soft}) is the same as the modulus of the soil immediately above the soft layer (E_{hard}); and s" is the compression of the soft layer alone.

$$s' = \frac{2}{9E_d} q B_o \left(\lambda_d \frac{B}{B_o} \right)^{\alpha} + \frac{\alpha}{9E_c} q \lambda_c B, \text{and} \tag{61}$$

$$s'' = \alpha \left(\frac{1}{E_{soft}} - \frac{1}{E_{hard}} \right) \Delta\sigma_v H \tag{62}$$

$\Delta\sigma_v$ is the average increase in vertical stress in the soft layer and H is the thickness of the soft layer. The settlement s" is calculated using an elasticity formula with a modulus equal to E/α. See example 4 in section 7.7.

* Thin soft layer close to the ground surface

If the raft or the embankment rests on a soft layer which is thinner than B/2, the settlement of the soft layer is calculated as:(10)

$$s = \sum_{1}^{n} \frac{\alpha_i \beta \Delta\sigma_i}{E_i} \Delta z_i \tag{63}$$

where n is the number of layers constituting the soft layer and β is a function of the safety factor, F.

$$\beta = \frac{2}{3} \times \frac{F}{F-1} \tag{64}$$

F is the ratio of the ultimate bearing capacity to the pressure applied by the foundation, $\Delta\sigma_i$ is the average increase in vertical pressure in the i^{th} layer computed by elastic theory, α_i is the rheological factor for the i^{th} layer, E_i is the pressuremeter modulus for the i^{th} layer, and Δz_i is the thickness of the i^{th} layer. Equation 63 above is based on the theory of elasticity using a modulus E/α.

The coefficient β tends to take into account the increase in compressibility beyond the preconsolidation pressure and is explained as follows:

1. S is a consolidation settlement.
2. If the factor of safety is 3, the bearing pressure is likely to be close to or smaller than the preconsolidation pressure, and β is 1 in this case.
3. If the factor of safety is less than 3, the bearing pressure is likely to exceed the preconsolidation pressure and β increases accordingly.

See example 5 in section 7.7.

7.6 Settlement: Precision of the Design Rules

A number of footing load tests in stiff clay, silt and sand (table 7) were used to compare the settlement calculated by Menard's equation to the measured settlement.(30,32) The procedure followed was to use the design curves of figure 20 in order to obtain a bearing capacity factor k, to evaluate the ultimate bearing capacity and use a factor of safety of 3 to obtain the safe bearing pressure q_{safe}.

$$q_{safe} = \frac{k p^*_{Le}}{3} + q_o \qquad (65)$$

The pressure q_{safe} was then used to calculate the footing settlement. This settlement was compared to the settlement measured at q_{safe} during the load tests. Figure 32 is a comparison of the measured and predicted settlement obtained. Figure 32 indicates that a precision of ± 50 percent can be expected from the Menard's rules.

In 1978, Baguelin, Jezequel and Shields showed the results of 45 comparisons between predicted and measured settlements on various structures; the results are plotted on figure 33.

As an example of the precision obtained in current practice, one result of a settlement data base study for footings on sand is shown in figure 34.(52) This figure shows a comparison of measured settlement with predicted settlement by the Peck and Bazaraa method.(87)

The consolidation test applies well to the prediction of the spherical part of the settlement, s_c while the pressuremeter test which is theoretically a pure deviatoric test applies well to the prediction of the deviatoric part of the settlement. Therefore for a wide foundation

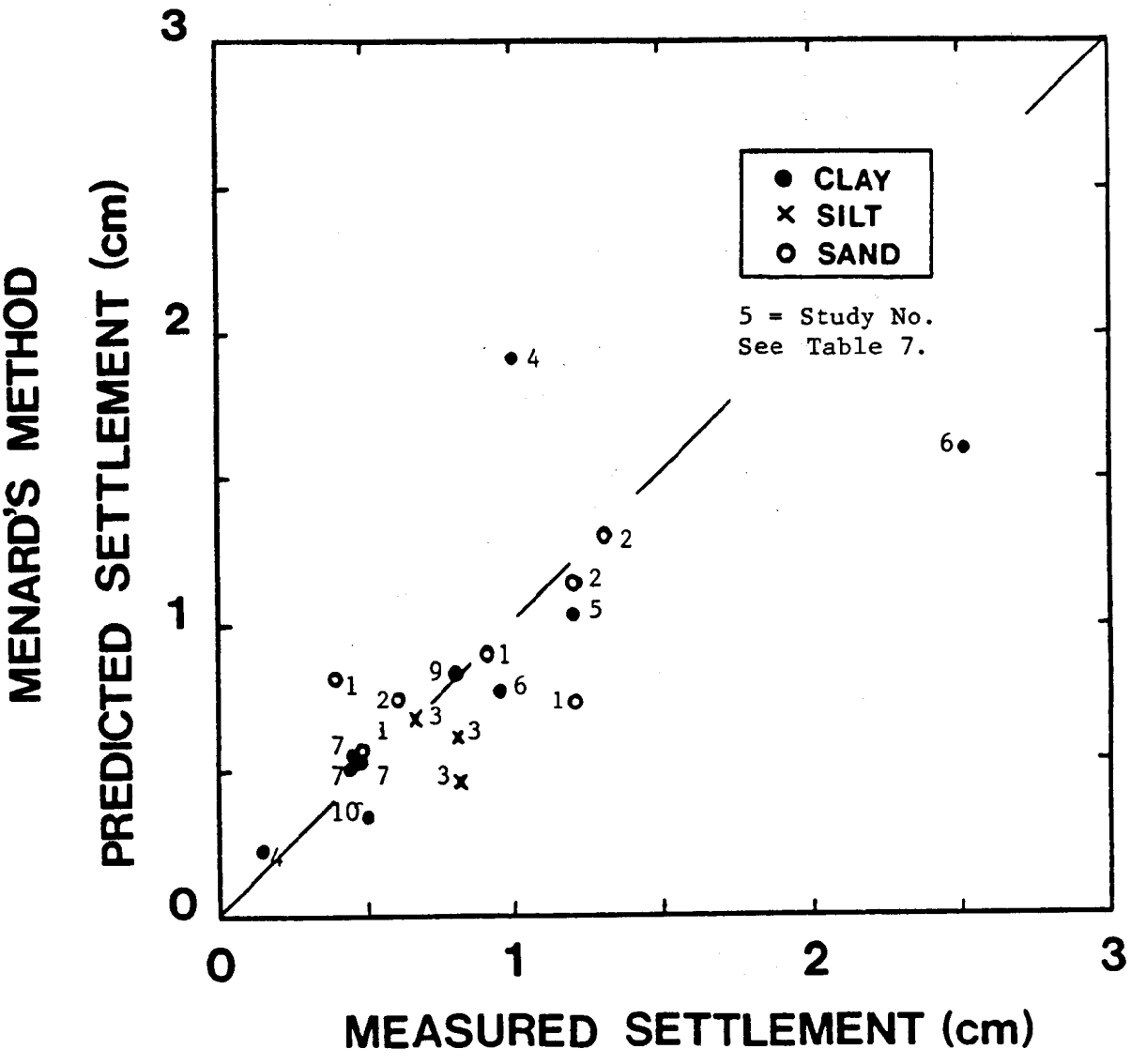

Figure 32. Measured settlement vs. predicted settlement by Menard's method, for data base 1.

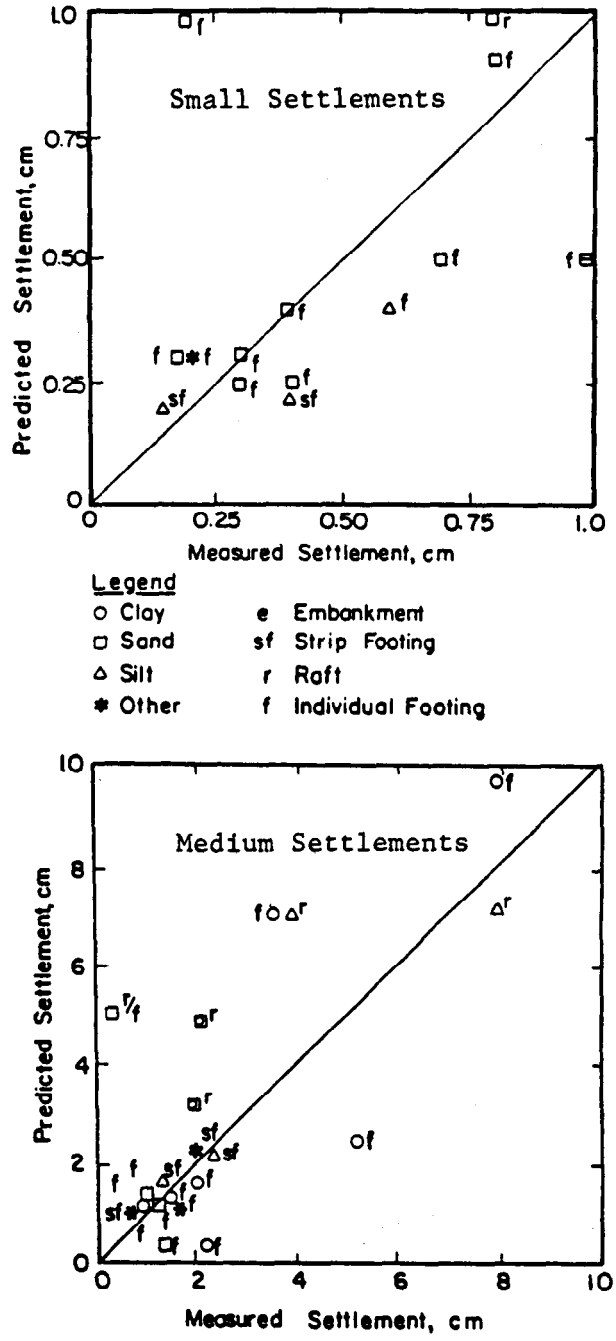

Figure 33. Measured settlement vs. predicted settlement by Menard's method, for data base 2.(10)

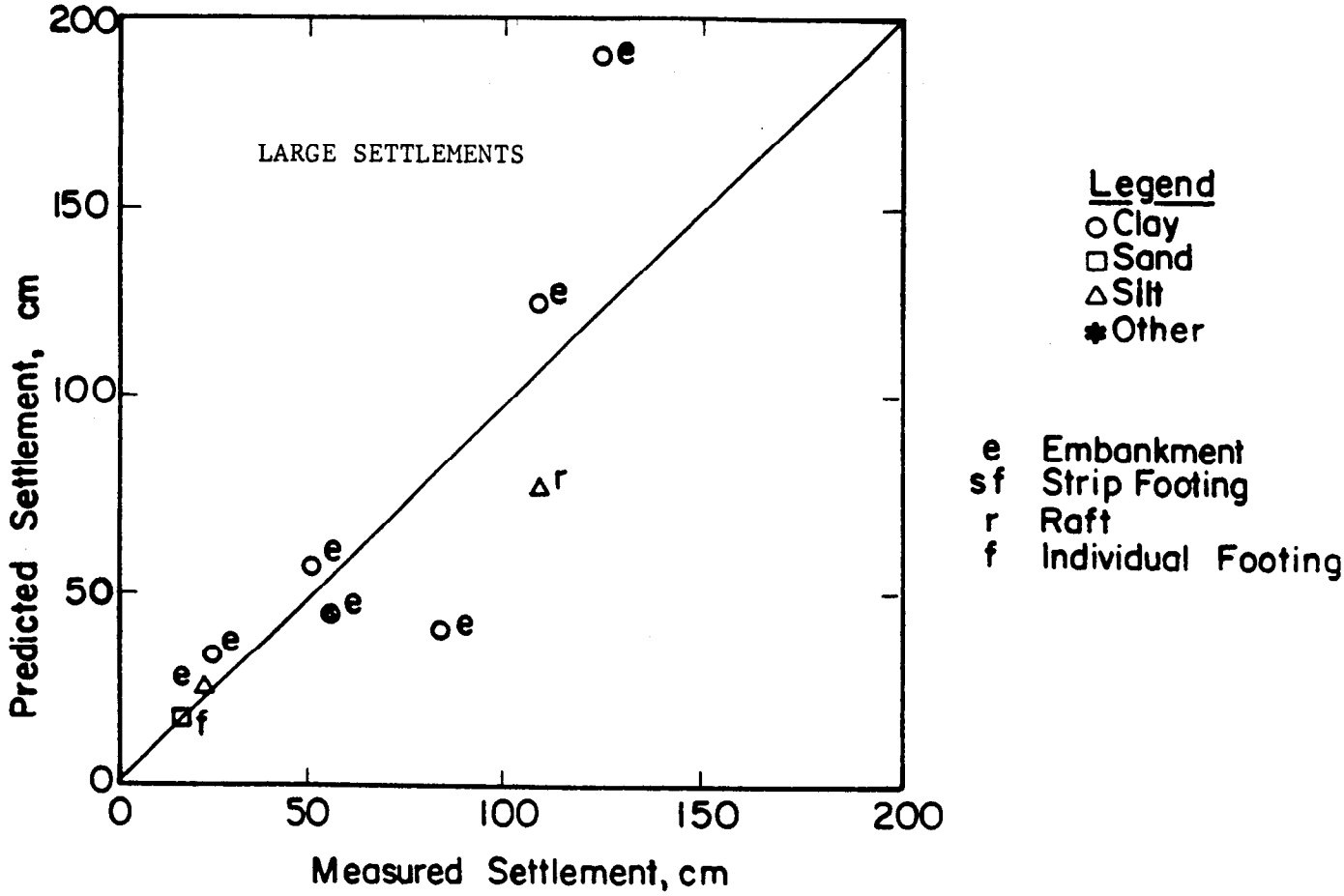

Figure 33. Measured settlement vs. predicted settlement by Menard's method (continued).

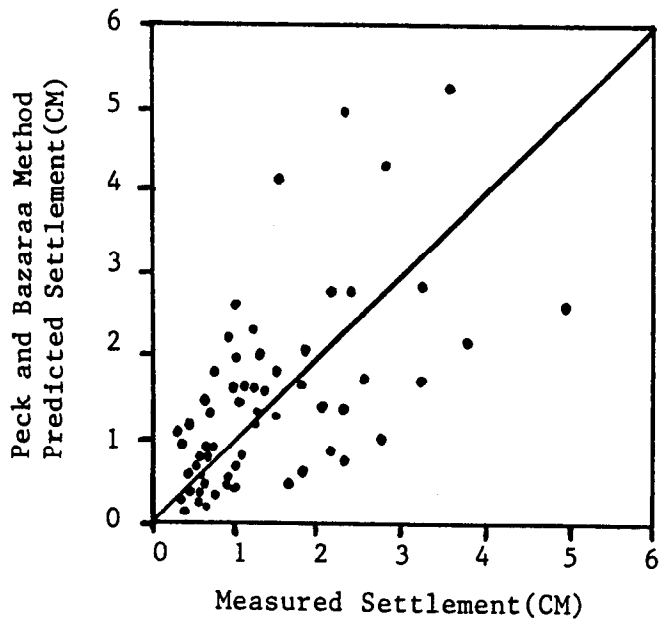

Figure 34. Measured settlement vs. predicted settlement by Peck and Bazaraa'S method.(52)

over a thin compressible layer where s_c will predominate, the consolidation test approach is to be favored. For footings on deep relatively uniform deposits where s_d will predominate, the pressuremeter test approach is to be favored.

7.7 Design Examples

EXAMPLE PROBLEM 1: RECTANGULAR FOOTING ON CLAY

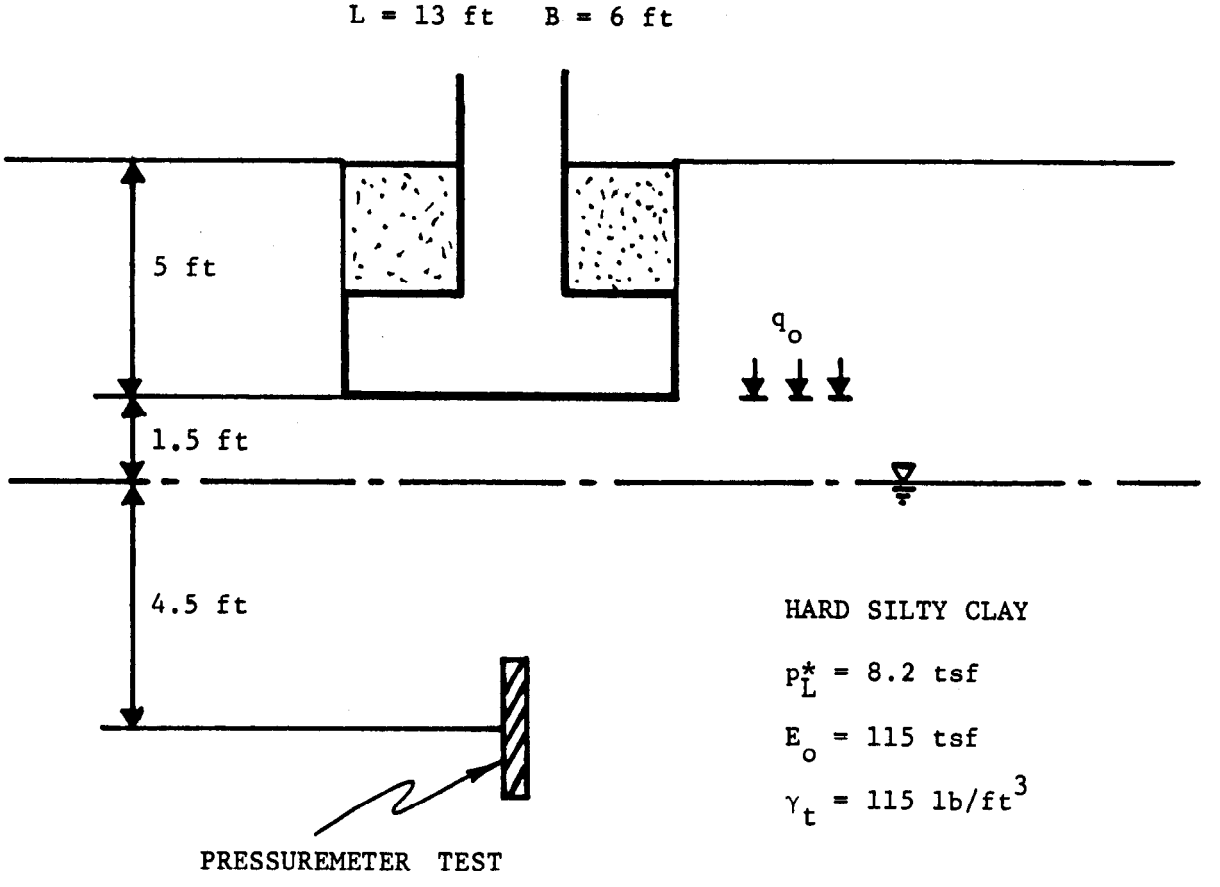

Figure 35. Example problem 1.

EXAMPLE 1 - Shallow Footing on a Clay (Figure 35)

Bearing Capacity

$q_L = k\ p^*_{Le} + q_o$

$p^*_{Le} = p^*_L$ $\quad$ He = 5.0 ft

B = 6 ft $\quad$ He/B = 0.83 $\quad$ B/L = 0.46

From Figure 20 : $\quad$ k(square footing) = 0.95

then, $\quad$ k(strip footing) = 0.95/1.2 = 0.79

and by interpolation,

$$k(B/L = 0.46) = 0.79 + 0.46 \times (0.95-0.79) = 0.86$$

$q_L = 0.86 \times 8.2 + (115 \times 5)/2000 = 7.34$ tsf.

$q_{safe} = 0.86/3 \times 8.2 + (115 \times 5)/2000 = 2.64$ tsf.

$q_{net} = 2.35$ tsf.

Settlement

$$s = \frac{2}{9E_d}\, q_{net}\, B_o \left[\lambda_d \frac{B}{B_o}\right]^{\alpha} + \frac{\alpha}{9E_c}\, q_{net}\, \lambda_c\, B$$

$E_d = E_c = 115$ tsf.

$E/p_L = 14$, then from Table 8 $\quad \alpha = 0.66$

$L/B = 2.2$. then from Figure 31 $\quad \lambda_c = 1.22$ and $\lambda_d = 1.58$

$$s = \frac{2}{9}\,\frac{1}{115} \times 2.35 \times 2.0 \times \left(1.58\,\frac{6.0}{2.0}\right)^{0.66} + \frac{0.66}{9 \times 115} \times 2.35 \times 1.22 \times 6.0$$

$s = 0.025 + 0.011 = 0.036$ ft = 0.43 in. < s(allowable) = 1 in.

therefore, $p_{all} = q_{safe} = 2.64$ tsf.

EXAMPLE PROBLEM 2: RECTANGULAR FOOTING ON LAYERED SOIL

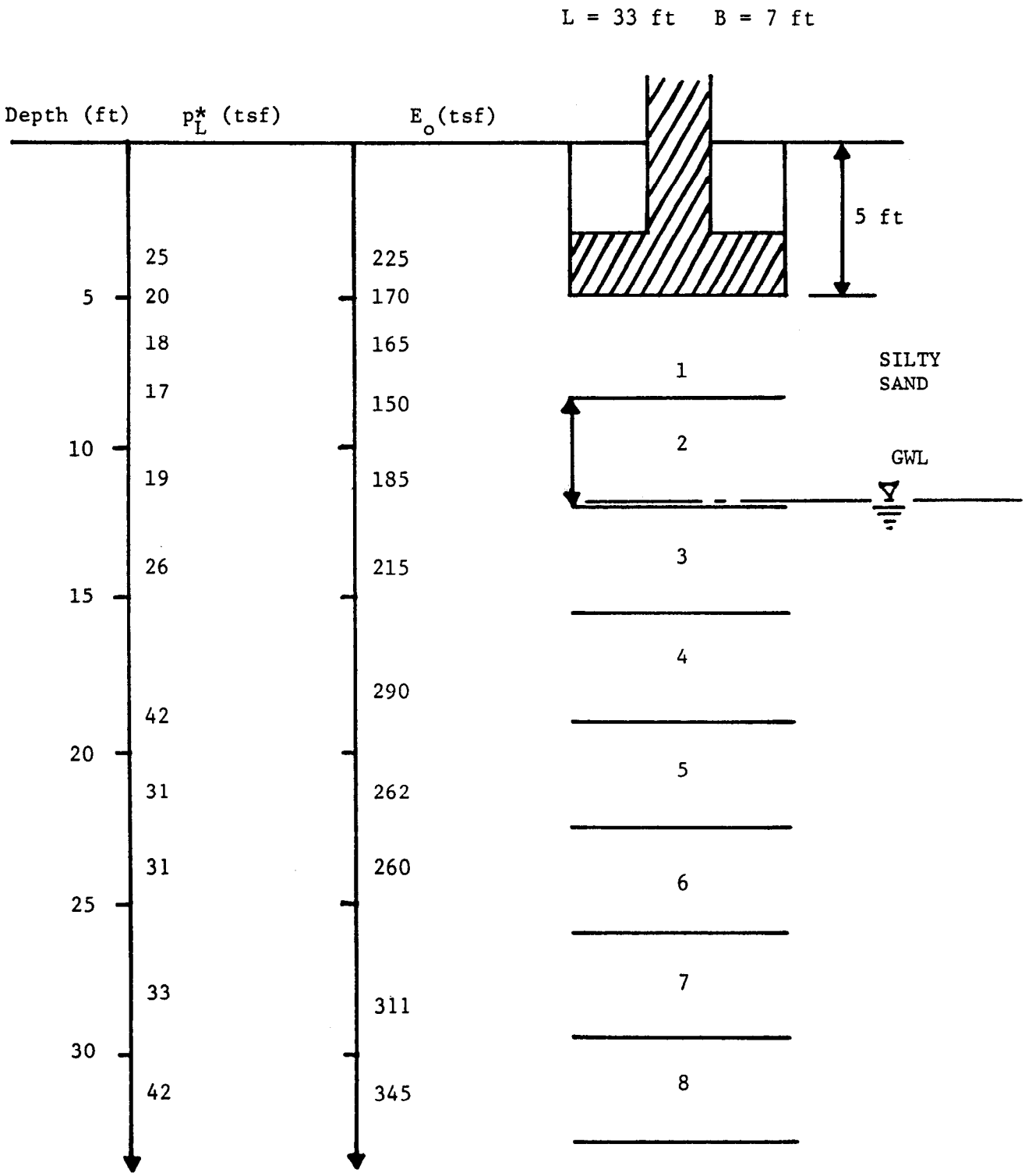

Figure 36. Example problem 2.

EXAMPLE 2 - Rectangular Footing on Layered Soil (Figure 36)

Bearing Capacity

$$q_L = k\ p^*_{Le} + q_o$$

where $p^*_{Le} = \sqrt[n]{p^*_{L1} \times p^*_{L2} \times \ldots \times p^*_{Ln}}$

= equivalent net limit pressure

5 values of p^*_L exist within the zone $\pm$ 1.5B above and below the footing depth.

$$p^*_{Le} = \sqrt[5]{25 \times 20 \times 18 \times 17 \times 19} = 19.6 \text{ tsf}$$

$$He = \frac{1}{p^*_{Le}}(p^*_{L1}\ z_1 + p^*_{L2}\ z_2 + \ldots + p^*_{Ln}\ z)$$

= equivalent embedment depth

1 value of p^*_L exists within the zone of embedment.

$$He = \frac{1}{19.6}\ (25 \times 5) = 6.4 \text{ ft.}$$

Determination of k,

He = 6.4 ft, B = 7 ft He/B = 6.4/7 = 0.91 B/L = 0.21

From figure 20: k(square footing) = 1.31

then k(strip footing) = 1.31/1.2 = 1.09

and by interpolation,

k(B/L = 0.21) = 1.09 + 0.21 (1.31 - 1.09) = 1.14

$q_L = 1.14 \times 19.6 + (12.4 \times 5)/2000 = 22.65$ tsf.

$q_{safe} = (1.14 \times 19.6)/3 + (124 \times 5)/2000 = 7.76$ tsf.

$q_{net} = 7.45$ tsf.

Settlement

$$s = \frac{2}{9E_d} q_n B_o \left(\lambda_d \frac{B}{B_o}\right)^{\alpha} + \frac{\alpha}{9E_c} q_n \lambda_c B$$

where E_c = harmonic mean of E's within layer 1

E_c = weighted average of E's from layers 1 - 16

E_c, $\frac{3}{E_c} = \frac{1}{170} + \frac{1}{165} + \frac{1}{150}$

$E_c = 161.2$ tsf

E_d, $E_1 = 161.2$ tsf

$$\frac{2}{E_2} = \frac{1}{150} + \frac{1}{185}$$

$E_2 = 165.7$ tsf

$$\frac{3}{E_{3/4/5}} = \frac{1}{215} + \frac{1}{290} + \frac{1}{262}$$

$E_{3/4/5} = 251.8$ tsf

$$\frac{3}{E_{6/7/8}} = \frac{1}{260} + \frac{1}{311} + \frac{1}{345}$$

$E_{6/7/8} = 301.2$ tsf

$E_{9/16}$ is taken as equal to $E_{6/7/8}$. This is conservative since the modulus appears to increase with depth.

$$\frac{4}{E_d} = \frac{1}{161.2} + \frac{1}{(0.85)\ 165.7} + \frac{1}{251.8} + \frac{1}{(2.5)\ 301.2} + \frac{1}{(2.5)\ 301.2}$$

$E_d = 200.7$ tsf

$$\frac{E_d}{p^*_{Le}} = \frac{200.7}{19.6} = 10.24$$

From table 8, $\alpha_d = 0.33$

$$\frac{E_c}{p^*_{Le}} = \frac{161.2}{19.6} = 8.22$$

From table 8, $\alpha_c = 0.33$

$$\frac{L}{B} = \frac{33}{7} = 4.7$$

From figure 31, $\lambda_d = 2.09$ and $\lambda_c = 1.38$

$$s = \frac{2}{9} \times \frac{7.45}{200.7} (2.0)(2.09 \frac{7.0}{2.0})^{0.33} + \frac{0.33}{9} \frac{7.45}{161.2} (1.38)(7.0)$$

$s = 0.032 + 0.016 = 0.048$ ft $= 0.58$ in.

EXAMPLE PROBLEM 3: FOOTING NEAR A SLOPE

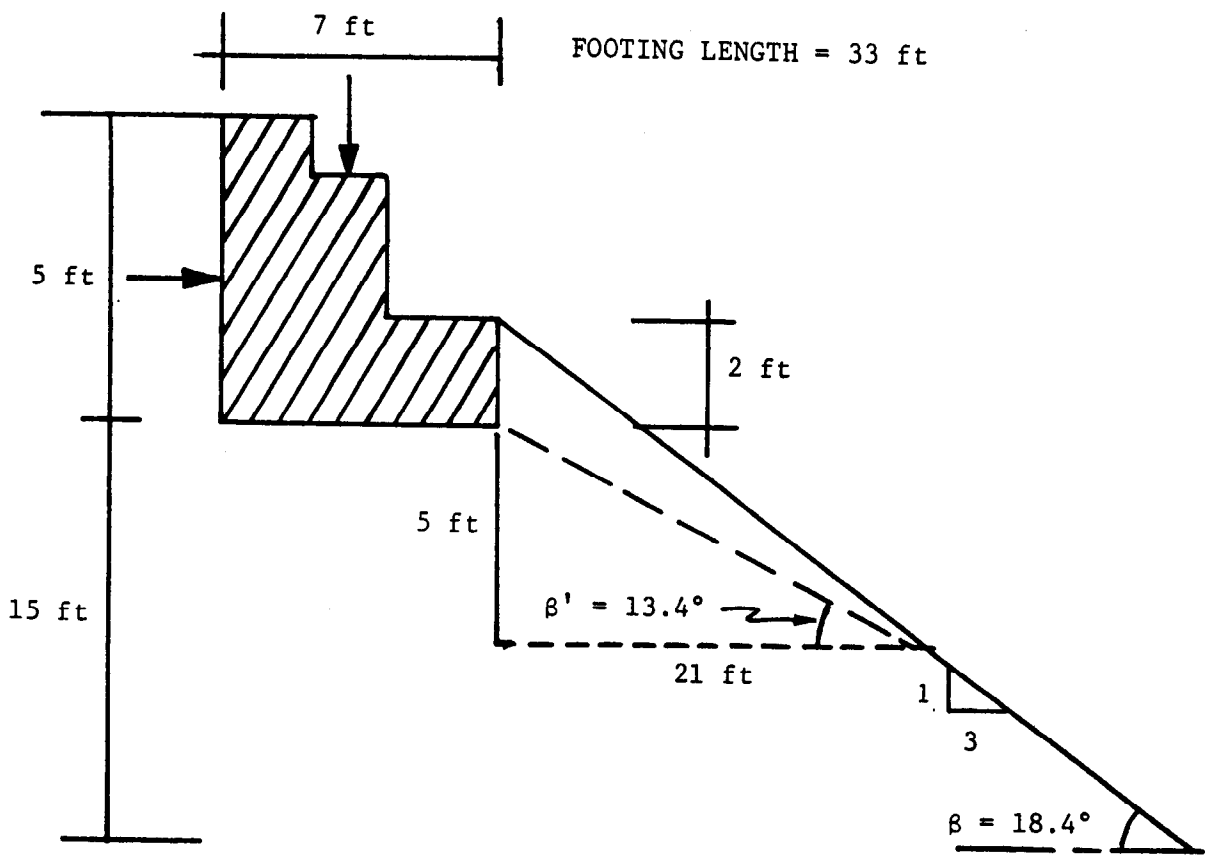

Pressuremeter data is the same as example problem 2.

Figure 37. Example problem 3.

EXAMPLE 3 - **Rectangular Footing with Inclined Load Near a Slope** (Figure 37).

The footing has been designed in such a way that the load will be centered. However the horizontal push from the backfill induces an inclination of 5° in the load. The case is therefore the one of a concentric inclined loading near a slope where the inclined load is directed towards the slope. In this case the reduction factor i_{is} is calculated by using equations 40 to 46 with the angle $\delta + \beta'$ instead of δ in the equations.

$$i_{is} = \left(1 - \frac{\delta+\beta'}{90}\right)^2 (1-\lambda) + \left(1 - \frac{\delta+\beta'}{20}\right) \lambda$$

$\delta = 5°$, $\beta' = 13.4°$ (see the figure)

$\lambda = \lambda_d \lambda_m$

$\lambda_d = 1 - D/B = 1 - 2/7 = 0.714$ because $0 < D/B < 1$

$\lambda_m = 1 - m = 1 - (p^*_L \text{ at } z = D)/(p^*_L \text{ at } z = D+B)$

$\lambda_m = 1 - 20/19 = -0.053$

$\lambda m = 0$ since $m > 1$

$\lambda = 0.714 \times 0 = 0$

$$i_{is} = \left(1 - \frac{5 + 13.4}{90}\right)^2 (1-0) + \left(1 - \frac{5 + 13.4}{20}\right) 0 = 0.633$$

The ultimate load for the footing on horizontal ground and embedded 2 ft into the soil was calculated separately to be $Q_u = 1600$ tons. Therefore the ultimate load for problem 5 is:

$Q_{uis} = 0.633 \times 1600 = 1013$ tons.

EXAMPLE PROBLEM 4 : RECTANGULAR FOOTING WITH SOFT LAYER

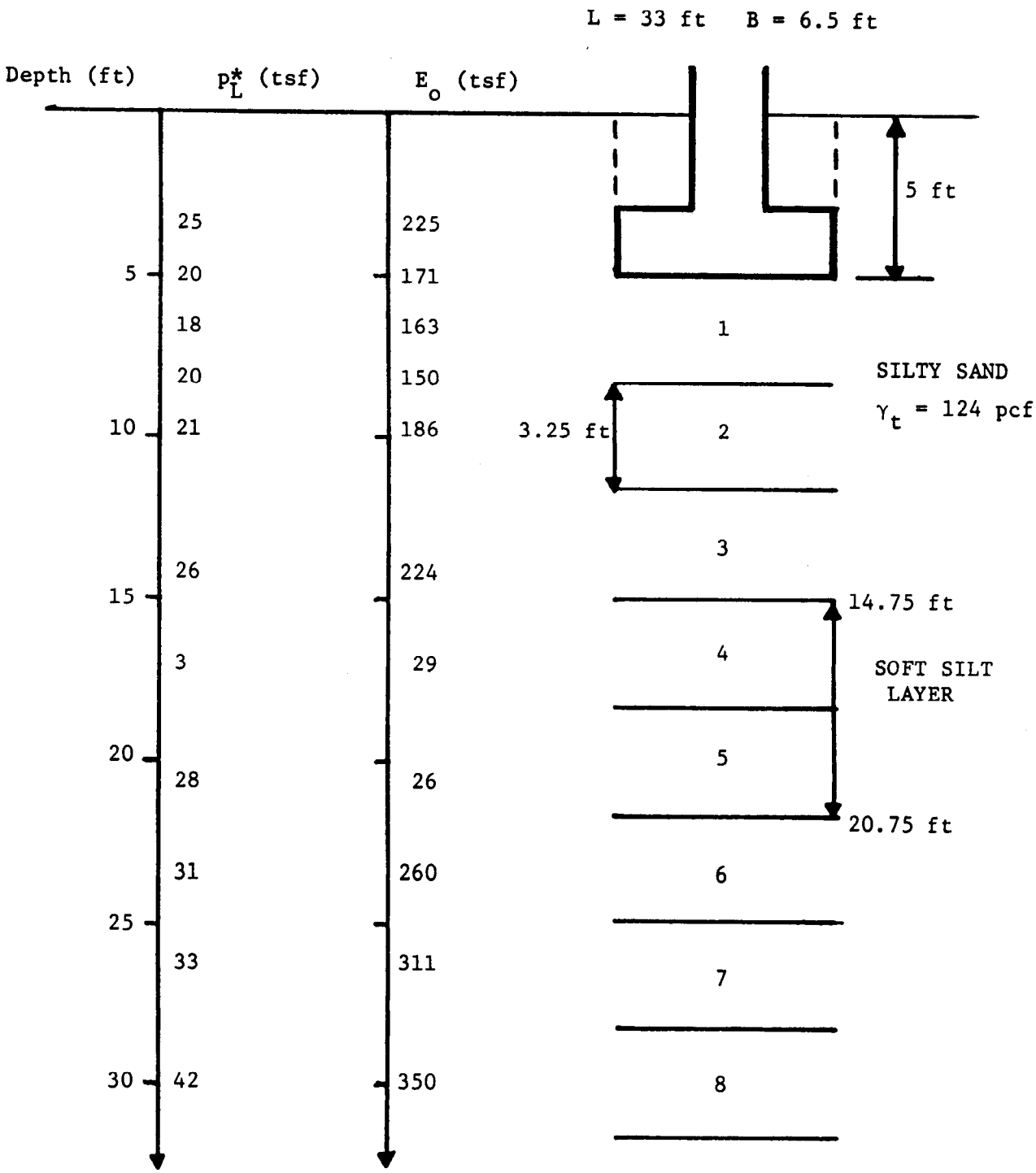

Figure 38. Example problem 4.

EXAMPLE 4 - **Rectangular Footing on a Soft Layer at Depth** (Figure 38).

Bearing Capacity

Estimate

$$q_{safe} = \frac{1}{3} k\, p^*_{Le} + q_o$$

$$q_{net} = q_{safe} - q_o = \frac{1}{3} k\, p^*_{Le}$$

$$\frac{B}{L} = \frac{6.5}{33.0} = 0.2 \qquad \frac{He}{B} = \frac{5.0}{6.5} = 0.77$$

Now, from fig. 20, k(square) = 1.21

$$k(\text{strip}) = \frac{1.21}{1.2} = 1.0$$

$$k\left(\frac{B}{L} = 0.2\right) = 1.0 + 0.2\,(1.21 - 1.0) = 1.04$$

Assume that p^*_{Le} is probably controlled by weak layer. (This is conservatively false.)

$$p^*_{Le} = (3 \times 2.8)^{1/2} = 2.9 \text{ psf}$$

$$q_{safe} = \frac{1}{3}(1.04)(2.9) + \left(\frac{5 \times 124}{2000}\right) = 1.30 \text{ tsf}$$

$$q_{net} = 1.0 \text{ tsf}$$

Settlement

Here: $s_T = s' + s''$

Where: $$s' = \frac{2}{9E_d} q_n B_o \left(\lambda_d \frac{B}{B_o}\right)^{\alpha} + \frac{\alpha}{9E_c} q_n \lambda_c B$$

$$s'' = \alpha \left(\frac{1}{E_c} - \frac{1}{E_m}\right) \Delta p_c H$$

Using the procedures already described, s' was calculated to be:

$$s' = 0.042 \text{ ft} = 0.50 \text{ in.}$$

Now consider the softness of the silt layer:

E_c = pressuremeter modulus of soft layer

$$\frac{2}{E_c} = \frac{1}{29} + \frac{1}{26}$$

$$E_c = 27.4 \text{ tsf}$$

$E_m = E_d$ (for the case where there is no soft layer)

E_d was calculated separately as 200 tsf

From Boussinesq theory and Newmark's chart, the vertical stresses at the upper and lower surfaces of the soft layer have changed by:

$z = 14.75$ ft $\quad \Delta\sigma_v = 0.24\ q_{net}$

$z = 20.75$ ft $\quad \Delta\sigma_v = 0.17\ q_{net}$

$q_{net} = 1.0$ tsf, therefore $(\Delta\sigma_v)$ at 14.75 ft = 0.24 tsf

and $(\Delta\sigma_v)$ at 20.75 ft= 0.17 tsf

Average $\Delta p = (0.24 + 0.17)/2$ 0.205 tsf

$$s'' = \alpha \left(\frac{1}{E_c} - \frac{1}{E_m}\right) \Delta p\ H$$

$$\frac{E_c}{p^*_L} = \frac{27.4}{2.9} = 9.5, \text{ from Table 3, silt } \alpha = 0.5$$

$$s'' = 0.5 \left(\frac{2}{27.4} - \frac{1}{200}\right) (0.205)(20.75 - 14.75)$$

$$s'' = 0.0194 \text{ ft} = 0.23 \text{ in.}$$

thus, $s_T = 0.50 + 0.23 = 0.73$ in.

EXAMPLE PROBLEM 5: MAT FOUNDATION ON A SOFT LAYER

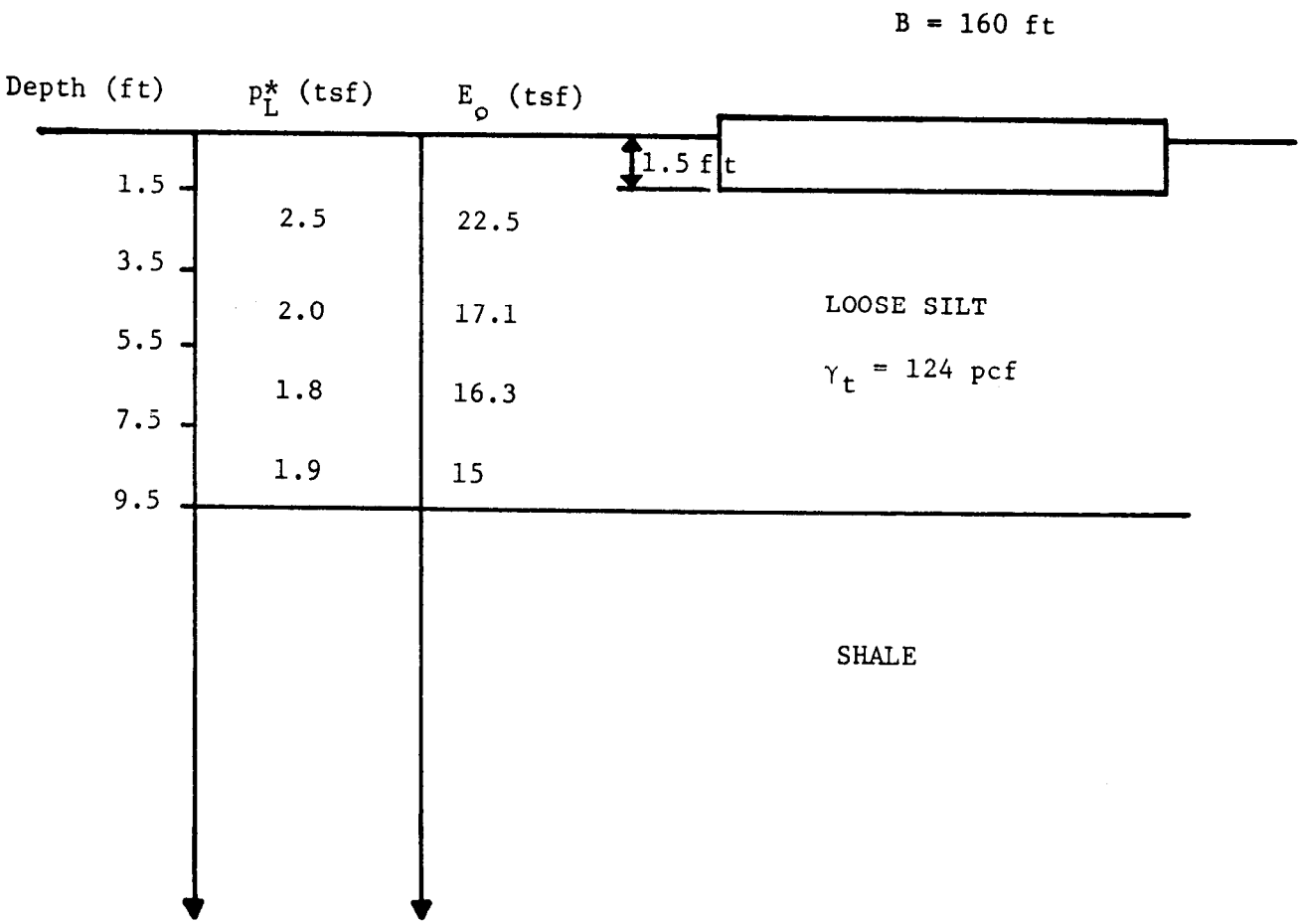

Figure 39. Example problem 5.

EXAMPLE 5- **Mat Foundation on a Soft Layer** (Figure 39).

Bearing Capacity

$$\text{Estimate } q_{safe} = \frac{1}{3} k\, p^*_{Le}\, q_o$$

$$q_{net} = \frac{1}{3} k\, p^*_{Le}$$

$$\text{Since } \frac{He}{B} \sim 0 \rightarrow k = 0.8$$

Assume that the silt layer controls bearing capacity; then let:

p^*_{Le} = average of the compressible layer

$$p^*_{Le} = (2.5 \times 2.0 \times 1.8 \times 1.9)^{1/4} = 2.03 \text{ tsf}$$

$$q_{safe} = \left(\frac{1}{3} \times 0.8 \times 2.03\right) + \left(\frac{124 \times 1.5}{2000}\right) = 0.63 \text{ tsf}$$

$$q_{net} = 0.54 \text{ tsf}$$

Settlement

For a wide foundation underlain by a soft layer (i.e. relatively thin, soft layer)

$$s = \int_o^h \frac{\alpha(z)\ \beta(F)\ p(z)}{E(z)}\, dz = \sum_1^n \frac{\alpha_i\ \beta_i\ p_i}{E_i}\, \Delta z_i$$

For silt layer:

$$\frac{E}{p^*_L} \sim 9, \text{ from table 8} \quad \alpha = 0.5$$

$$F = \text{safety factor} = \frac{k\, p^*_{Le}}{q_{net}}, \text{ where } k = 0.8$$

$$F = (0.8)\frac{2.03}{0.54} = 3.0$$

$$\text{thus, } \beta(F) = \frac{2}{3}\left(\frac{F}{F-1}\right) = \frac{2}{3}\left(\frac{3.0}{3.0-1.0}\right) = 1.0$$

Assume that Δp_v due to foundation loading is equal to actual foundation pressure since the layer of silt is thin compared to the foundation width.

Then: $$s = \sum \frac{\alpha\beta q_n}{E}\Delta z = \alpha\beta q_n \Sigma\left(\frac{\Delta z}{E}\right)$$

$$s = (0.5)(1.0)(0.54)\left(\frac{(3.5-1.5)}{22.5} + \frac{2.0}{17.1} + \frac{2.0}{16.3} + \frac{2.0}{15}\right)$$

$$s = 0.125 \text{ ft} = 1.5 \text{ in.}$$

8. DESIGN OF VERTICALLY LOADED PILES

8.1 Ultimate Load: Step-by-Step Procedure

A microcomputer program exists for automatic calculations.(101) This procedure follows the recommendations outlined in the "Regles de Justification des Fondations sur Pieux," published by the LCPC and the SETRA as an official French design document.

* Equation for ultimate point pressure q_L

$$q_L = k(p_{Le} - p_{OH}) + q_{ov} \tag{66}$$

where k is the bearing capacity factor

p_{Le} is the equivalent limit pressure (from test)

p_{OH} is the total horizontal stress at rest (from test)

p_{OV} is the total vertical stress at rest (calculated)

* Calculating the equivalent limit pressure p_{Le} (figure 40)

The equivalent limit pressure represents the average limit pressure in the homogeneous bearing layer near the point of the pile. A homogeneous layer is defined as a layer where the maximum limit pressure is not larger than 1.5 times the minimum limit pressure $p_{L\,min}$. In this case

$$p_{Le} = \frac{1}{2a}\int_{-a}^{+a} p_{L(z)}\,dz \tag{67}$$

If B is the pile equivalent diameter, the value of a is taken as:

$$a = 1.65 \text{ ft} \quad \text{if} \quad B \leq 3.3 \text{ ft} \tag{68}$$

$$a = B/2 \quad \text{if} \quad B > 3.3 \text{ ft} \tag{69}$$

The pile equivalent diameter is taken as:

$$B = \frac{4A}{P} \tag{70}$$

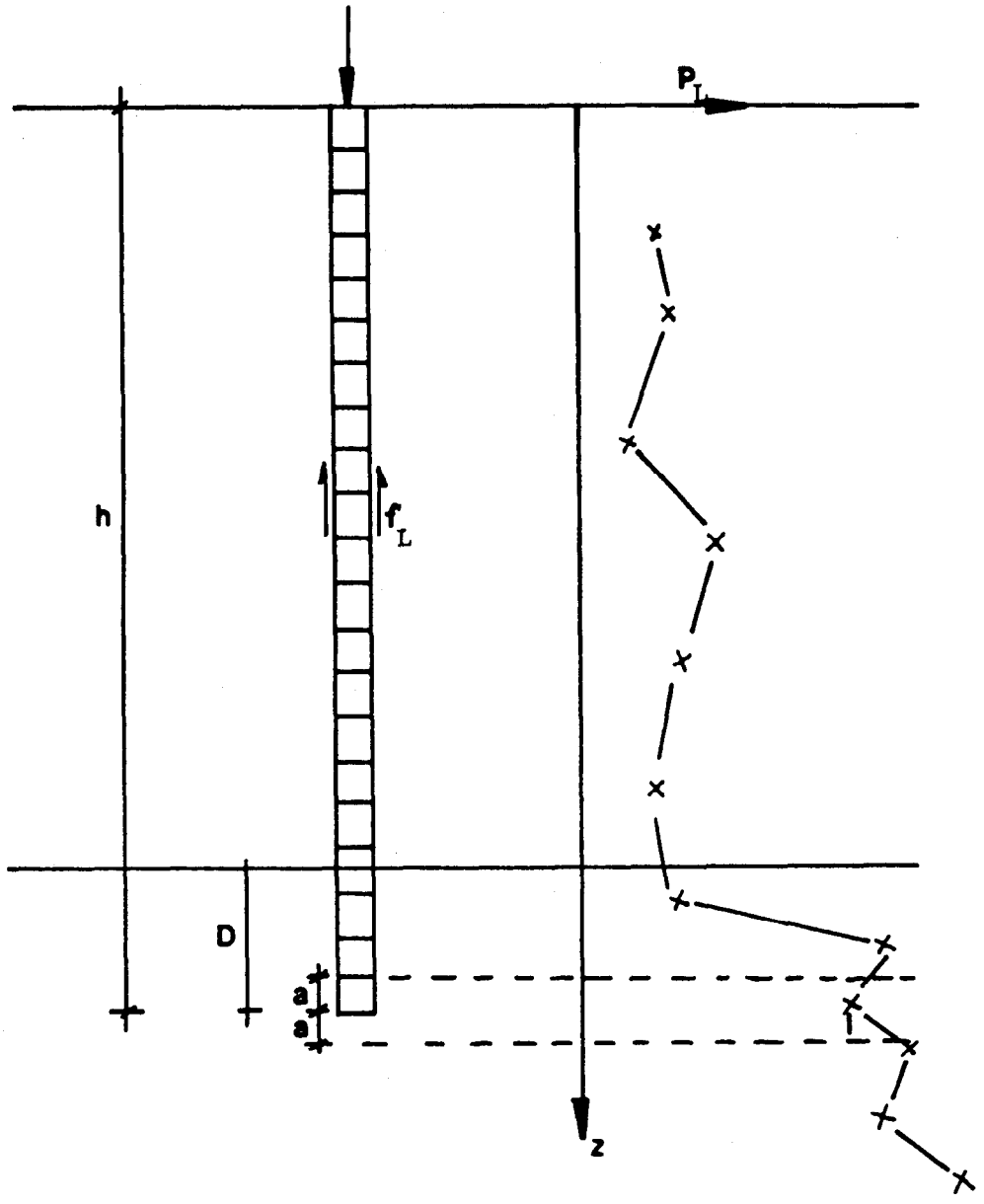

Figure 40. Parameters for determining the equivalent limit pressure for the point capacity.

where A and P are the area and perimeter of the pile cross section, respectively.

The quantity $\int_{-a}^{+a} p_{L(z)}\, dz$ is the area under the limit pressure versus depth profile obtained by joining the points on the profile. If the bearing layer is not homogeneous, a limit of 1.5 times $p_{L\,min}$ is imposed on the profile before applying equation 67. The value of a above is relatively small; one must ensure that the bearing layer is underlain by layers which are as strong or stronger. If weaker layers exist below the bearing layer, careful attention must be given to the influence of these weaker layers on the point resistance of the pile and the pile group. If the embedment D of the pile into the bearing layer is less than a, then p_{Le} is calculated as

$$p_{Le} = \frac{1}{a + D} \int_{-D}^{+a} p_{L(z)} dz \qquad (71)$$

* Determining k, the pressuremeter bearing capacity factor

The bearing capacity factor k is obtained from table 9. This k value is for a circular or square pile as opposed to a slurry trench wall used as a foundation element. For this "strip footing" type of deep foundations the k value is taken as the k of table 9 divided by 1.2. Interpolation is used for intermediary shapes.

The k values of table 9 are for full embedment of the pile in the bearing layer. The equivalent embedment D_e is defined as:

$$D_e = \sum_i \Delta z_i \frac{P_{Li}}{P_{Le}} \qquad (72)$$

where z_i are the thicknesses of the elementary layers corresponding to the p_{Li} values, p_{Li} are the limit pressures within the depth of embedment D in the bearing layer. Full embedment is considered to be achieved when:

$$D_e > 5B \qquad (73)$$

If not, the k values must be reduced to k (D_e/B) as follows:

$$k(D_e/B) = 0.8 + \left(\frac{k - 0.8}{25}\right)\frac{D_e}{B}\left(10 - \frac{D_e}{B}\right) \qquad (74)$$

where k is obtained from table 9.

* Calculating the point capacity

The ultimate point pressure is calculated using equation 66.

$$q_L = k(p_{Le} - p_{OH}) + q_{ov} \tag{75}$$

then the ultimate point load is:

$$Q_p = q_L A_p \tag{76}$$

where A_p is the area of the pile point. For open-end pipe piles the value of A_p is limited to one-half the value of Q_p obtained for the closed end pipe pile.

* Obtaining the ultimate unit friction, f_L

The value of f_L at a depth z is obtained as a function of the soil type, the pile type, and the limit pressure at the depth z. First table 10 is used to choose the proper curve on figure 41. Then figure 41 is used together with the limit pressure p_{Le} at depth z to obtain the ultimate unit friction f_L at that depth.

* Obtaining the ultimate friction load

The ultimate friction load Q_S is obtained by:

$$Q_s = P \int_o^h f_{L(z)} dz \tag{77}$$

where $f_{L(z)}$ is the profile of the ultimate unit friction versus depth, P is the pile perimeter and h the depth of embedment (figure 40).

* Obtaining the total ultimate load

$$Q_L = Q_p + Q_s - W_p \tag{78}$$

where W_p is the weight of the pile. The ultimate load Q_L is the load which corresponds to a settlement of the pile equal to one-tenth of the pile diameter. Note that for H piles, Q_L is taken as the smallest of the two values of Q_L obtained by considering that the pile fails along the soil-steel interface and by considering that the pile fails along the enclosing perimeter.

* Obtaining the safe load and the creep load

The safe load Q_{safe} is defined as:

$$Q_{safe} = \frac{Q_p + Q_s}{F} - W_p \tag{79}$$

Table 9. k values for piles
(after LCPC-SETRA, 1985).

	Piles with NO Soil Displacement	Piles with Full Soil Displacement
Clay-Silt	1.2	1.8
Sand-Gravel	1.1	3.2 to 4.2 (1)
Chalk-Marl Marly Limestone	1.8	2.6
Weathered or Fractured Rock	1.1 to 1.8 (2)	1.8 to 3.2 (2)

(1) Use 3.2 for dense sand or gravel (p_L > 30 tsf) and 4.2 for loose sand or gravel (p_L < 10 tsf). Interpolate in between.

(2) Data are limited. Treat the rock as the soil that might have a similar behavior.

Table 10. Choice of design curves for ultimate friction (after LCPC-SETRA, 1985).

PILE \ SOIL	CLAY/SILT	SAND	GRAVEL	CHALK	MARL/ MARLY LIMESTONE	WEATHERED OR FRACTURED ROCK
Drilled - Dry	Q1* Q2(2) Q3(3)			Q3* Q6*(2)	Q4* Q5(2)	Q6*
Drilled - with Mud	Q1* Q2(2)	Q1*(6) Q2	Q2(6) Q3	Q3* Q6*(2)	Q4* Q5(2)	Q6*
Drilled - with Casing (Casing retrieved)	Q1* Q2(4)	Q1*(6) Q2	Q2(6) Q3	Q3* Q4*(4)	Q4	
Drilled - with Casing (Casing left in place)	Q1	Q1	Q2	Q2	Q3*	
Caissons (1)	Q2 Q3(5)			Q4*	Q5	Q6*
Driven - Metal (Closed end)	Q1* Q2(5)	Q2	Q3	Q4	Q4	Q4*(7)
Driven - Concrete	Q2	Q3	Q3	Q4*	Q4*	Q4*(7)
Driven - Molded (10)	Q2	Q2*	Q3	Q4	Q4	
Driven - Coated (11)	Q2	Q3*	Q4	Q5*	Q4*	
Injected - Low Pressure	Q2*	Q3*	Q3*	Q5*	Q5*	Q6*
Injected - High Pressure (8)	Q5*	Q5*	Q6*	Q6*	Q6*	Q7*(9)

(1) Without casing left in place (rough contact).
(2) Reaming and grooving before pouring concrete.
(3) Reaming and grooving before pouring concrete, for very stiff clays only ($p_L \geq 15$ tsf).
(4) Drilling in the dry. without twisting the casing.
(5) Stiff clays ($p_L > 15$tsf).
(6) Long piles (> 100 ft).
(7) If driving is possible.
(8) Selective and repetitive injection at a low rate of flow.
(9) (8) and proper grouting of the fissured mass. Especially for micropile for which load tests are recommended.
(10) Driven closed-end casing; once at final penetration the casing is filled with concrete, the point is left in place and the casing is retrieved.
(11) Driven pipe or H pile with an oversize shoe (2 in. oversize); as the pile is driven, mortar is injected in the annulus.
* Probably conservative, but the friction cannot be increased without a verification by load testing.

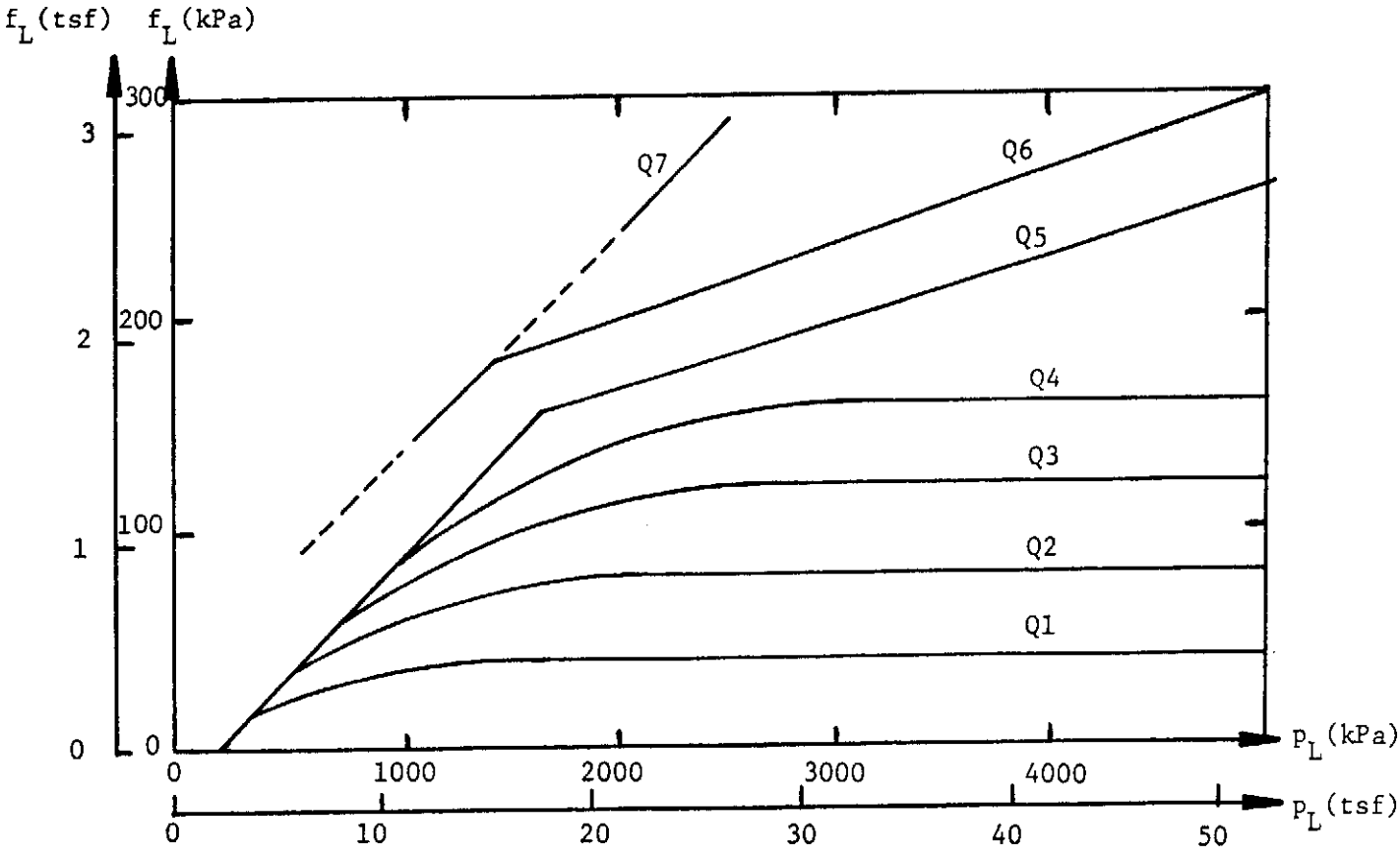

Figure 41. Ultimate unit friction on the shaft of a pile. See table 10 for choice of curve (after LPC-SETRA, 1985).

where F is a factor of safety. Using a pile load test data base Briaud and Tucker showed that for that data base and for a method very similar to the recommended method, a factor of safety of 2.8 would lead to a risk of failure of zero.(33) Risk was defined as the probability that the predicted ultimate load divided by the factor of safety is larger than the ultimate load measured in the load test. For a factor of safety of 2 the risk was 13.3 percent. A factor of safety of 2.8 is recommended.

The creep load Q_c is defined as the load beyond which the slope of the load-settlement curve for the pile starts to increase rapidly. Below Q_c the settlement is generally small and creep is limited. The load Q_c is given in the LCPC-SETRA document as:(61)

$$Q_c = \frac{Q_p}{2} + \frac{Q_s}{1.5} \quad \text{for bored piles} \tag{80}$$

$$Q_c = \frac{Q_p}{1.5} + \frac{Q_s}{1.5} \quad \text{for driven piles} \tag{81}$$

Examples of calculations are shown in section 8.5.

8.2 Ultimate Load: Precision of the Design Rules

Several comparisons have been made between measured and predicted ultimate loads using various pressuremeter methods.(14,15,18,20,21,23,26,33,35,41,47)

A data base of 51 pile load tests was assembled (table 11). These pile load tests were all performed in the United States between 1982 and 1987. Pressuremeter tests were performed next to those load tests and predictions were made for the ultimate capacity. The PMT method used for this data base is the earlier version of the method described in section 8.1.

The load settlement curve for each load test was used to determine the measured ultimate load, Q_m. The load Q_m was defined as the load reached for a settlement equal to one tenth of the diameter or equivalent diameter of the pile plus the elastic compression of the pile under Q_m ($D/10 + Q_M L/AE$). This load was not always reached during the load tests collected; only the piles where Q_m or a plunging load was reached (88% of the data) or where Q_m could be obtained with reasonable confidence by extension of the load test curve were used. Note in table 11 that, especially for piles in sand, at the ($D/10 + Q_L/AE$) settlement the tangent to the load-settlement curve did not indicate plunging failure. It is estimated that in those cases the true ultimate load was larger than the "D/10" ultimate load listed in table 11 by at least 20 percent.(35)

Table 11. Full scale vertical pile load tests.

Pile ID	Site	Pile Type	Pile Length (m)	Pile Diam. (m)	Load Test	Soil	Ult. Load Predicted (tons)	Measured Load at B/10 (tons)
1	L&D 26	HP 14x73	16.5	0.36	Tens	Sand/Grav	304	120**
2	L&D 26	HP 14x73	16.5	0.36	Comp	Sand/Grav	356	356**
3	L&D 26	HP 14x73	16.5	0.36	Tens	Sand/Grav	304	45
4	L&D 26	HP 14x73	16.2	0.36	Comp	Sand/Grav	350	430**
5	L&D 26	HP 14x73	16.2	0.36	Comp	Sand/Grav	380	320**
6	L&D 26	HP 14x73	16.8	0.36	Tens	Sand/Grav	313	130**
7	L&D 26	HP 14x73	18.0	0.36	Tens	Sand/Grav	338	180*
8	L&D 26	HP 14x73	21.1	0.36	Tens	Sand/Grav	405	150
9	L&D 26	HP 14x73	17.7	0.36	Tens	Sand/Grav	331	100**
10	L&D 26	HP 14x73	18.0	0.36	Comp	Sand/Grav	391	225
11	L&D 26	HP 14x73	12.2	0.36	Tens	Sand/Grav	223	50
12	L&D 26	Pipe	14.2	0.30	Comp	Sand/Grav	230	130**
13	L&D 26	Pipe	11.0	0.30	Tens	Sand/Grav	111	61
14	L&D 26	Pipe	14.4	0.36	Comp	Sand/Grav	284	125**
15	L&D 26	Pipe	11.1	0.36	Tens	Sand/Grav	132	68
16	L&D 26	Pipe	14.6	0.41	Comp	Sand/Grav	343	180**
17	L&D 26	Pipe	11.1	0.41	Tens	Sand/Grav	151	100
18	L&D 26	HP 14x73	11.9	0.36	Tens	Sand/Grav	185	130*
19	L&D 26	HP 14x73	11.3	0.36	Tens	Sand/Grav	172	90
20	L&D 26	HP 14x73	11.3	0.36	Tens	Sand/Grav	172	95
21	Miss.	Bored	12.5	0.36	Comp	Clay	93	124
22	Miss.	Sq. Conc	6.3	0.36	Comp	Clay	66	90
23	Miss.	Sq. Conc	7.6	0.46	Comp	Clay	176	120
24	Miss.	Sq. Conc	10.4	0.46	Comp	Clay	255	200*
25	Miss.	Sq. Conc	7.0	0.36	Comp	Sand	152	55
26	Miss.	Sq. Conc	7.1	0.36	Comp	Clay/Sand	75	100**
27	Miss.	Sq. Conc	8.6	0.36	Comp	Clay/Sand	93	67
28	Miss.	Sq. Conc	10.2	0.36	Comp	Clay/Sand	115	108
29	Miss.	Bored	10.6	0.36	Comp	Clay	138	130
30	MIss.	HP 12x53	19.1	0.30	Comp	Sand	113	154**
31	Miss.	Sq. Conc	16.0	0.36	Comp	Sand	243	120
32	Miss.	HP 12x53	12.4	0.30	Comp	Sand	58	58
33	Miss.	HP 12x53	8.6	0.30	Comp	Sand	37	35
34	Miss.	Sq. Conc	14.0	0.41	Comp	Clay/Sand	184	117
35	Miss.	Sq. Conc	16.4	0.41	Comp	Clay/Sand	283	143
36	L&D 2	HP 14x89	16.5	0.36	Comp	Clay/Sand	293	200**
37	L&D 2	HP 14x89	18.0	0.36	Tens	Clay/Sand	284	85
38	L&D 2	HP 14x89	19.5	0.36	Comp	Clay/Sand	366	250**
39	L&D 2	Sq. Conc	16.2	0.41	Comp	Clay/Sand	213	220
40	L&D 2	Sq. Conc	19.7	0.41	Comp	Clay/Sand	266	230
41	L&D 2	Sq. Conc	22.7	0.41	Comp	Clay/Sand	325	325*
42	L&D 2	HP 14x73	15.9	0.36	Tens	Clay/Sand	240	100
43	L&D 2	HP 14x73	18.3	0.36	Tens	Clay/Sand	287	60
44	LADWP	Bored	2.9	0.66	Tens	Clay	19	55
45	LADWP	Bored	2.9	0.64	Tens	Clay	18	55
46	LADWP	Bored	4.4	0.66	Tens	Clay	46	85
47	LADWP	Bored	2.9	0.71	Tens	Sand	79	125*
48	LADWP	Bored	2.2	0.75	Tens	Sand	61	75
49	Lackland	Bored	10.5	0.46	Comp	Clay	121	170*
50	U of Hous	Driven	13.1	0.27	Comp	Clay	55	80
51	U of Hous	Bored	2.36	2.41	Comp	Clay	252	336
52	Hous Ship	Bored	30.5	0.91	Comp	Sand/Clay	989	965
53	Hous Ship	Sq. Conc	30.5	0.51	Comp	Sand/Clay	689	850?
54	Hous Ship	Pipe	36.9	0.61	Comp	Sand/Clay	393	650?

* Load test curve extended to B/10 + Q_mL/AE with reasonable confidence.
** Slope at B/10 + Q_mL/AE does not indicate plunging failure; true ultimate load most probably higher than load listed in table by at least 20%.

Table 11. Full scale vertical pile load tests (continued).

Pile I.D.	References
1 to 20	Corps of Engineers, St. Louis District and Tucker, Briaud, 1987
21 to 32	Mississippi State Highway Department and Briaud et al., 1986
36 to 43	Corps of Engineers, Vicksburg District and Briaud Engineers, 1984
44 to 48	Los Angeles Department of Water and Power, Earth Technology Corporation, and Briaud et al., 1984
49	U.S. Army Engineers Waterways Experiment Station, and Briaud Engineers, 1982
50, 51	O'Neill et al., 1980, O'Neill, Sheikh, 1985, and Briaud, Riner, 1984
52 to 54	Texas State Department of Highways and Public Transportation, McClelland Engineers and Briaud Engineers, 1986

The predictions were performed automatically by using an IBM-PC computer program written for that purpose. For the H piles the ultimate pile capacity was calculated first by using the steel-soil contact areas for point and shaft resistance, Q_{U1}, and second by using the enclosing rectangular areas for point and shaft resistances, Q_{U2}. For these H piles the predicted ultimate load was considered to be the lowest of the two loads Q_{U1} and Q_{U2}. In all cases Q_{U2} was smaller than Q_{U1}. Note that Q_{U2} corresponds to a plugged condition where a soil plug exists between the flanges of the H piles.

Figure 42 shows predicted versus measured ultimate loads for compression tests. On the average the method overpredicted the measured loads by 20 percent. However, as was mentioned earlier, for a significant number of piles (table 11) no plunging failure was reached at a settlement of $D/10 + Q_m L/AE$ and the true ultimate load for those piles was estimated to be at least 20 percent larger. Therefore if the true ultimate load had been measured and plotted on figure 42 instead of the $(D/10 + Q_m L/AE)$ ultimate load, the overprediction of the PMT method would have been lower.

Figure 43 shows predicted versus measured ultimate load for tension tests. On the average the method overpredicts the measured loads by a factor of 2.5. However almost all the tension tests in the data base were performed on H piles and there is evidence showing that for H piles the friction in tension is approximately one-half of the friction in compression; this may explain in part the overprediction of the PMT method.(35,23) Indeed, if the H piles are ignored on figure 43, the few other piles (3 pipe piles and 5 bored piles) do not show the overprediction trend.

Inspection of figure 42 shows that for compression loading the use of a factor of safety of 2.8 may be appropriate to determine the design working load. Indeed for this data base this would ensure that at the design working load none of the piles would be loaded to failure and that the design working load would be on the average one-half the measured $(D/10 + Q_m L/AE)$ ultimate load.

8.3 Settlement: Method

A microcomputer program PILPMT exists for automatic calculations.(101) The settlement of a single pile at half the ultimate load is always quite small. Another data base study was performed on 98 pile load tests.(33) For each full scale pile load test the following settlement was calculated:

$$s_a = s_m - 0.5\frac{QL}{AE} \qquad (82)$$

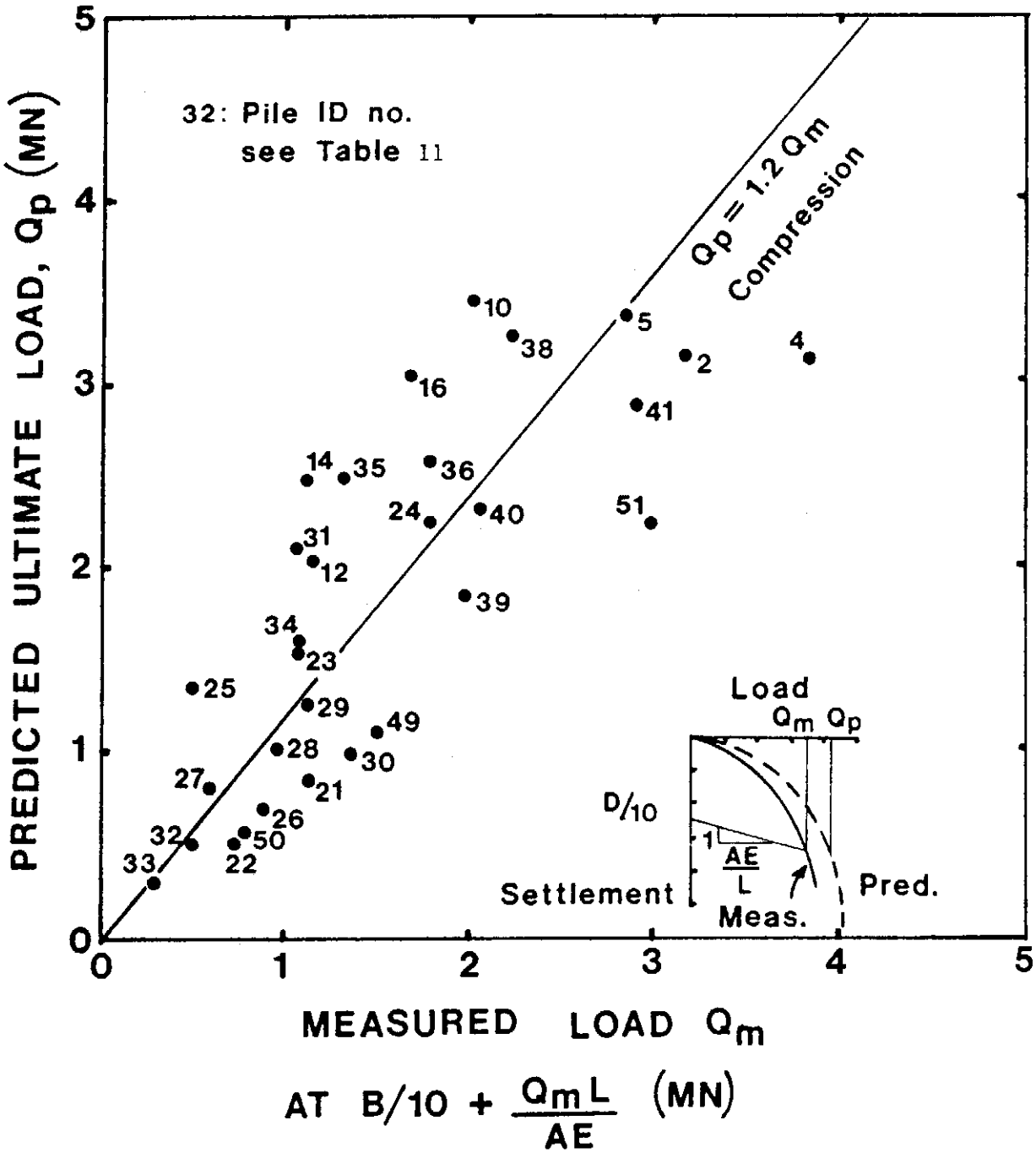

Figure 42. Predicted vs. measured ultimate loads for compression tests.

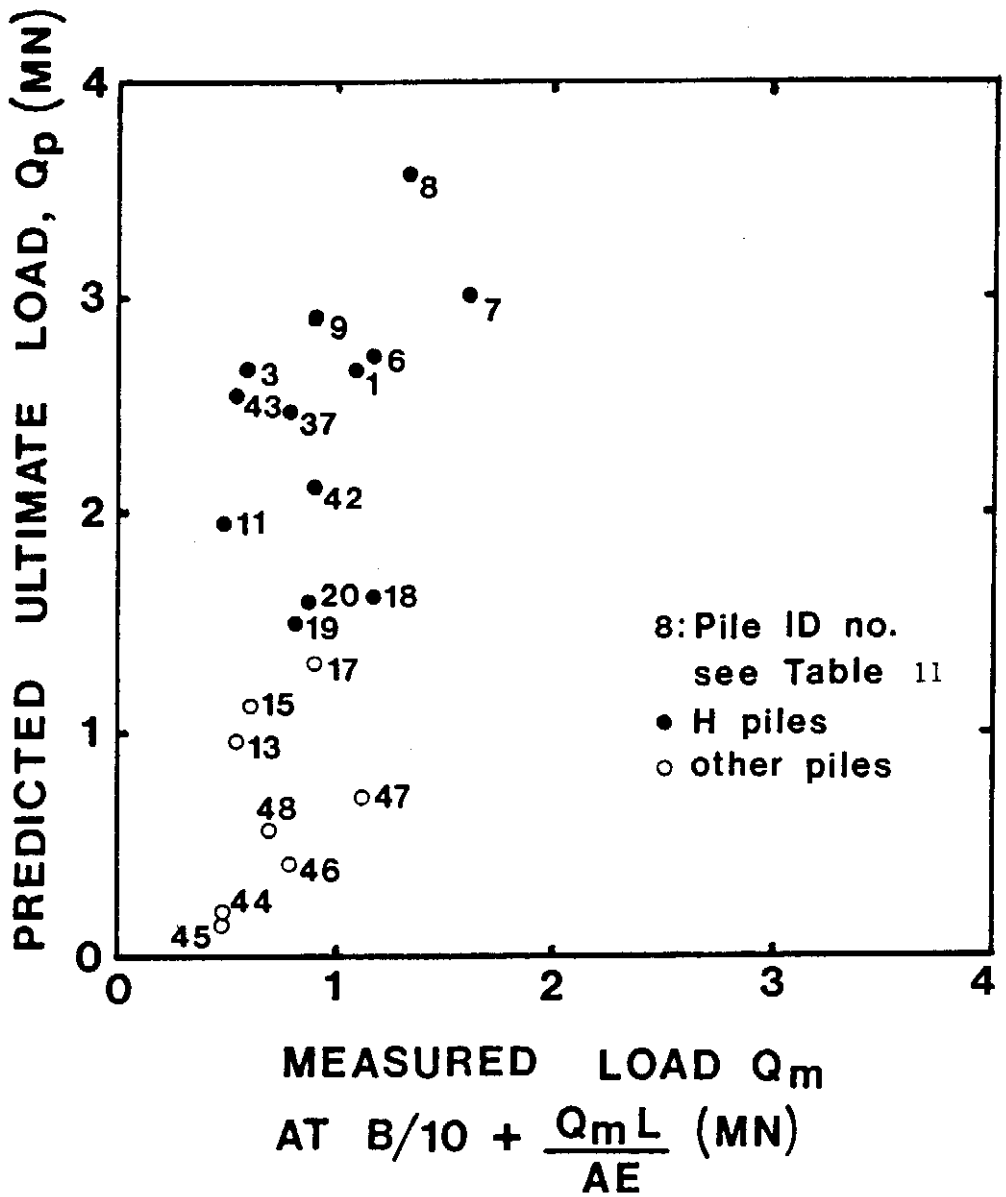

Figure 43. Predicted vs. measured ultimate loads for tension tests.

where s_a is the adjusted settlement, s_m is the measured settlement at one-half the measured ultimate load, Q is one-half the measured ultimate load, L is the embedded length of the pile. A is the pile cross section area, E is the pile modulus of elasticity. Equation 82 assumes that, at one-half the measured ultimate load, the load in the pile decreases linearly from one-half the measured ultimate load at the ground surface to zero at the pile point. A relative frequency plot of the ratio of S_a / B where B is the pile diameter is shown on figure 44 together with the mean and standard deviation of S_a / B. The log-normal distribution based on this mean and standard deviation is also shown and fits the data quite well. Based on this distribution there is a 95 percent probability that the adjusted settlement will be 1.25 percent of the pile diameter or less or that the settlement will be 1.25 percent of the pile diameter plus QL/AE or less.

The LCPC-SETRA document (1985) makes the following recommendations for calculating the pile settlement, s, at working loads:

$$s = 0.006B \quad \text{for} \quad \text{bored} \quad \text{piles} \tag{83}$$

$$s = 0.009B \quad \text{for} \quad \text{driven} \quad \text{piles} \tag{84}$$

where B is the pile diameter. One should add the elastic shortening of the pile (QL/AE) if the pile is long.

The complete load-settlement curve at the top of the pile can be generated if the q-w curve and the f-w curves are obtained. The q-w curve is the load transfer curve at the tip of the pile, where q is the average point pressure developed for a pile tip movement w. An f-w curve is a load transfer curve along the shaft of the pile where f is the pile soil friction developed for a pile shaft movement w.

The recommended method models the f-w and q-w curves as elastic-plastic models. The method evolved from the method proposed by Baguelin et Al.[10] The recommended slope for the f-w curve is $E_R / 2R(1+\upsilon)(1+\text{Ln}(L/2R))$ where E_R is the unload-reload pressuremeter modulus, R the pile radius, υ Poisson's ratio for the soil, L the embedded length of the pile (figure 45). The slope for the q-w curve is $2E_R/(1-\upsilon^2)R$ for driven piles and $2E/(1-\upsilon^2)R$ for drilled shafts where E is the first load pressuremeter modulus. These slopes correspond to the equation for the settlement of a rigid plate at the surface of an elastic half space and therefore makes the reasonable assumption that the decrease in settlement due to the embedment of the pile point is offset by the increase in settlement at the pile point due to the shear stresses in the soil induced by the pile shaft friction (figure 45).[88] Note that the q-w

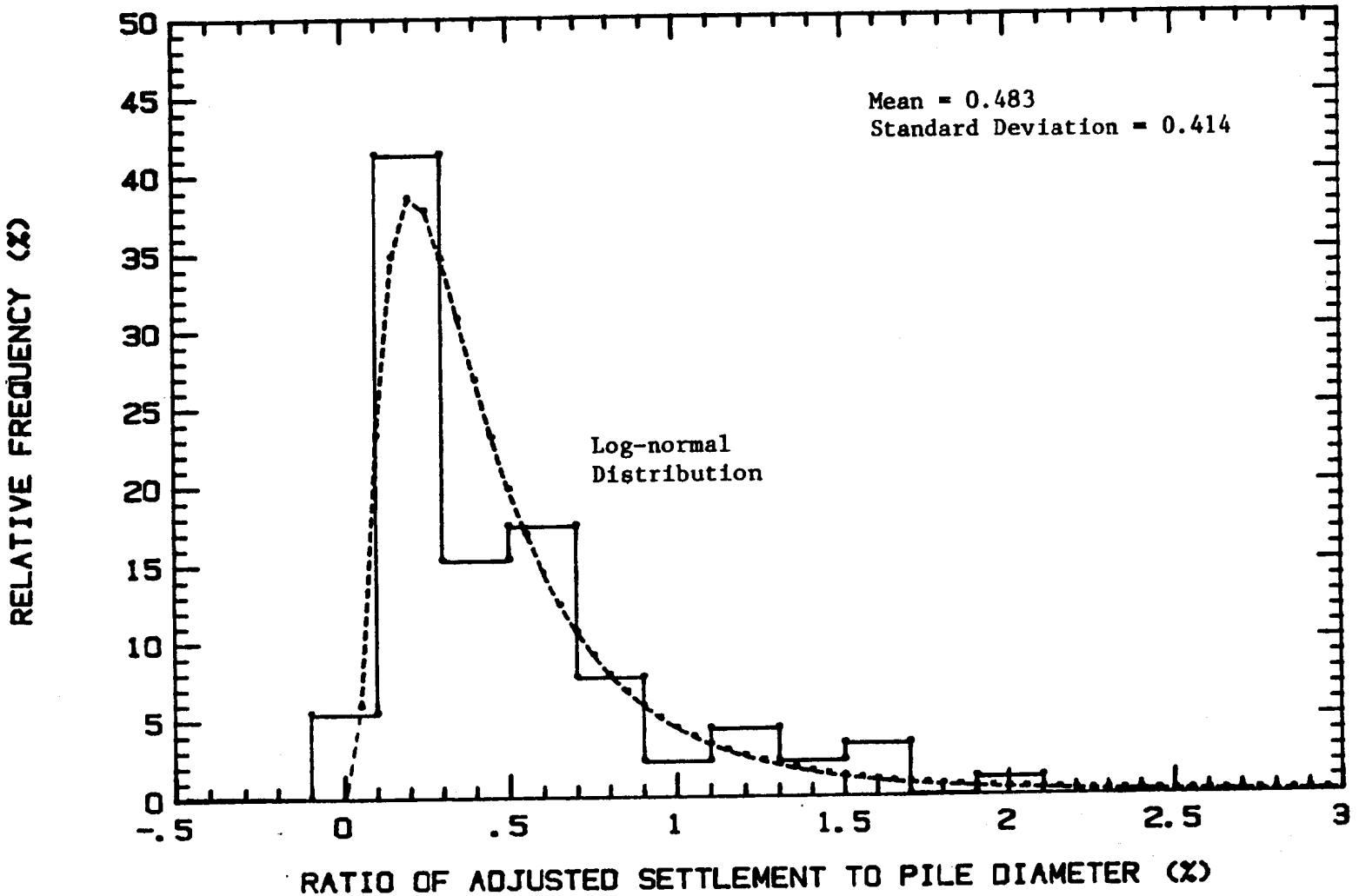

Figure 44. Relative frequency plot of the ratio of settlement to pile diameter for 98 piles.

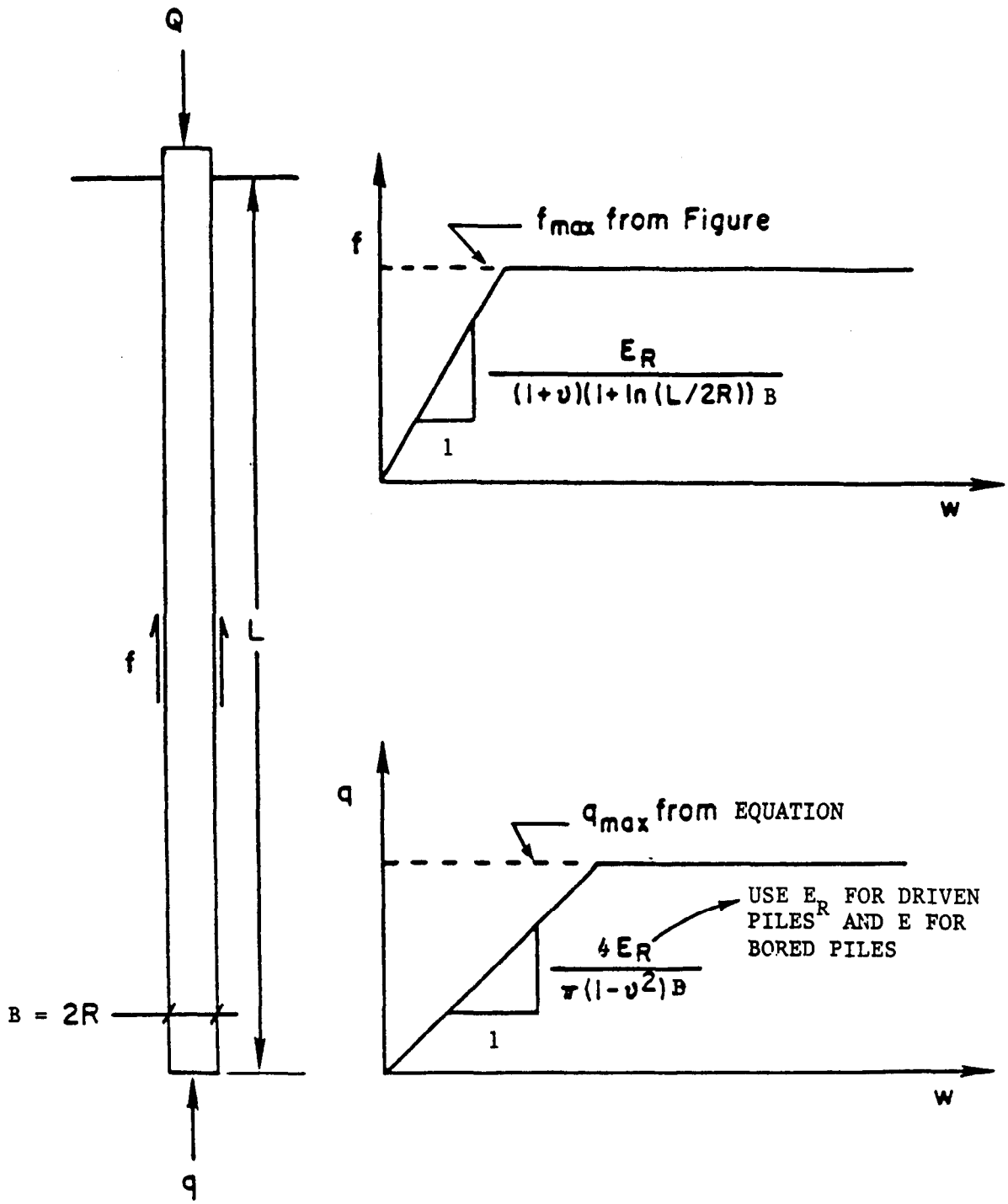

Figure 45. Load transfer curves from pressuremeter data.

E_R is used for driven piles. If the bottom of the hole for the drilled shaft was bored cleanly and if it was cleaned thoroughly before pouring the concrete, it may be possible after careful evaluation of the soil type to use E_R for the q-w curve of drilled shafts.

Examples of settlement calculations are given in section 8.5.

8.4 Settlement: Precision of the Design Rules

The method above was used to develop the complete load settlement curve for the piles of the data base (table 11). Then a factor of safety of 2.5 was applied to the predicted ultimate load. This gave the design working load. The predicted and measured settlements were obtained at the design working load; they are plotted on figure 46. Only the compression pile load tests are considered because of the problems associated with the tension tests on H piles. As can be seen the predictions compare favorably with the measured values. The settlement magnitude of these single piles is very small since it averages 2.5 mm (0.1 in).

8.5 Design Examples

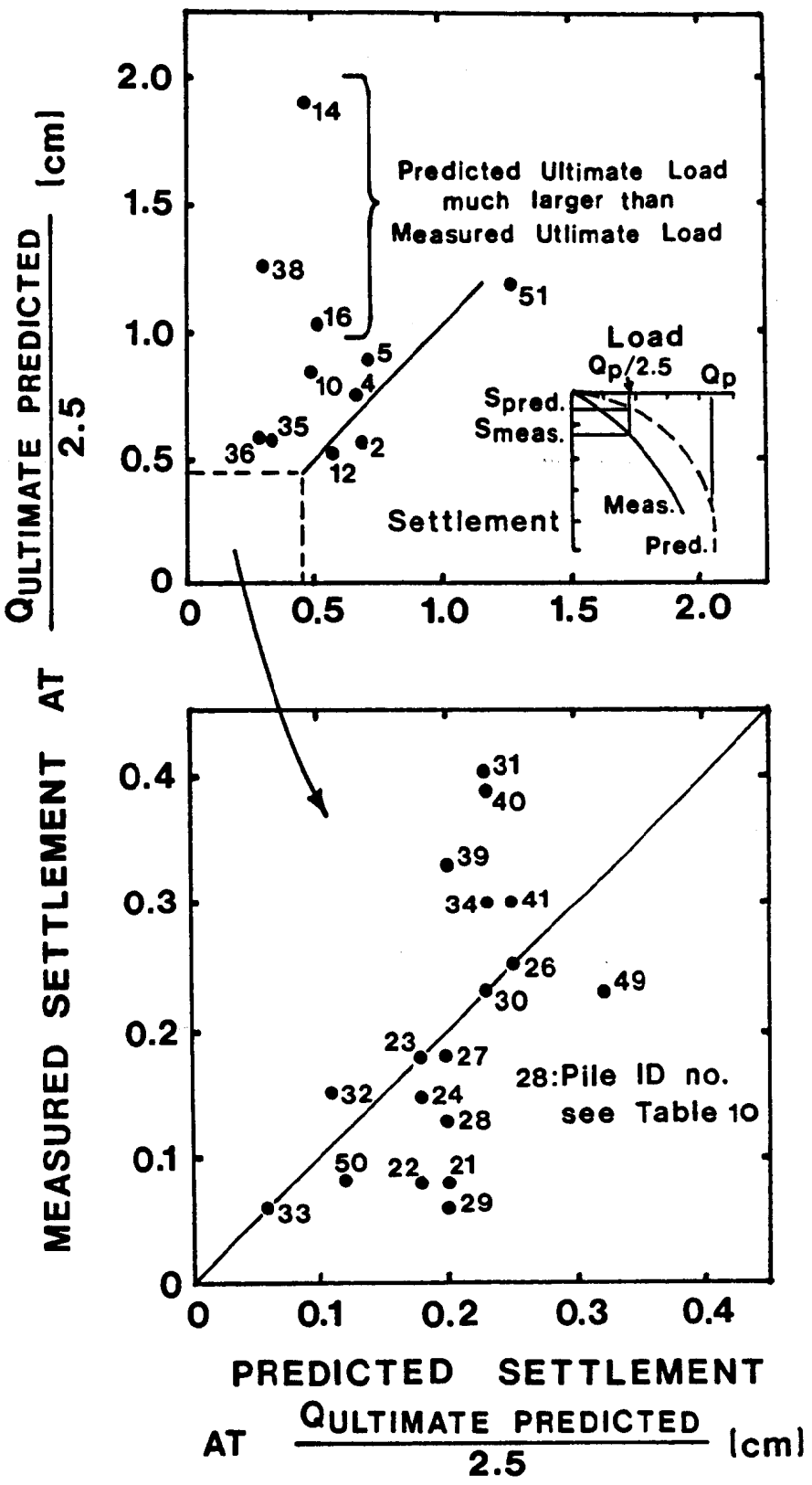

Figure 46. Predicted vs. measured settlement at 1/2.5 the predicted ultimate load.

EXAMPLE 1: PILE IN CLAY

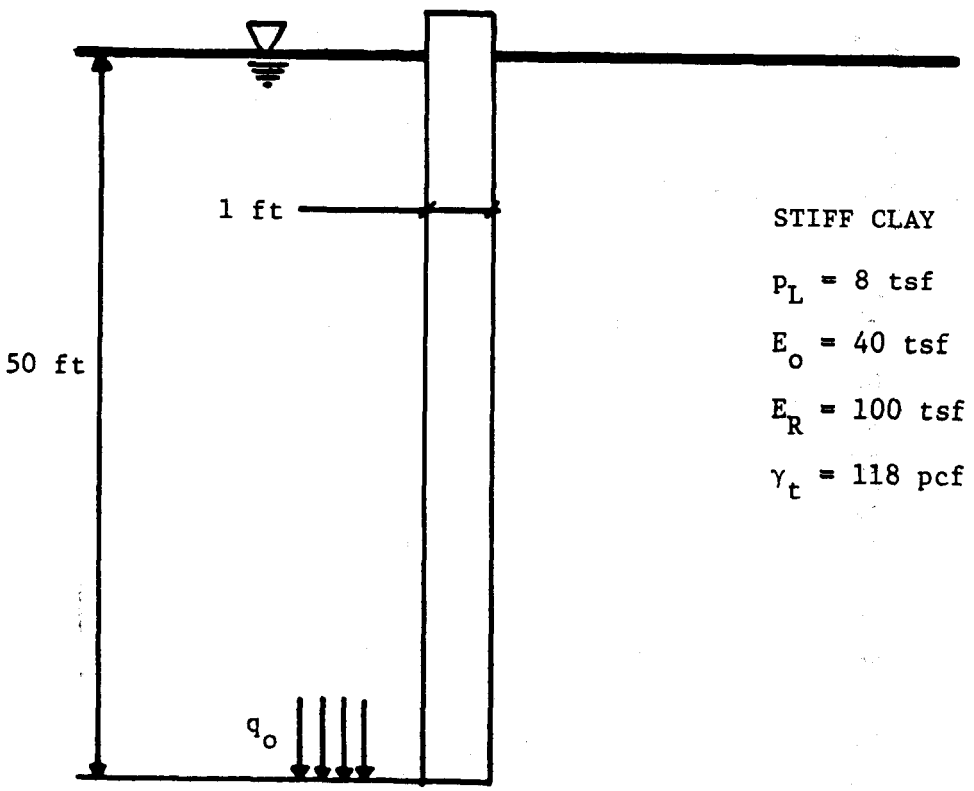

BORED CONCRETE PILE

(DRILLED SHAFT, DRILLED DRY)

Figure 47. Example 1.

EXAMPLE 1 : ULTIMATE CAPACITY

Point

Since the soil is uniform $p_{Le} = p_L = 8$ tsf, p_{OH} obtained from the test at 50 ft depth is 2.1 tsf. From table 8, no displacement pile, clay, k = 1.2.

$$q_L = k(p_{Le} - p_{OH}) + q_{ov}$$

$$= 1.2 \times (8 - 2.1) + 50 \times \frac{118}{2000} = 10.0 \text{ tsf}$$

$$Q_p = A_p \cdot q_L = \pi \times 0.5^2 \times 10 = 7.85 \text{ tons}$$

Side

From table 9, the pile is drilled dry and therefore curve Q1 is used. Note that if reaming and grooving is ensured before pouring concrete curve Q_2 can be used. From figure 84 and for p_{Le}, curve Q_1 leads to an f_L value of:

$$f_L = 0.31 \text{ tsf}$$

$$Q_s = A_s \cdot f_L = \quad \times 1 \times 50 \times 0.31 = 48.7 \text{ tons}$$

Total Capacity

$$Q_L = 7.85 + 48.7 \times 56.5 \text{ tons}$$

total recommended load at the ground surface is

$$Q = \frac{Q_L}{2.8} - W_p = \frac{56.5}{2.8} - \pi \times 0.5^2 \times 50 \times \frac{100}{2000} = 17.2 \text{ tons}$$

check creep load

$$Q_c = \frac{7.85}{2} + \frac{48.7}{1.5} = 36.4 \text{ tons} > 17.2 \text{ tons, o.k.}$$

EXAMPLE 1 : q-w AND f-w CURVES

q-w Curve

$$\frac{q}{w} = \frac{4 E_o}{\pi (1-\nu^2) B} = \frac{4 \times 40}{3.14 (1-0.35^2) \times 1} = 58 \text{ tsf/ft}$$

$$q_L = 10.0 \text{ tsf} \qquad w_q = \frac{10.0}{58} = 0.17 \text{ ft} = 2.07 \text{ in}$$

f-w Curve

$$\frac{f}{w} = \frac{E_R}{(1+\nu)(1+\text{Ln}(\frac{L}{B}) B} = \frac{100}{(1+0.33)(1+\text{Ln} \frac{50}{1}) 1} = 15.3 \text{ tsf/ft}$$

$$f_L = 0.31 \text{ tsf} \qquad w_f = 0.24 \text{ in}$$

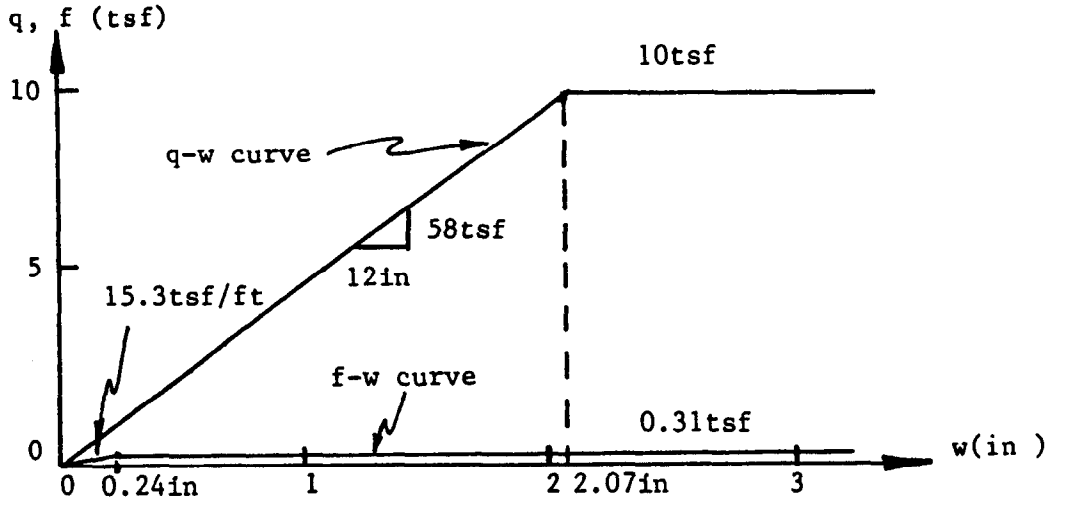

EXAMPLE 2: PILE THROUGH LOOSE SILT INTO DENSE SAND

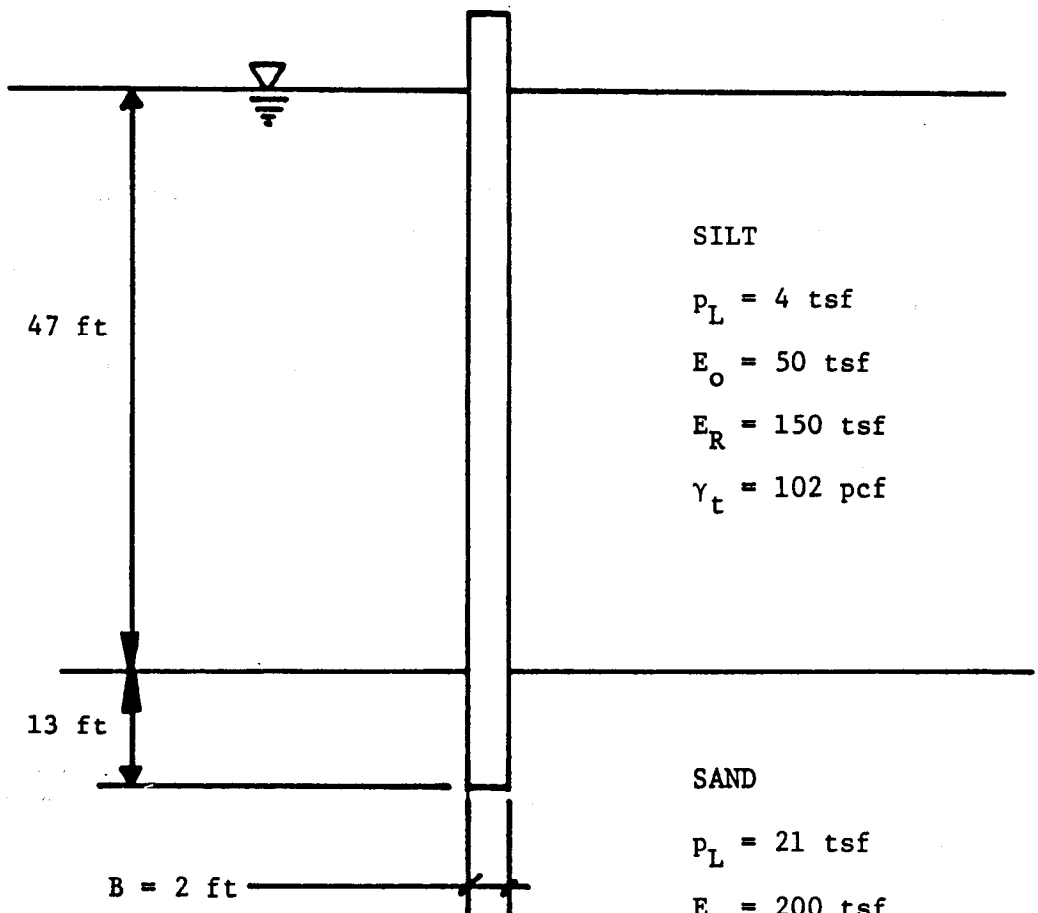

STEEL PIPE PILE

(OPEN END, WALL THICKNESS = 3/8 IN)

Figure 48. Example 2.

EXAMPLE 2 : ULTIMATE CAPACITY

Point

The equivalent limit pressure is

$$p_L = \frac{1}{2a} \int_{-a}^{+a} p_L(z)\, dz$$

a is 1.65 ft since $B \leqslant 3.3$ ft

Since the p_L value does not vary within $\pm$ 1.65 ft around the pile point, the bearing layer is homogeneous and:

$$p_{Le} = 21 \text{ tsf}$$

From table 8, for a full displacement pile (assumes that the pipe pile plugs),

$k = 3.2$ for $p_L > 30$ tsf

$k = 4.2$ for $p_L < 10$ tsf

for this example $p_L = 21$ tsf and by interpolation

$$k = 3.65$$

The embedment in the bearing layer is 13 ft > 5B ; therefore there is no need to reduce k for lack of embedment. The total horizontal pressure at rest is obtained from the test at 63 ft depth as being $p_{OH} = 2.5$ tsf.

$$q_L = 3.65\ (21 - 2.5) + \frac{60 \times 125}{2000} = 71.3 \text{ tsf.}$$

$$Q_p = A_p q_L = \pi \times 1^2 \times 71.3 = 223.9 \text{ tons.}$$

All calculations above assumed that the pile was close ended. For the open ended pipe pile a reduced value of Q_p equal to one-half times the Q_p value for the close ended pipe pile is used.

$$Q_p \text{ (open end)} = \frac{1}{2} Q_p \text{ (close end)} = \frac{1}{2} \times 223.9 = 112 \text{ tons}$$

Side

From table 9, the pile fits under the category Driven Metal. For silts curve Q_1 is used, while for sand curve Q_2 is used. From figure 84 and for the p_{Le} values of the example, the f_L values are: in the silt $f_L = 0.20$ tsf and in the sand $f_L = 0.84$ tsf. Therefore:

$$Q_s = 47 \times \pi \times 1 \times 0.20 + 13 \times \pi \times 1 \times 0.84 = 29.5 + 34.3$$

$$Q_s = 63.8 \text{ tons}$$

Total Capacity

$$Q_L = 112 + 63.8 = 175.8 \text{ tons}$$

total recommended load at the ground surface.

$$Q = \frac{Q_L}{2.8} - W_p = \frac{175.8}{2.8} - \frac{\pi(12^2 - (12 - \frac{3}{8})^2)60}{144} \times \frac{450}{2000} = 62.8 - 2.6$$

$$Q = 60.2 \text{ tons}$$

check creep load

$$Q_c = \frac{Q_L}{1.5} = \frac{175.8}{1.5} = 117.2 \text{ tons} > 60.2 \text{ tons o.k.}$$

EXAMPLE 2 : q-w and f-w CURVES

q-w Curve

$$\frac{q}{w} = \frac{4E_R}{\pi(1-\nu^2)\,B} = \frac{4 \times 830}{\pi(1-0.3^2) \times 2} = 581 \text{ tsf/ft}$$

$$q_L = \frac{1}{2} \times 71.3 = 35.6 \text{ tsf because pipe is open ended.}$$

$$w_q = \frac{35.6}{581} = 0.06 \text{ ft} = 0.74 \text{ in}$$

f-w Curve in the Sand

$$\frac{f}{w} = \frac{E_R}{(1+\nu)(1+\text{Ln}\frac{L}{B})\,B} = \frac{830}{(1+0.3)(1+\text{Ln}\frac{60}{2}) \times 2} = 72.5 \text{ tsf/ft}$$

$$f_L = 0.84 \text{ tsf.}$$

$$w_f = \frac{0.84}{72.5} = 0.012 \text{ ft} = 0.14 \text{ in}$$

f-w Curve in the Silt

$$\frac{f}{w} = \frac{E_R}{(1+\nu)(1+\text{Ln}\frac{L}{B})\,B} = \frac{150}{(1+0.3)(1+\text{Ln}\frac{60}{2})\,2} = 13.1 \text{ tsf/ft}$$

$$f_L = 0.2 \text{ tsf}$$

$$w_f = \frac{0.2}{13.1} = 0.015 \text{ ft} = 0.18 \text{ in}$$

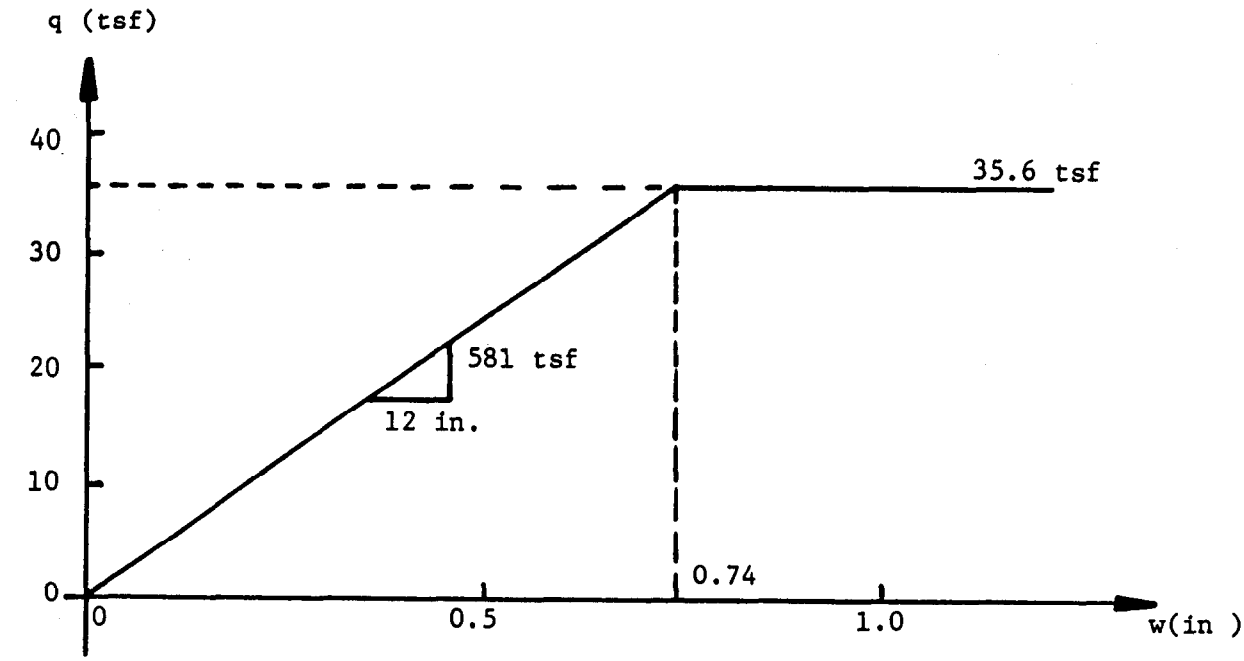
q (tsf)
40
30
20
10
0
35.6 tsf
581 tsf
12 in.
0.74
0
0.5
1.0
w(in)

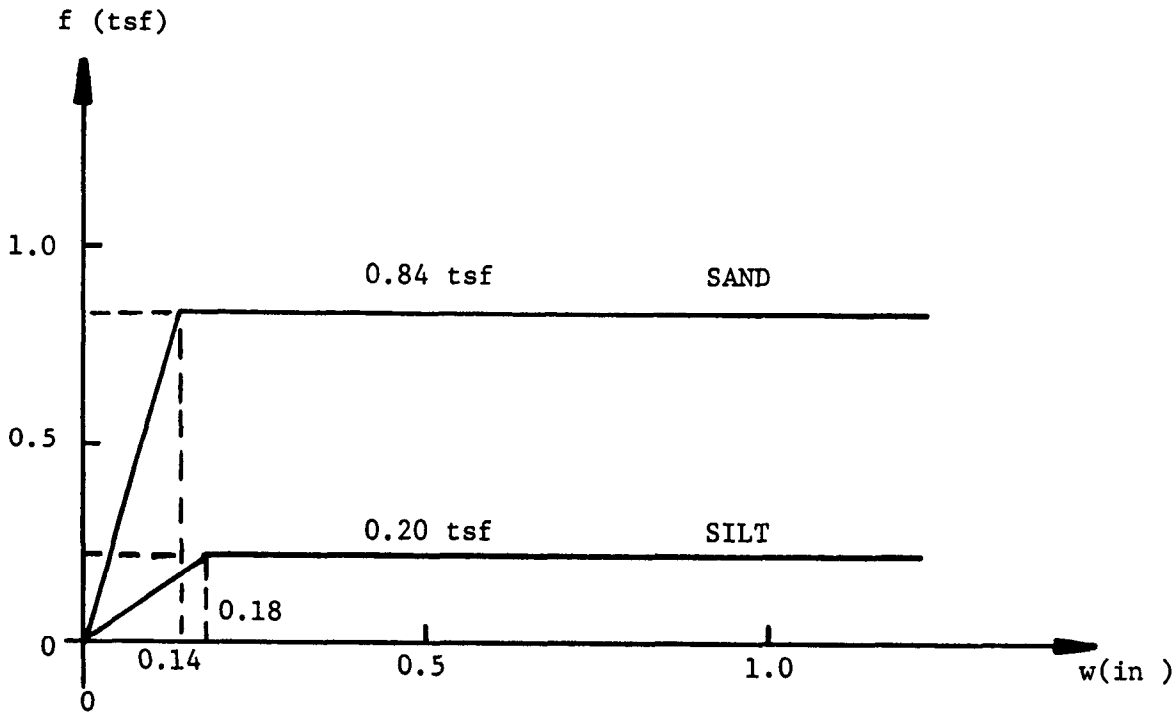
f (tsf)
1.0
0.5
0
0.84 tsf
SAND
0.20 tsf
SILT
0.18
0.14
0.5
1.0
w(in)
0

8.6 Pile Groups

No specific pressuremeter method exists to calculate the settlement of pile groups; however, potentially two approaches are possible. The first one would consist of using a PILGP1 type of approach by combining the load transfer curves and the pressuremeter reload modulus as elastic modulus.(84) The second one would be to use the concept of an equivalent footing at a depth equal to two-thirds of the pile length and treat it as a shallow foundation settlement problem. These two methods have not been checked against case histories.

9. DESIGN OF HORIZONTALLY LOADED PILES

9.1 The Phenomenon

When a pile is loaded horizontally there are several components to the soil resistance (figure 49). The front resistance due to normal stresses, σ_{rr} the shaft friction resistance due to shear stresses, $\tau_{r\theta}$ and $\tau_{r\theta}$ the base friction resistance due to shear stresses $\tau_{z\theta}$ and τ_{zr} and the base moment resistance due to normal stresses, σ_{zz}. Except for very short stubby piles ($D/B < 3$) the major components of soil resistance are due to σ_{rr} and $\tau_{r\theta}$. At working loads the contribution due to the $\tau_{r\theta}$ effect may be as much as 50 percent of the total resistance.(29)

At any depth, z, the resultant of the above soil resistance is the P-y curve where P is the resultant soil resistance in force per unit length of pile, and y is the horizontal displacement of the pile. The horizontal load versus horizontal deflection of the pile at the ground surface is then obtained by finite difference solution of the governing differential equation using the P-y curve.(89)

Close to the ground surface there is a zone of reduced soil resistance due to the lack of vertical confinement. This phenomenon affects both the pressuremeter expansion and the laterally loaded pile down to a critical depth, D_{pm} for the pressuremeter and D_{pi} for the pile (figure 49). Below the critical depth the deformation process is no longer influenced directly by the ground surface. Within the critical depth the soil resistance decreases from the "deep" resistance at the critical depth to a minimum resistance at the ground surface.

9.2 Subgrade Modulus Approach for Long Flexible Piles

Here, the soil is assumed to have a linear P-y curve (figure 50):

$$p = -Ky \tag{85}$$

where P is the soil reaction in load per unit length of pile (lb/in), K is the horizontal spring constant (lb/in^2), and y is the pile deflection (in). Furthermore, it is assumed that K is a constant independent of depth (uniform soil).

The horizontal subgrade modulus k (lb/in^3) is defined as:

$$\frac{P}{B} = -ky \tag{86}$$

where B is the width of the pile. Therefore, the relationship between the horizontal spring constant K and the horizontal subgrade modulus k is:

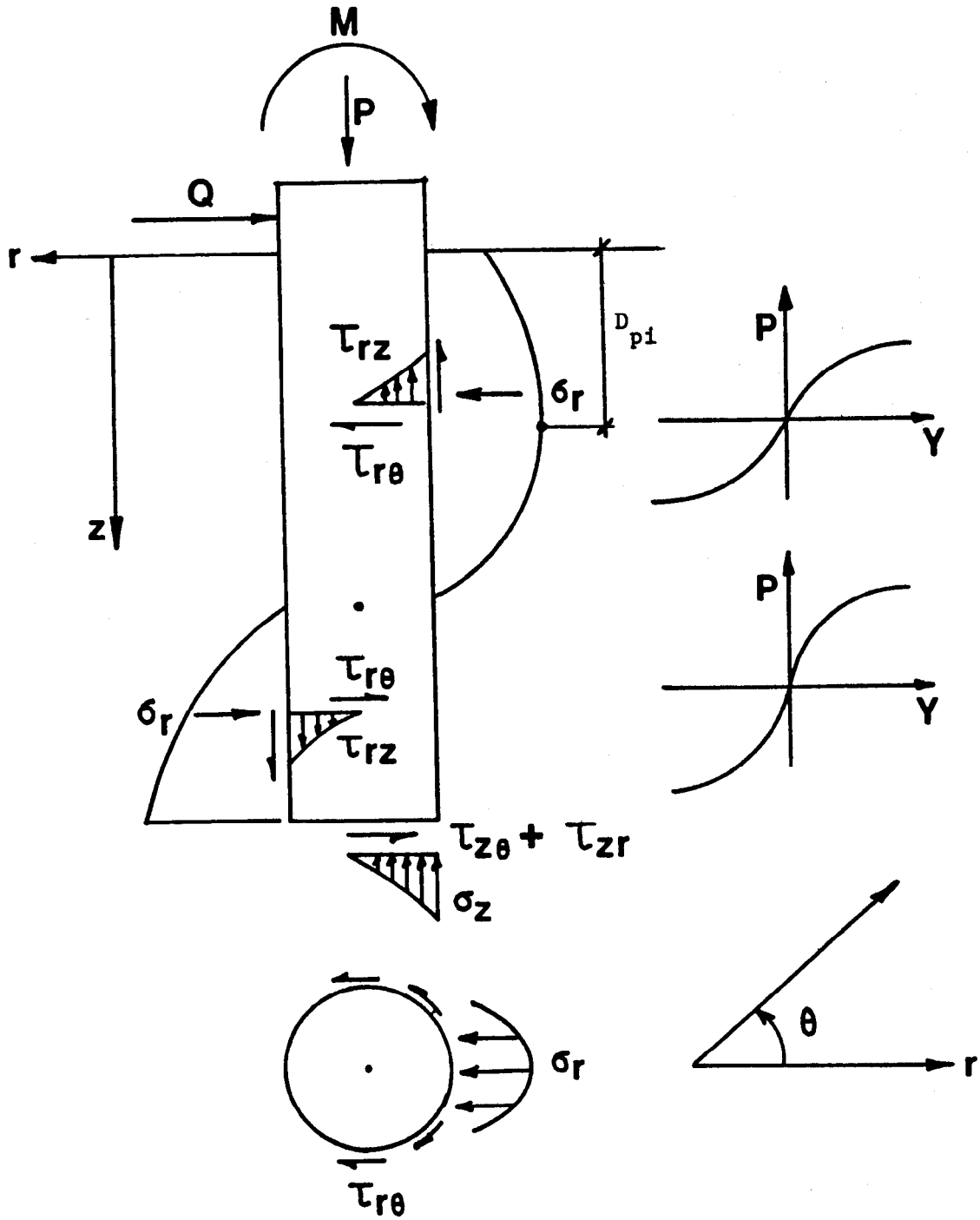

Figure 49. Components of soil resistance (after GAI Consultants, 1982).

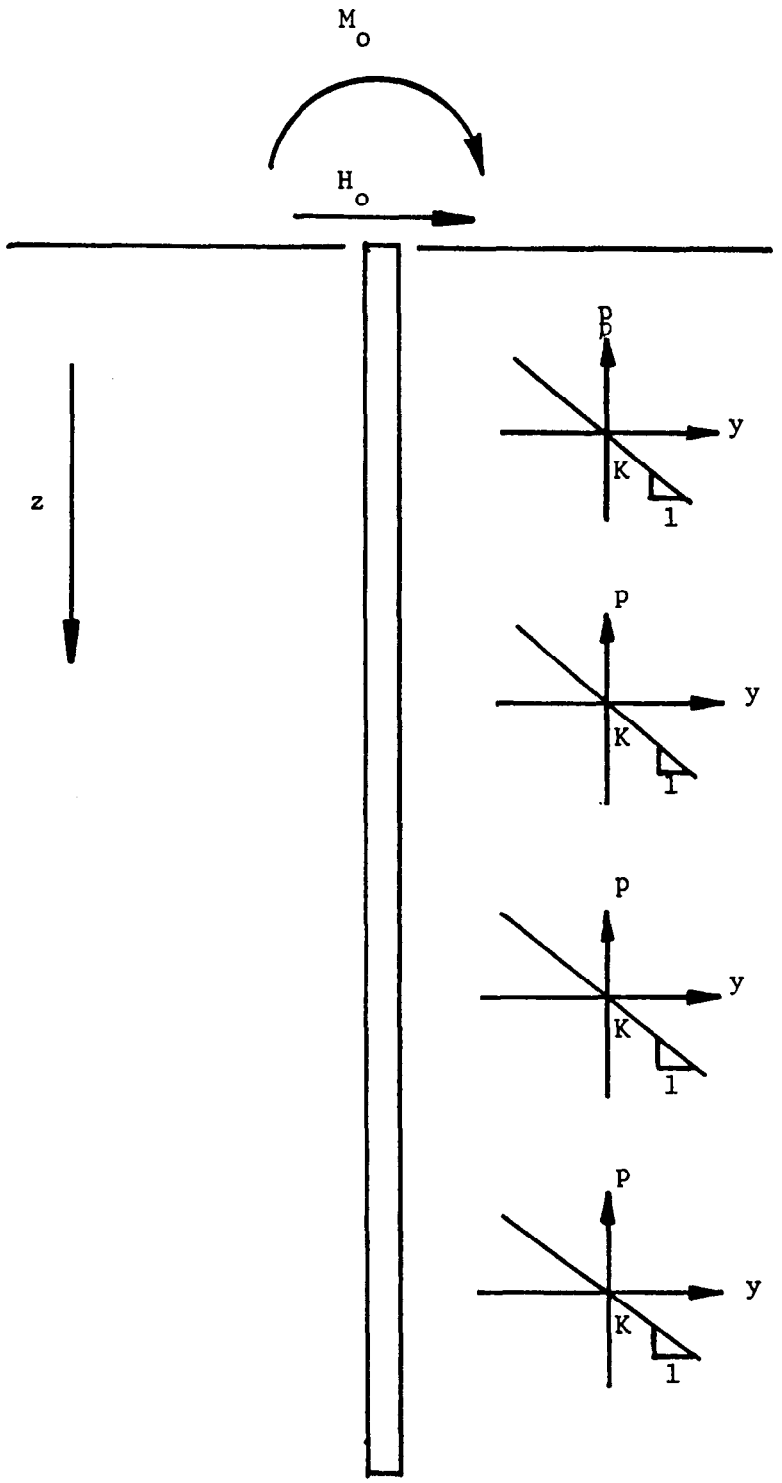

Figure 50. Assumptions for the subgrade modulus approach.

$$K = kB \tag{87}$$

It is recommended that, in first approximation, the horizontal spring constant k be taken as:

$$K = E_o + E_r \qquad \text{for nondisplacement or low displacement piles} \tag{88}$$

$$K = 2E_r \qquad \text{for full displacement piles} \tag{89}$$

where E_o is the pressuremeter first load modulus and E_R is the pressuremeter reload modulus. Nondisplacement piles are bored piles; low displacement piles are H-piles and unplugged pipe piles. Note that a pipe pile which would form a plug at a penetration larger than 5 to 10 pile diameters should be considered as unplugged for horizontal load purposes. Indeed, this 5-to 10-pile-diameter zone close to the ground surface, which controls the horizontal behavior of the pile, would have been subjected only to low displacements. Full displacement piles are, for example, prestressed concrete piles and closed end pipe piles.

The horizontal spring constant K is selected after preparing a profile of K versus depth. The K value should be selected as a conservative average within the zone of influence near the ground surface.

The assumptions made are: the P-y curves are linear, the soil is uniform (all P-y curves are the same), the pile is infinitely long. The limitations due to these assumptions are discussed at the end of this section. The governing differential equation is:

$$EI\frac{d^4y}{dz^4} + Ky = 0 \tag{90}$$

or

$$y + \frac{l_o^4}{4}\frac{d^4y}{dz^4} = 0 \tag{91}$$

with

$$l_o = \sqrt[4]{\frac{4EI}{K}} \tag{92}$$

This parameter l_o is called the transfer length. A pile will be considered as infinitely long if:

$$L \geq 3l_o \tag{93}$$

where L is the embedded length of the pile. This condition must be satisfied for the solution to apply. The boundary conditions are:

$$\text{for } z = \infty, \qquad y = 0 \tag{94}$$

$$\text{for } z = 0, \qquad V = H_o \text{ and } \quad M = M_o \tag{95}$$

where H_o and M_o are the horizontal load and the applied moment at the ground surface, respectively. Given these boundary conditions the solution to the differential equation is:(10)

$$y_{(z)} = \frac{2H_o}{l_o K} e^{-\frac{z}{l_o}} \cos\frac{z}{l_o} + \frac{2M_o}{l_o^2 K} e^{-\frac{z}{l_o}} \left(\cos\frac{z}{l_o} - \sin\frac{z}{l_o} \right) \tag{96}$$

so that the deflection at the ground surface is:

$$y_o = \frac{2H_o}{l_o K} + \frac{2M_o}{l_o^2 K} \tag{97}$$

The solution for the slope y' is:

$$y'_{(z)} = -\frac{2H_o}{l_o^2 K} e^{-\frac{z}{l_o}} \left(\cos\frac{z}{l_o} + \sin\frac{z}{l_o} \right) - \frac{4M_o}{l_o^3 K} e^{-\frac{z}{l_o}} \cos\frac{z}{l_o} \tag{98}$$

At the ground surface the slope is:

$$y'_o = -\frac{2H_o}{l_o^2 K} - \frac{4M_o}{l_o^3 K} \tag{99}$$

The solution for the bending moment M is:

$$M_{(z)} = H_o l_o e^{-\frac{z}{l_o}} \sin\frac{z}{l_o} + M_o e^{-\frac{z}{l_o}} \left(\cos\frac{z}{l_o} + \sin\frac{z}{l_o} \right) \tag{100}$$

At the ground surface the bending moment is M_o. More importantly the maximum bending moment in the pile M_{max} must be found. This is done by finding the value of z (z_{max}) which satisfies $dM/dz = 0$. Since dM/dz is the shear force V, the solution for V is given first.

$$V_{(z)} = H_o e^{-\frac{z}{l_o}} \left(\cos\frac{z}{l_o} - \sin\frac{z}{l_o} \right) - \frac{2M_o}{l_o} e^{-\frac{z}{l_o}} \sin\frac{z}{l_o} \tag{101}$$

Therefore z_{max} is given by:

$$H_o e^{-\frac{z_{max}}{l_o}} \left(\cos\frac{z_{max}}{l_o} - \sin\frac{z_{max}}{l_o}\right) - \frac{2M_o}{l_o} e^{-\frac{z_{max}}{l_o}} \sin\frac{z_{max}}{l_o} = 0 \qquad (102)$$

or

$$\tan\frac{z_{max}}{l_o} = \frac{1}{1 + \frac{2M_o}{l_o H_o}} \qquad (103)$$

Note that z_{max}/l_o is expressed in radians, not in degrees or grades.

The load per unit length of pile P (lb/in) can be obtained from the deflection y (in) at any depth by:

$$P = Ky \qquad (104)$$

At the surface,

$$P_o = Ky_o \qquad (105)$$

and the average pressure on the pile close to the ground surface is

$$p_o = \frac{Ky_o}{B} \qquad (106)$$

This pressure p_o is compared to the soil limit pressure close to the ground surface in order to minimize the creep problem under sustained horizontal loads.

$$F = \frac{p_L}{p_o} \qquad (107)$$

The factor of safety F must be 2 or more. An example of calculations given in section 9.7.

The above approach applies to the case of long flexible piles as defined by the condition:

$$L > 3l_o \qquad (108)$$

where L is the embedded pile length and l_o is the transfer length (equation 92). The solution given by equation 211 corresponds to a straight line on the H_o versus y_o plot (figure 51). In reality the $H_o - y_o$ plot shows a curvature, so that the straight line solution of equation 96 intersects the real plot at one point. With the recommended values of K (equations 88 and 89), this point corresponds to a horizontal deflection y_o equal to 0.5 in on the average. This statement is based on 3 comparisons with full scale load tests.(45) If the deflection is less

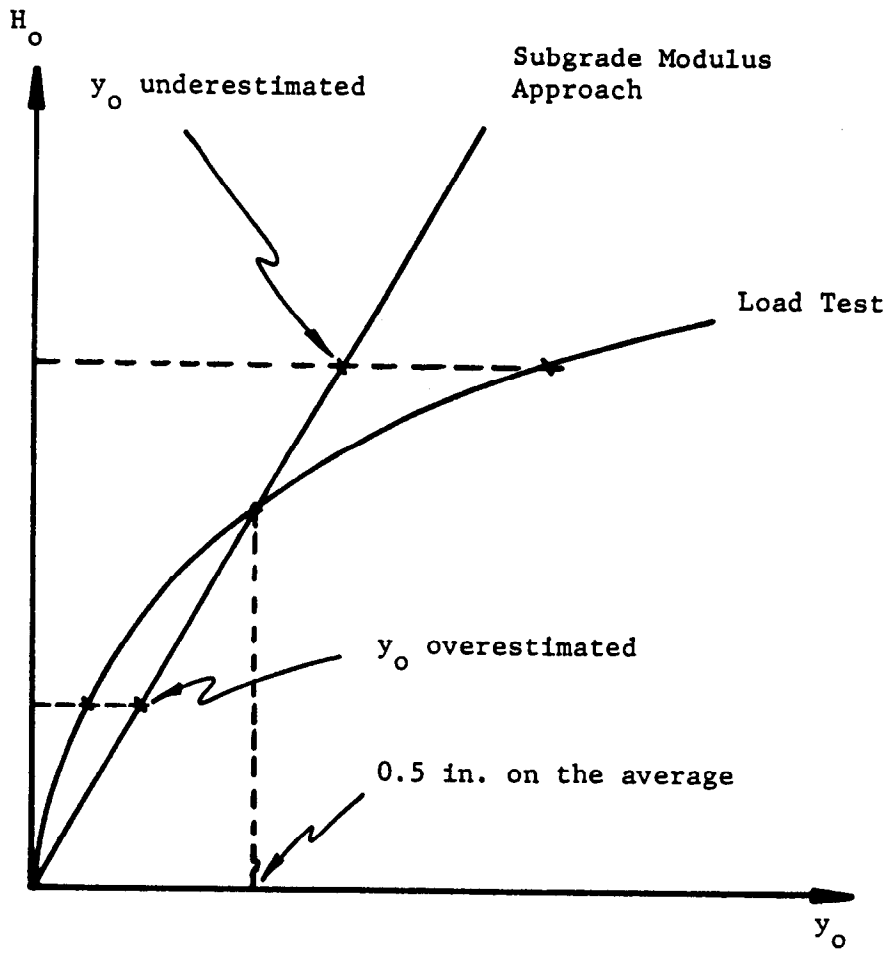

Figure 51. Evaluation of the subgrade modulus prediction.

than 0.5 in, the deflection is likely to be overestimated; if the deflection is more than 0.5 in it is likely to be underestimated. The recommendations for K come from the simplifications of the more detailed recommendations for constructing P-y curves from preboring pressuremeter curves (section 9.4). A design examples is presented in section 9.7.

9.3 Subgrade Modulus Approach for Short Rigid Piles

The following assumptions are made: 1. the P-y curves are linear, 2. the soil is uniform (all P-y curves are the same), 3. the pile is rigid and therefore there is no curvature in the pile. With these assumptions a solution was proposed by Baguelin, Jezequel and Shields as follows.(10) Assumption 1 leads to:

$$P = Ky \tag{109}$$

Assumption 2 states that K is a constant independent of depth. Assumption 3 which describes the fact that the pile is rigid leads to a linear variation of y versus depth.

$$y = Rz + S \tag{110}$$

The pile is considered rigid if the embedded length L is smaller or equal to the transfer length l_o:

$$L \leq l_o \tag{111}$$

where

$$l_o = \sqrt[4]{\frac{4EI}{K}} \tag{112}$$

and E is the pile modulus, I the moment of inertia, and K the horizontal spring constant for the soil. As for long flexible piles:

$$K = E_o + E_R \quad \text{for no displacement or low displacement piles} \tag{113}$$

$$K = 2E_R \quad \text{for full displacement piles} \tag{114}$$

where E_o and E_R are the load and reload preboring pressuremeter modulus respectively. The proper K value is chosen as a conservative value near the surface of the K versus depth profile. With these assumptions, the shear in the pile is calculated as:(10)

$$V = H_o - \int_o^z P\,dt \tag{115}$$

or

$$V = H_o - KR\frac{z^2}{2} - KSz \tag{116}$$

Also the bending moment is given by:

$$M = M_o + H_o z - \int_o^z P(z-t)dt \tag{117}$$

or

$$M = M_o + H_o z - KR\frac{z^3}{6} - KS\frac{z^2}{2} \tag{118}$$

The boundary conditions are:

$$\text{for} \quad z = L, V = 0, M = 0 \tag{119}$$

This leads to the values of R and S:(10)

$$R = -\frac{6(H_o L + 2M_o)}{KL^3} \tag{120}$$

$$S = \frac{2(2H_o L + 3M_o)}{KL^2} \tag{121}$$

The displacement at the ground surface is:

$$y_o = S = \frac{2(2H_o L + 3M_o)}{KL^2} \tag{122}$$

The slope at the ground surface is:

$$y'_o = \left(\frac{dy}{dz}\right)_o = R = -\frac{6(H_o L + 2M_o)}{KL^3} \tag{123}$$

Note that the slope y' is a constant independent of z since there is no curvature in the pile (rigidity). The maximum bending moment M_{max} is found by determining first the depth z_{max} at which M_{max} acts. The value of z_{max} is found by setting $V_{(z)} = 0$.

$$V = H_o - KR\frac{z_{max}^2}{2} - KSz_{max} = 0 \tag{124}$$

which leads to:

$$z_{max} = -\frac{2S}{R} - L = -\frac{2y_o}{y'_o} - L \tag{125}$$

The maximum bending moment is then calculated as (equation 118):

$$M_{max} = M_o + H_o z_{max} - KR\frac{z_{max}^3}{6} - KS\frac{z_{max}^2}{2} \qquad (126)$$

The load per unit length of pile P (lb/in) can be obtained from the deflection y (in) at any depth by:

$$P = Ky = KRz + KS \qquad (127)$$

At the surface,

$$P_o = Ky_o \qquad (128)$$

and the average pressure on the pile close to the ground surface is:

$$p_o = \frac{Ky_o}{B} \qquad (129)$$

This pressure p_o is compared to the soil limit pressure close to the ground surface in order to minimize the creep problem under sustained horizontal loads:

$$F = \frac{p_L}{p_o} \qquad (130)$$

The factor of safety F must be 2 or more.

An example of calculations is given in section 9.7.

9.4 P-y Curve Approach: The Procedure

In the two previous sections it was assumed that the P-y curve was linear and that the same P-y curve applied at all depths. In the general case the P-y curve is nonlinear and various P-y curves exist at various depths. This is the case which is addressed in the following sections.

A microcomputer program PYPMT exists for automatic calculations using this method.(65) This method was presented in 1985.(15,95) It cannot be performed by hand and is not described in detail. Instead a summary of the procedure is given, then the precision of the method is evaluated.

1. Perform pressuremeter tests in a prebored hole at the site with close spacing near the surface and down to a depth of approximately 20 pile diameters or down to the pile tip, whichever is smallest.

2. Correct the pressuremeter curves for membrane resistance, system compressibility and pressuremeter critical depth effect.

3. Obtain the front reaction curves (Q-y) from the pressuremeter curves.

4. For any pressuremeter test within the pile critical depth apply the proper reduction factor to obtain the true Q-y curves.

5. Obtain the friction resistance curve (F-y) by applying the subtangent method to the reload pressuremeter curves.

6. Obtain the P-y curves by adding at each depth the Q-y curve to the F-y curve.

7. If the pile is short ($L/B < 3$) add a P-y curve at the bottom of the shaft to take the bottom friction into account.

8. Run the finite difference program to obtain the pile response.

9.5 Precision of the Method

A 27 pile load test data base is used to determine the precision of the method. The piles in the data base (table 12) cover a wide range of types and pile insertion techniques including bored piles, pipe piles, H piles, and concrete piles. The pile lengths vary from 3m (10 ft) to 25 m (82 ft) and the diameters from 0.27 m (0.88 ft) to 137 m (4.5 ft). The soil included sand, silt and clay as well as layered profiles.

For each pile, preboring pressuremeter tests were performed next to the pile and predictions were performed leading to a predicted horizontal load-horizontal deflection curve at the pile top. On the same graph the measured curve obtained during the load test was plotted (figure 52). The site names followed by an asterisk in table 12 represent cases where predictions were sent to the sponsor prior to receiving the load test results. In order to compare predicted with measured behavior, the loads obtained at a value of the horizontal deflection equal to 10 percent (ultimate) and 2 percent (small movements) of the pile diameter were compared (figures 52 and 53). Figures 52 and 53 show that the method predicts the measured behavior very satisfactorily. Note that only piles 1 to 7 were used to develop the method initially.

The work done by Matlock and Reese from 1955 to 1970 has represented a major step forward in the solution to the problem of horizontally loaded piles.[71,90,70,104] It is believed that the pressuremeter can represent an additional step forward by allowing to improve the quality and range of applicability of the P-y curve approach. The PMT P-y curve approach has the drawback of requiring the performing of PMT tests which are not routine tests in the

Table 12. Full scale horizontal pile load test data base.

Pile I.D. Number	Site	Pile Type	Pile Embedded Length (m)	Pile Diam. (m)	Soil
1	Sabine	Pipe	12.2	0.32	Clay
2	Mustang Island	Pipe	21.0	0.61	Sand
3	Lake Austin	Pipe	12.2	0.32	Clay
4	Houston	Bored	13.0	0.76	Clay
5	Texas A&M (1977)	Bored	6.1	0.91	Clay
6	Texas A&M (1978)	Bored	4.6	0.76	Clay
7	Texas A&M (1979)	Bored	4.6	0.76	Clay
8	Univ. of Houston*	H	11.8	0.27	Clay
9	Univ. of Houston*	Pipe	11.4	1.22	Clay
10	L&D 26 (1983)	HP14x73	20.4	0.36	Sand
11	L&D 26 (1983)	HP14x73	20.4	0.36	Sand
12	L&D 26 (1978)	H	15.2	0.36	Sand
13	L&D 26 (1978)	Pipe	15.2	0.36	Sand
14	Virginia	Bored	3.5	1.37	Clay
15	Carolina	Bored	4.5	1.37	Sand
16	Iowa	Bored	4.6	1.37	Clay
17	LADWP Delta*	Bored	3.0	0.61	Clay
18	LADWP Caliente*	Bored	3.0	0.74	Sand
19	LADWP Alamo*	Bored	3.0	0.65	Clay
20	Baytown	Bored	11.9	0.61	Clay
21	Lackland*	Bored	10.5	0.46	Clay
22	La Baule 1	Rd. Conc.	6.0	0.61	Sand/Clay
23	La Baule 2	Rd. Conc.	6.0	0.61	Sand/Clay
24	Plancoet	Caisson	4.4	0.95	Silt
25	Plancoet	H	6.1	0.36	Silt
26	Cubzac	Pipe	24.7	0.91	Clay
27	Provins	Pipe	23.0	0.93	Silt/Peat

*Load test results unknown at time of predictions

Table 12. Full scale horizontal pile load test data base (continued).

Pile I.D. Number	Reference
1	Matlock, Tucker, 1961 and Smith, 1983
2	Reese et al., 1967 and Smith, 1983
3	Matlock et al., 1956 and Smith, 1983
4	Welch, Reese, 1972 and Smith, 1983
5	Kasch et al., 1977 and Smith, 1983
6	Holloway et al., 1978 and Smith, 1983
7	Bierschwale et al., 1981 and Smith, 1983
8 and 9	O'Neill, Dunnavant, 1984 and Briaud et al., 1985
10 and 11	Corps of Engineers, St. Louis District and Briaud et al., 1984
12 and 13	Woodward-Clyde Consultants, 1979 and Smith, 1983
14 to 16	GAI Consultants, 1982 and Smith, 1983
17 to 19	Los Angeles Department of Water and Power and Briaud et al., 1984
20	Soil Mechanics, Inc., 1982 and Smith, 1983
21	Corps of Engineers, Fort Worth District and Briaud Engineers, 1982
22 and 23	LeMauff, Peignaud, 1973 and LCPC, 1982
24 and 25	Baguelin, Jezequel, 1972, LCPC, 1982 and Smith, 1983
26	Ambrosino et al., 1973 and LCPC, 1982
27	Bigot et al., 1982 and LCPC, 1982

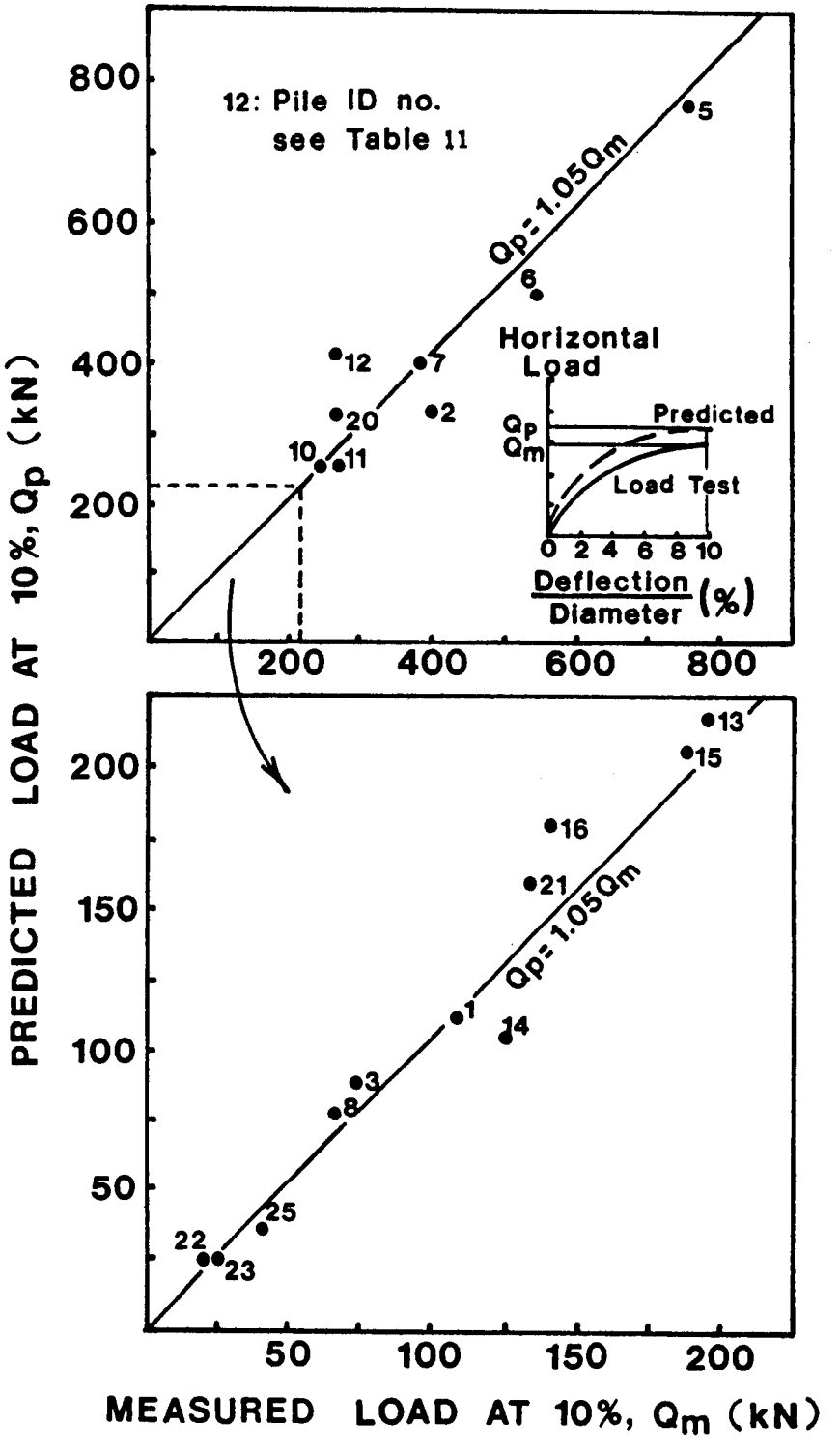

Figure 52. Predicted vs. measured horizontal loads at a deflection equal to 10 percent of the pile diameter.

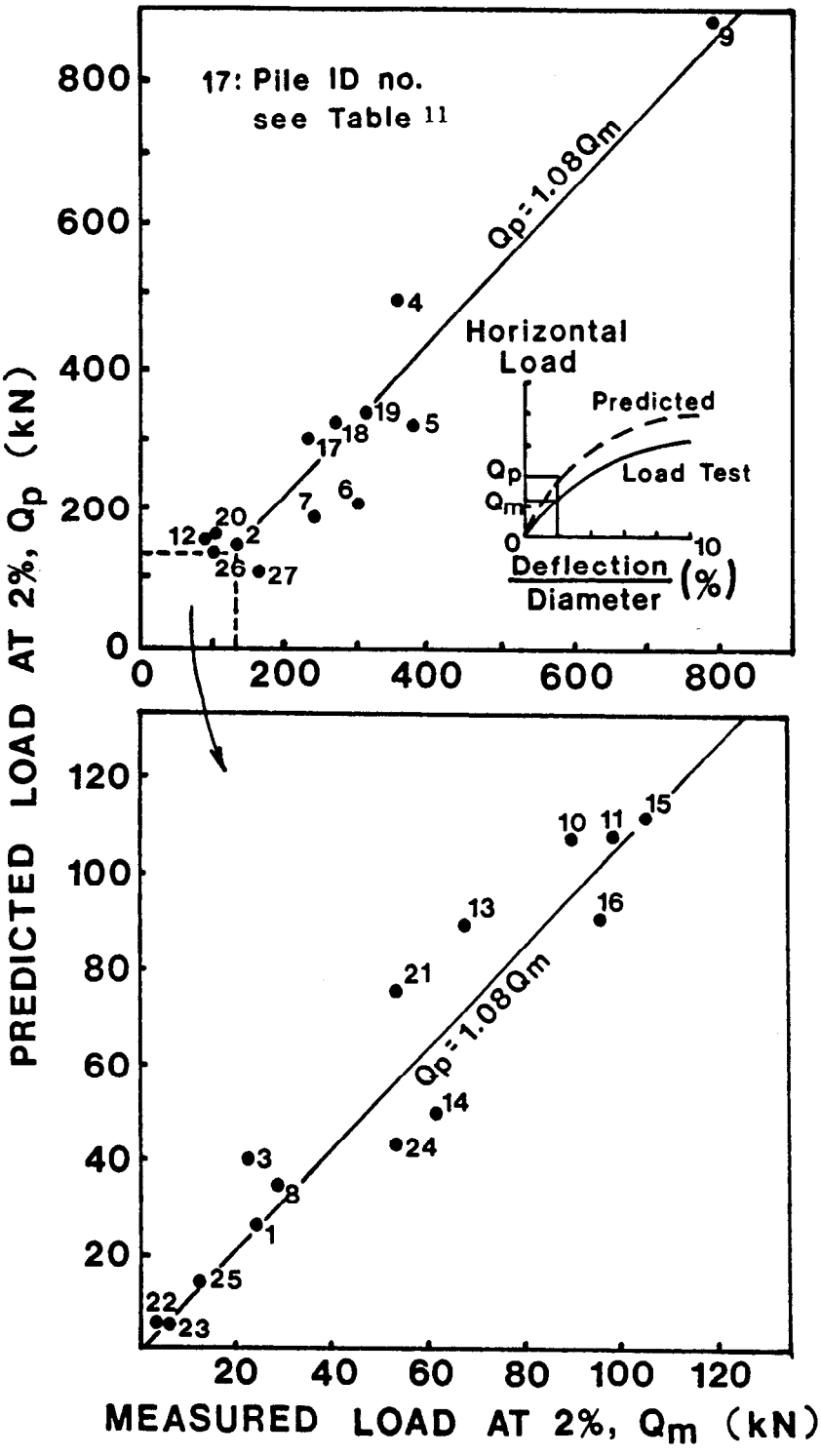

Figure 53. Predicted vs. measured loads at a groundline deflection equal to 2 percent of the pile diameter.

United States. The advantages over the current P-y curves are: the PMT P-y curve is obtained point by point in situ with the pressuremeter, the pressuremeter test can be performed in almost all soils and rocks including calcareous soils, permafrost, peat, and rock; therefore, the method can always be used, the method of installation of the pile can be duplicated by the method of installation of the pressuremeter such as prebored holes for bored piles and driven probes for driven piles, the type of loading can be easily simulated during the PMT test including long-term sustained loads, cyclic loads, and rate of loading effects.

9.6 Rule of Thumb to Estimate the Horizontal Behavior

The ultimate horizontal load Q_U is defined as the load reached for a pile horizontal deflection equal to $1/10^{th}$ of the pile diameter if the pile has not been overstressed when this point is reached. In other words this ultimate load is the soil ultimate load for a given pile and not the pile ultimate load. This ultimate load Q_U can be estimated in first approximation by:

$$Q_U = p_L^* B D_c \tag{131}$$

where B is the pile diameter, p_L^* is the average pressuremeter net limit pressure within the pile critical depth D_c. The value of D_c is obtained from the following equations:

$$D_c = B \quad \text{if} \quad \frac{1}{B}\sqrt[4]{\frac{EI}{p_L^*}} \le 6.33 \tag{132}$$

$$D_c = \frac{3B}{4}\left(\frac{1}{B}\sqrt[4]{\frac{EI}{p_L^*}} - 5\right) \quad \text{if} \quad \frac{1}{B}\sqrt[4]{\frac{EI}{p_L^*}} > 6.33\ldots \tag{133}$$

where E is the modulus of the pile material, I is the moment of inertia of the pile cross section around its centroidal axis. This rule of thumb does not take into account the strength of the pile but helps in estimating the ultimate load.

A factor of safety of 3 on this ultimate load usually leads to a load for which the deflection will be approximately 1.5 percent of the pile diameter.

At working loads, the subgrade modulus approach can be used to calculate the deflection and the maximum bending moment (section 9.2 for long flexible piles and section 9.3 for short rigid piles).

9.7 Design Examples

EXAMPLE 1: LONG FLEXIBLE PILE

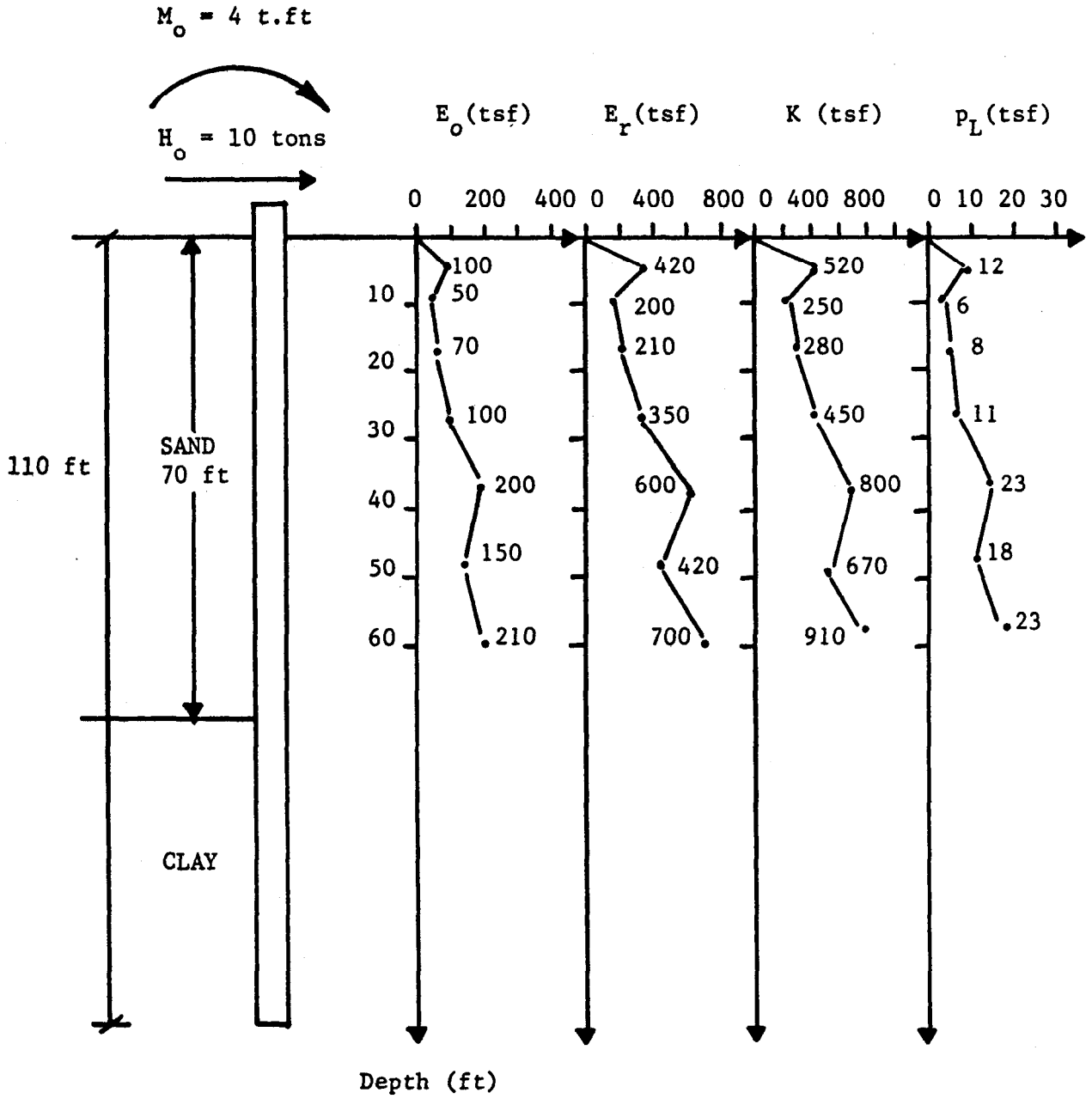

24 IN PIPE PILE UNPLUGGED, WALL THICKNESS = 3/8 IN

Figure 54. Example 1.

EXAMPLE 1: LONG FLEXIBLE PILE UNDER HORIZONTAL LOAD

Select horizontal spring constant.

From the profile a conservative value of 250 tsf is selected:

$$K = 250 \text{ tsf}$$

Calculate the transfer length.

$$l_o = \sqrt[4]{\frac{4EI}{K}}$$

$$E = 30 \times 10^6 \text{ psi} = 30 \times 10^6 \times \frac{144}{2000} \text{ tsf} = 2.16 \times 10^6 \text{ tsf.}$$

$$I = \frac{\pi D_o^4}{64} - \frac{\pi D_1^4}{64} = \frac{\pi \times 24^4}{64} - \frac{\pi (24-2\times0.375)^4}{64} = 1941 \text{ in.}^4 = 0.0936 \text{ ft}^4$$

$K = 250$ tsf.

$$l_o = \sqrt[4]{\frac{4 \times 2.16 \times 10^6 \times 0.0936}{250}} = 7.54 \text{ ft}$$

Check that pile can be considered as "long flexible"

$$L = 110 \text{ ft} > 3\, l_o = 22.6 \text{ ft} \quad \text{ok.}$$

Displacement and slope at ground surface

$$y = \frac{2H_o}{l_o K} + \frac{2M_o}{l_o^2 K}$$

$$y_o = \frac{2 \times 10}{7.54 \times 250} + \frac{2 \times 4}{7.54^2 \times 250}$$

$$y_o = 0.0106 + 0.00056 = 0.0112 \text{ ft} = 0.13 \text{ in.}$$

$$y'_o = -\frac{2H_o}{l_o^2 K} - \frac{4M_o}{l_o^3 K}$$

$$y'_o = - \frac{2 \times 10}{7.54^2 \times 250} - \frac{4 \times 4}{7.54^3 \times 250}$$

$$y'_o = - 0.00141 - 0.00015 = - 0.00156 \text{ radians}$$

$$y'_o = - 0.089 \text{degrees.}$$

Find depth to maximum bending moment.

$$\tan \frac{Z_{max}}{l_o} = \frac{1}{1 + \frac{2M_o}{l_o H_o}} = \frac{1}{1 + \frac{2 \times 4}{7.54 \times 10}} = 0.904$$

$$\frac{Z_{max}}{l_o} = 0.735 \text{ radians} \qquad Z_{max} = 0.735 \times 7.54 = 5.54 \text{ ft}$$

Find maximum bending moment.

$$M_{max} = H_o l_o e^{-\frac{Z_{max}}{l_o}} \sin \frac{Z_{max}}{l_o} + M_o e^{-\frac{Z_{max}}{l_o}} \left(\cos \frac{Z_{max}}{l_o} + \sin \frac{Z_{max}}{l_o}\right)$$

$$M_{max} = 10 \times 7.54 \, e^{-0.735} \sin 0.735 + 4 \, e^{-0.735} (\cos 0.735 + \sin 0.735)$$

$$M_{max} = 24.24 + 2.71 = 26.95 \text{ t.ft}$$

Check for creep.

$$P = Ky \qquad P = 250 \times 0.0112 = 2.8 \text{t/ft.}$$

$$\text{Average corresponding pressure } p_a = \frac{P}{B} = \frac{2.8}{2} = 1.4 \text{tsf.}$$

The limit pressure close to the surface is at least 6 tsf.

$$\text{Therefore } F = \frac{p_L}{p} = \frac{6}{1.4} = 4.29$$

The factor of safety is sufficient to ensure that there will be little creep versus time.

EXAMPLE 2: SHORT RIGID PILE

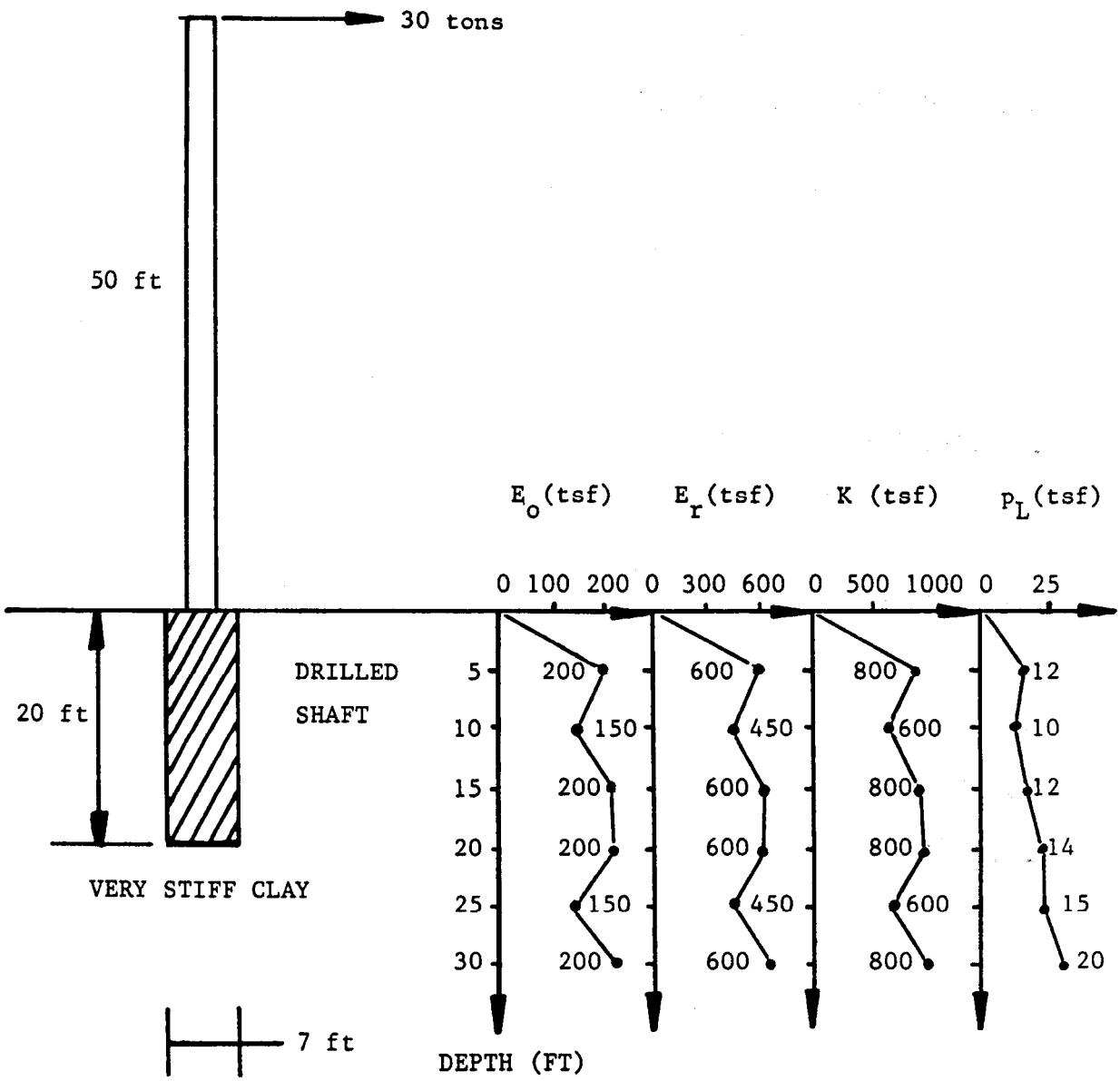

Figure 55. Example 2.

EXAMPLE 2: SHORT RIGID PILE UNDER HORIZONTAL LOAD

Select horizontal spring constant.

From the profile, a conservative value of 600 tsf is selected.

$$K = 600 \text{ tsf}$$

Calculate the transfer length.

$$l_o = \sqrt[4]{\frac{4EI}{K}}$$

$$E = 3 \times 10^6 \text{ psi} = 3 \times 10^6 \times \frac{144}{2000} \text{ tsf} = 2.16 \times 10^5 \text{ tsf}$$

$$I = \frac{\pi D^4}{64} = \frac{\pi \times 7^4}{64} = 117.8 \text{ ft}^4$$

$$K = 600 \text{ tsf}$$

$$l_o = \sqrt[4]{\frac{4 \times 2.16 \times 10^5 \times 117.8}{600}} = 20.29 \text{ ft}$$

Check that pile can be considered as "rigid short"

$$L = 20 \text{ ft} < l_o = 20.29 \text{ ft} \quad \text{ok}$$

Displacement at the ground surface.

$$H_o = 30 \text{ t}$$

$$M_o = 30 \times 50 = 1500 \text{ t.ft.}$$

$$y_o = \frac{2(2H_oL + 3M_o)}{KL^2}$$

$$y_o = \frac{2(2 \times 30 \times 20 + 3 \times 1500)}{600 \times 20^2} = 0.047 \text{ ft}$$

$$y_o = 0.57 \text{ in.}$$

Slope at the ground surface.

$$y'_o = - \frac{6(H_o L + 2M_o)}{KL^3}$$

$$y'_o = - \frac{6(30 \times 20 + 2 \times 1500)}{600 \times 20^3} = - 0.0045 \text{ radians}$$

$$y'_o = - 0.26 \text{ degrees.}$$

Calculate maximum bending moment.

The depth Z_{max} is: $Z_{max} = - \frac{2y_o}{y'_o} - L$

$$Z_{max} = - \frac{2 \times 0.047}{-0.0045} - 20 = 0.89 \text{ ft.}$$

Then $M_{max} = M_o + H_o Z_{max} - KR \frac{Z_{max}}{6} - KS \frac{Z_{max}^2}{2}$

$R = y'_o = - 0.0045$

$S = y_o = 0.047$ ft.

and $M_{max} = 1500+30x0.89-600\ (-0.0045) \frac{0.89^3}{6} - 600 \times 0.047 \times \frac{0.89^2}{2}$

$M_{max} = 1515.8$ t.ft.

Check for creep.

$P = Ky$ $\qquad P = 600 \times 0.047 = 28.2$ t/ft.

Average corresponding pressure $p = \frac{P}{B} = \frac{28.2}{7} = 4.03$ tsf

The limit pressure close to the surface is estimated at 10 tsf from the profile; therefore $F = p_L/p = 10/4.03 = 2.5$. The factor of safety is sufficient to ensure that there will be little creep versus time.

10. DESIGN OF RETAINING WALLS

10.1 General

The pressuremeter is of little help in the design of the following types of retaining walls: gravity walls, cantilever walls, reinforced earth walls. An exception would be the problems associated with the bearing capacity and settlement of such walls (section 7).

This chapter is devoted to the design of drilled shaft retaining walls, sheet pile walls, slurry trench walls, and more generally to the design of walls which develop part or all of the retaining force from the resistance of the embedded portion of the wall (figure 56).

There are various types of methods available to design such retaining walls. The first type of method is the limit equilibrium approach, where the global equilibrium of the wall is considered.

The second type of method is the finite element method where the wall and the soil surrounding the wall are modeled by finite elements.

The third type of method is the finite difference method where the wall is modeled by a series of elements acted upon by nonlinear spring models representing the soil reaction. This method gives a prediction of the wall displacement and can be considered as being of intermediate complexity between the first and second type of method. The nonlinear springs modeling the soil behavior are described by P-y curves where P is the load on the wall at depth z per unit length of wall and per unit width of wall (pressure) and y is the displacement of the wall at the same depth z (figure 56). This method is the one which is used throughout this chapter.

10.2 Preparing the P-y Curves within the Retained Soil Depth

Within the retained soil depth (figure 56), there is soil on one side of the wall and air on the other side. Consider figure 56 for sign convention. The at rest pressure is exerted on the wall. If the wall moves towards the positive y the pressure decreases until it reaches the active earth pressure p_A. The amount of wall displacement necessary to reach p_A is y_A (figure 56). If the wall moves towards the negative y the pressure increases until it reaches the passive earth pressure p_p. The amount of wall displacement necessary to reach p_p is y_p (figure 56).

The values of p_A and p_p are calculated from classical soil mechanics.

$$p_a = K_a \sigma'_v + u \qquad (134)$$

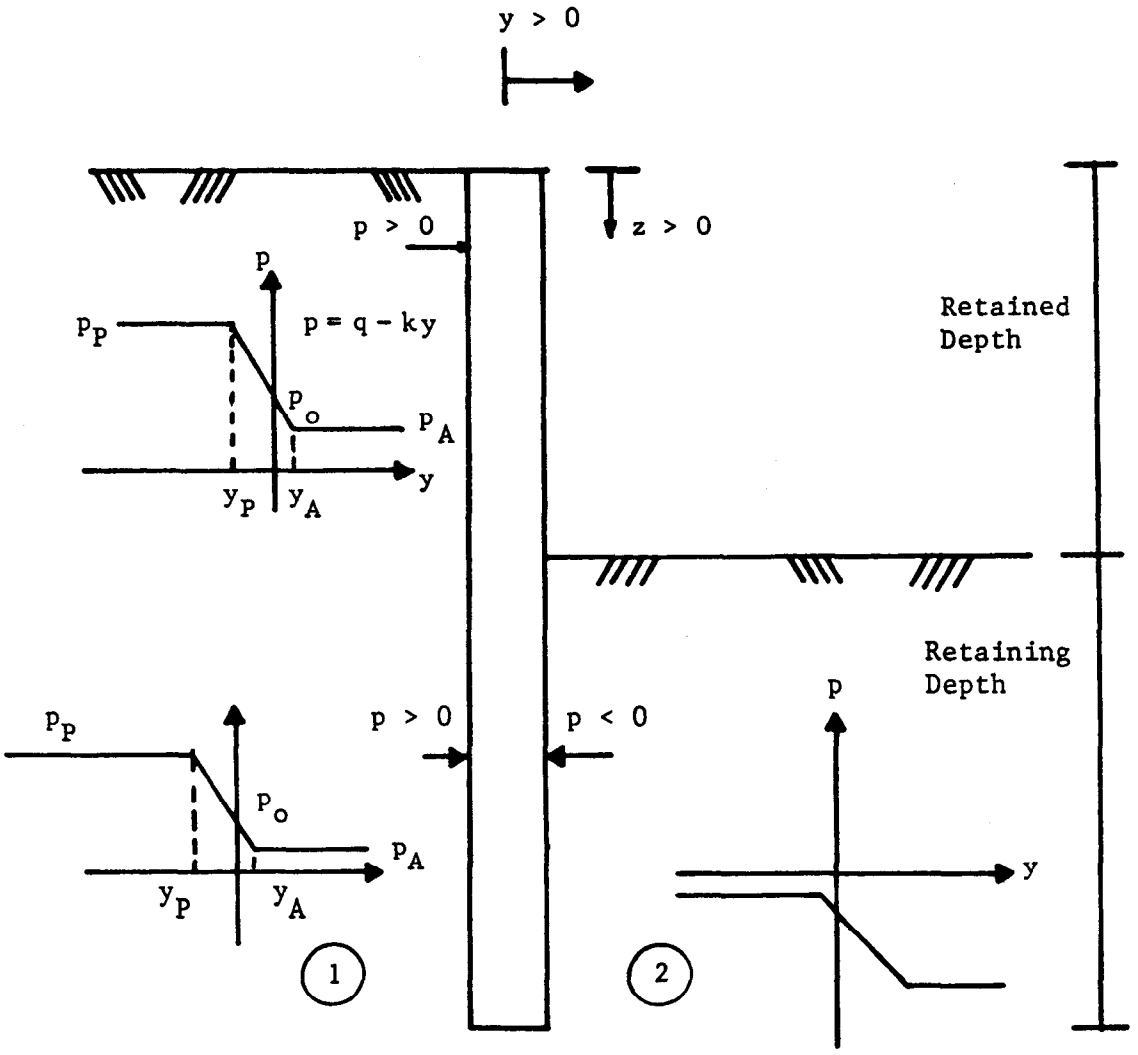

Figure 56. P-y curves for retaining walls.

$$p_p = K_p \sigma'_v + u \qquad (135)$$

where σ'_v is the vertical effective stress at depth z, K_a and K_p the coefficients of active and passive earth pressure respectively, and u, the water pressure at depth z against the wall. Many recommendations have been made for the values of y_A and y_p. Terzaghi (1954) shows data which suggest the following order of magnitude for y_a and y_p:

$$y_A = 0.0005H \qquad (136)$$

$$y_p = 0.005H \qquad (137)$$

where H is the height of the wall (height of retained soil).

The P-y curve is therefore completed as shown on figure 56 for any depth z within the retainined soil depth.

10.3 Preparing the P-y Curves within the Retaining Soil Depth

Within the retaining soil depth (figure 56), there is soil on both sides of the wall. The side where the soil to be retained is located is side 1 (figure 56); the side where the retaining soil is located is side 2 (figure 56). For side 1 the P-y curve is prepared as in the case of the P-y curve within the retained soil depth.

The P-y curve for side 2 is prepared in the same way except that the pressure P are negative since they are opposed to the direction of y (figure 56).

The resulting P-y curve in the retaining soil depth is obtained by adding the P-y curve on side 1 to the P-y curve on side 2 as shown on figure 57. These combined P-y curves can be prepared at various depths within the retaining soil depth.

10.4 Pressuremeter P-y Curves

Menard made some recommendations for obtaining the individual P-y curves within the retaining soil depth.(78,76,77) Figure 58 shows an individual P-y curve for side 2 in the retaining soil depth. Menard proposed to calculate the slope k of the P-y curve (figure 59).

$$k = \frac{E_o}{0.33\alpha h + 0.43(1.83h)^{\alpha}} \qquad (138)$$

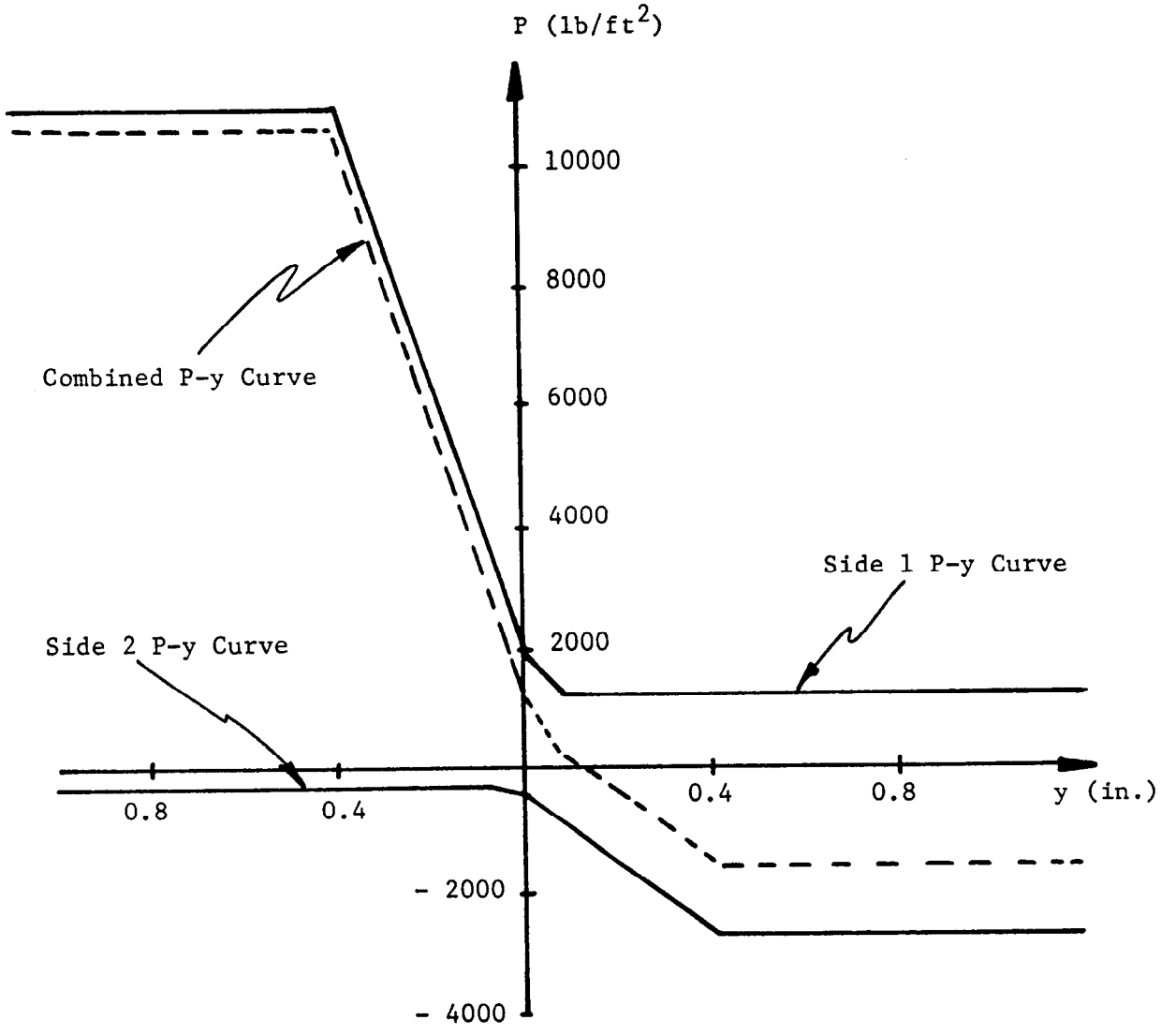

Figure 57. Preparing the combined P-y curve.

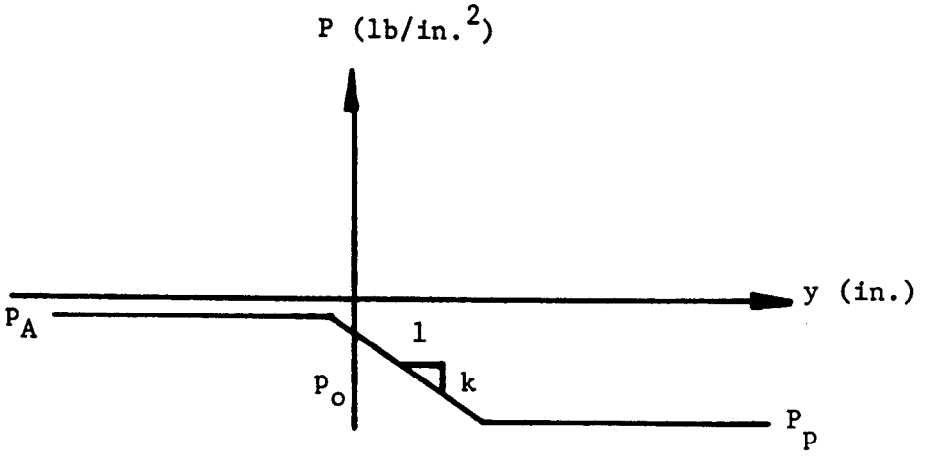

Figure 58. P-y curve for side 2 on figure 110.

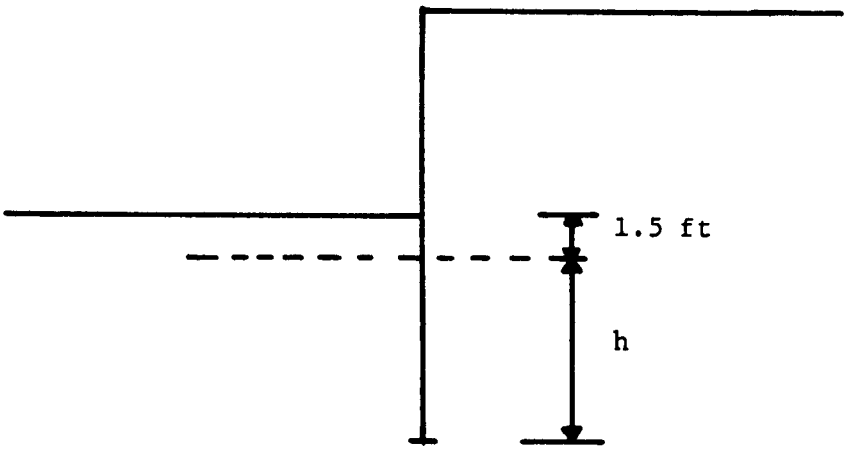

Figure 59. Definition of the corrected depth.

where E_o is the pressuremeter first load modulus in tsf at a depth z within the retaining soil depth, h is the corrected depth of embedment in feet as defined on figure 55, and α is a dimensionless coefficient (table 8, section 7) depending on the ratio of E_o over the pressuremeter limit pressure p_L.

Menard gives the following equation for the ultimate passive resistance of the soil:

$$p_p = \frac{p_L - p_o}{K_B} + p_o \qquad (139)$$

where p_L is the pressuremeter limit pressure, p_o is the at rest total horizontal stress in the soil and K_B is a dimensionless coefficient dependent upon the E_o / p_L ratio as follows:

clay for $E / p_L = 10$, $K_B = 2.7$

for $E / p_L = 15$, $K_B = 3.2$

sand for $E / p_L = 10$, $K_B = 3.5$

for $E / p_L = 15$, $K_B = 4.2$

Engineering judgement must be used to determine values of K_B for E_o / p_L values other than 10 and 15. The value of the passive resistance calculated using equation 139 probably represents a short term value. For long-term values the classical approach is recommended (equation 135).

For the ultimate active resistance of the soil, Menard does not make any PMT recommendations, therefore the classical approach is retained (equation 134).

Once the P-y curve for side 2 is prepared at a depth z, the P-y curve for side 1 at the same depth z is prepared according to the same recommendations. Then the P-y curves for side 1 and side 2 are added to give the combined P-y curve at depth z (section 10.3).

10.5 Examples

The site is located at the intersection of the West Belt and Kimberly Lane in Houston, Texas. The two retaining walls will allow for an underpass intersection. Each of the two retaining walls will be made of a line of drilled piers, 36-in in diameter with a 42-in spacing center-to-center. At the final stage of construction, those piers will have a total length of 68 ft and retain 22 ft of soil (figure 60).

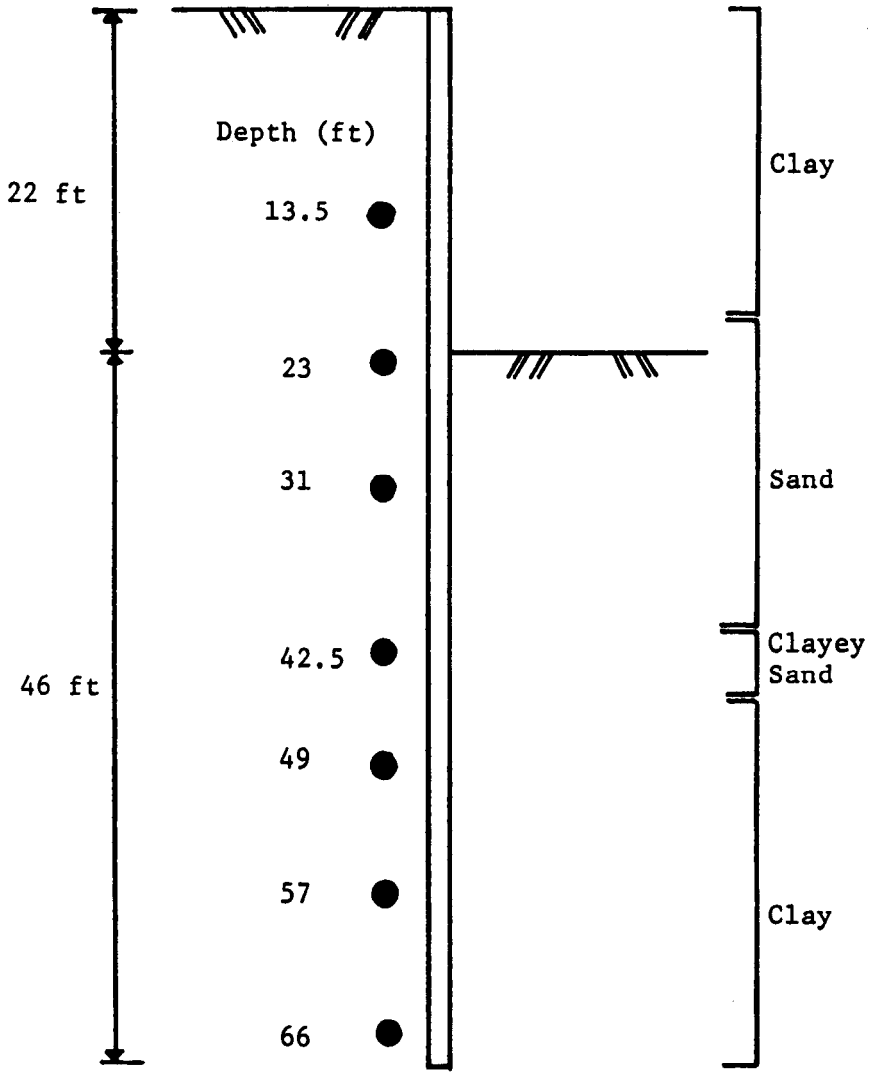

Figure 60. Underpass retaining wall in Houston.

A total of seven pressuremeter tests were performed on August 31, 1983. Their position is shown on figure 60 along with the observed soil layers. The results are presented in figure 61.

In order to analyze the retaining wall the following assumptions were made: each pier affects a width of soil equal to 3.5 ft, the reinforcing steel is such that the cracking moment is not exceeded in each pier, the modulus of elasticity for the concrete is 4×10^6 psi, the soil total unit weight is 120 lb/ft^3 and the soil friction angle is $\phi = 30°$ with no cohesion.

For the part of the analysis based on the conventional approach, the displacement needed to develop active pressure is 2 mm, the displacement needed to develop passive pressure is 10 mm.

For the Menard method, the procedure outlined in section 10.4 was used below the excavation level. Above the excavation level P-y curves based on the conventional approach were used.

Table 13 contains a summary of the P and Y coordinates used to analyze the wall. The depth z is the depth in ft from the top of the wall, P is the pressure in psf, and Y is the corresponding lateral displacement in ft. A, B, C, and D refer to the four points on the P-Y curve shown on table 13.

The results of the analysis are shown on figures 62 and 63.

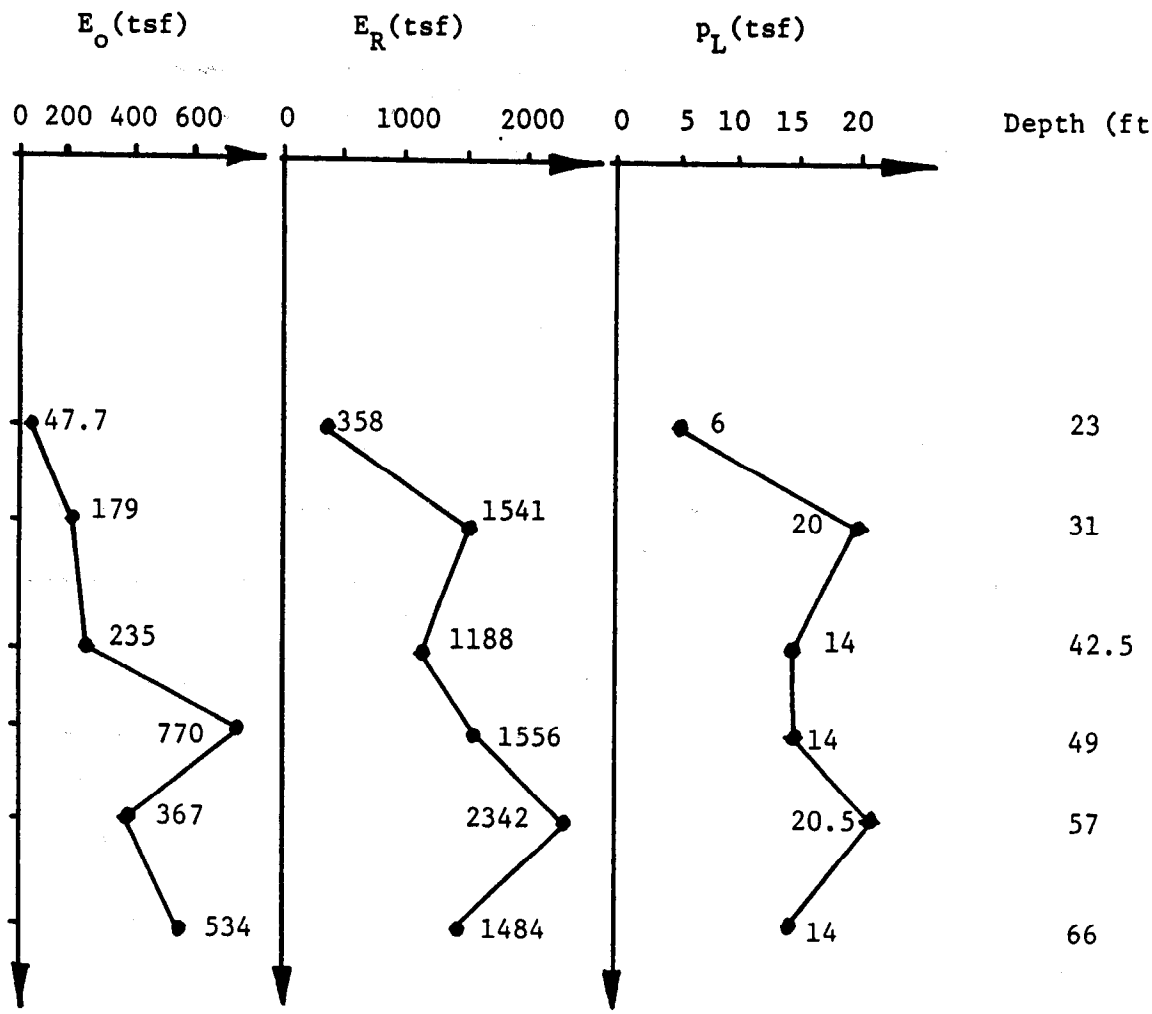

Figure 61. Summary of pressuremeter test results.

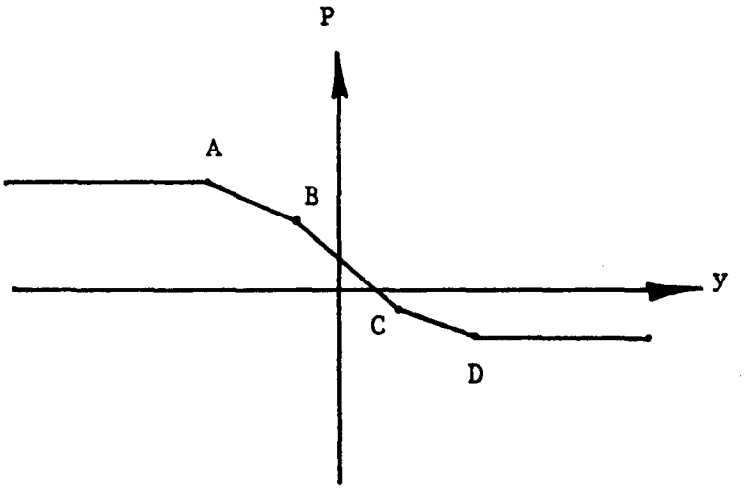

Table 13. P-y curve data for West Belt and Kimberly Wall.

Z	A		B		C		D	
	P (lb/ft)	Y (ft)	P (lb/ft)	Y (ft)	P (lb/ft)	Y (ft)	P (lb/ft)	Y (ft)
0	0	- 1000	-	-	-	-	0	1000
22	4740	- .245	1320	0	-	-	880	.031
31	12930	- .217	1660	- .003	70	.012	- 10730	.117
42	8400	- .106	2150	- .010	- 360	.020	- 6200	.160
49	10610	- .282	2390	- .017	- 650	.032	- 8410	.282
57	14830	- .866	2720	- .047	- 960	.077	- 12630	.866
66	10950	- .407	3080	- .041	-1310	.061	- 8750	.407

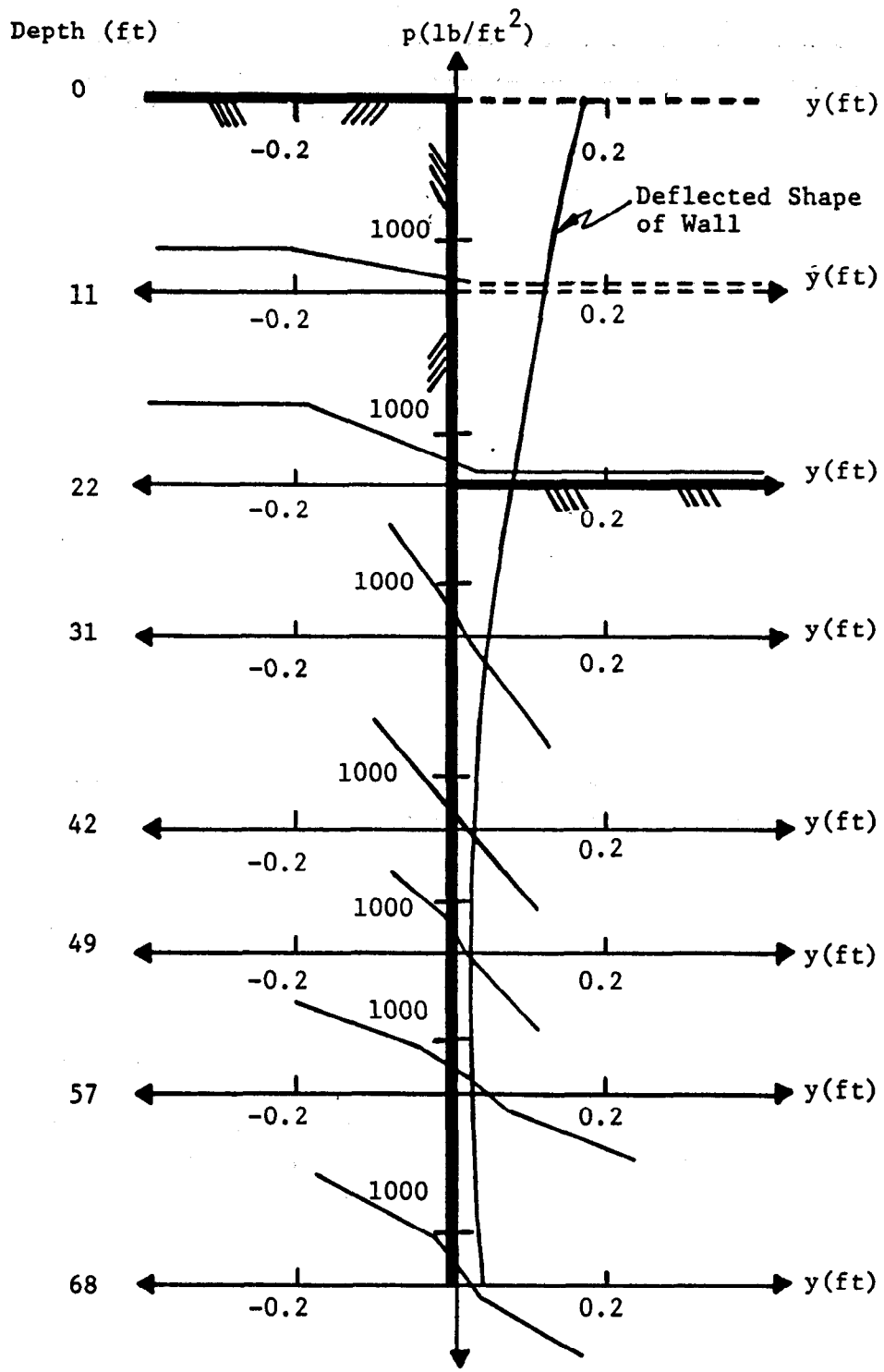

Figure 62. Results of analysis of the wall.

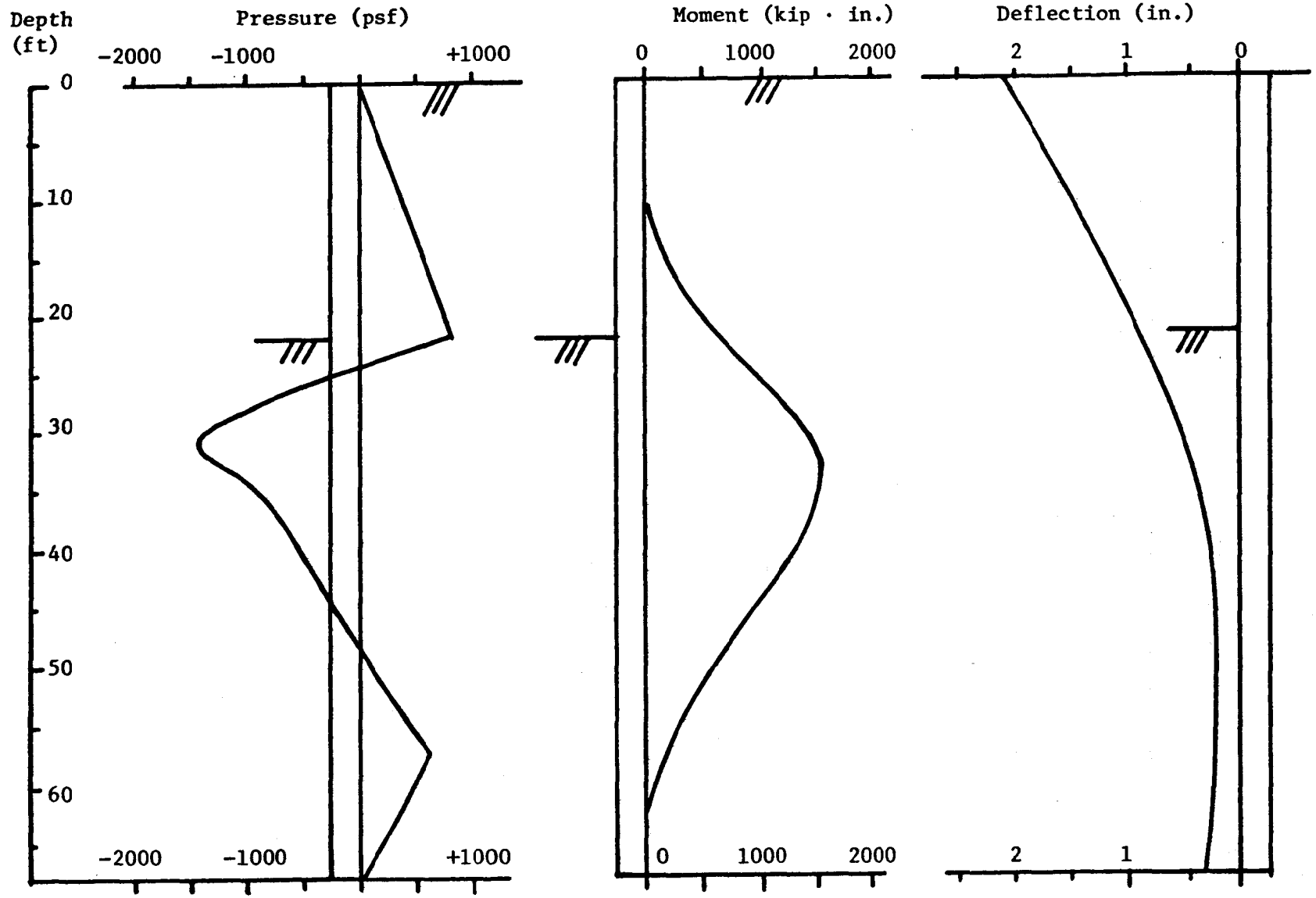

Figure 63. Pressure, bending moment, and deflection for the wall.

11. ADVANTAGES, DISADVANTAGES AND COSTS

11.1 Disadvantages

The quality of the borehole influences the quality of the test results. This induces variation in the results. This variation can be minimized if the recommended way to prepare the borehole is strictly followed and if proper training of the drilling crew takes place.

The probe dimensions are not standardized. This induces variation in the results. This problem can be solved by proposing a stricter ASTM Standard. A probe with a 3-in diameter and inflatable length-to-diameter ratio equal to 6.5 is recommended.

There are some soils in which it is difficult to prepare a quality borehole for the pressuremeter. These include soft clays (undrained shear strength $\leq$ 500 psf), loose clean sands under the water table (SPT blow count $\leq$ 10 blows/ft), large grained soils (maximum particle size > 2.5 in).

As with any other in-situ test, drainage cannot be controlled during the pressuremeter test. Furthermore pore pressures are not commonly measured with preboring pressuremeters.

From the design point of view the pressuremeter cannot be of direct help for the problem of slope stability. The pressuremeter is of limited use for the problem of retaining structures.

11.2 Advantages

From the testing point of view, one of the primary advantages of the preboring pressuremeter is that the test can be performed in most soils. This ensures the engineer that the site investigation will lead to useful results. In a study reported by Baguelin et al. 63 sites were tested with the pressuremeter (PMT), the cone penetrometer (CPT) and the retrieval of undisturbed samples.(6) The number of sites where the tests could be performed is shown on table 14. This table indicates that the PMT test could be performed and led to useful results in 95 percent of the cases. The CPT test could be performed and lead to useful results in only 43 percent of the cases. Undisturbed samples could be obtained and analyzed in only 40 percent of the cases.

The second advantage of the preboring pressuremeter test is that it represents an in-situ load test. With this in-situ load test a number of loading sequences can be duplicated: long pressure steps for long-term loading, rapid inflation for impact loading, unload reload cycles for cyclic loading.

Table 14. Feasibility and representativity of various geotechnical tests.

Type of Test Considered	Number of sites for which the tests ...						
	... were effectively performed	... were interpretable and representative		... were incomplete or non-interpretable	... could not be performed a priority	... could have been performed and interpreted but were not carried out.	Total
Cone Penetration Test (CPT) q_c	35	= 22	+	13 (premature refusal)	23 (soils too compact)	5	63
Menard (PM) Pressuremeter p_l	61	= 58	+	3 (p_l spacing too large)	0	2	63
Laboratory Tests c, ϕ	29	= 14	+	15 (unacceptable scatter)	23 (soils not appropriate)	11	63

The third advantage is that because of the simple geometry of the expansion process, theory allows to transform the PMT curve into an in-situ stress-strain curve. From this stress strain curve, a large number of important soil parameters can be deduced.

The fourth advantage is that the equipment is relatively inexpensive ($10,000 in 1987) and can be used readily with any drilling rig able to prepare a proper borehole.

The fifth advantage is that, to a certain extent, the quality of the test can be judged from the shape of the test curve.

From the design point of view, the first application is the design of horizontally loaded piles including onshore piles, offshore piles, guardrails and sign posts. Experimental data and common sense indicate that, short of a horizontal load test, the pressuremeter is at present the best tool for predicting the response of horizontally loaded piles. Indeed, the analogy is striking.

The second application is the design of shallow foundations and more specifically spread footings where the pressuremeter provides a unified approach to the problem. It is particularly useful for footings on stiff clays and medium dense to dense sands.

The third application is the design of vertically loaded piles and in particular end bearing piles.

11.3 Cost and Time Required

The cost of the basic equipent is about $10,000. On the average 8 tests can be performed in 1 day. In favorable soil conditions, 12 tests/day can be expected while only 4 quality tests/day may be possible in difficult soil conditions. One pressuremeter test cost approximately the same as a consolidation test.

12. REFERENCES

(1) Amar, S., Baguelin, F., Canepa, Y., "Etude Experimentale du Comportement des Fondations Superficielles," *Annales de l' I.T.B.T.P. No. 427, Serie Sols et Fondations 189*, September 1984.

(2) Amar, S., Jezequel, J.-F., "Essais en Place et en Laboratoire Sur Sols Coherents: Comparaison des Resultats," *Bulletin de Liaison des Laboratoires des Ponts et Chaussees*, No. 58, Mars-Avril 1972.

(3) Ambrosino, R., Bru, J.P. and Ledoux, J.L., "Comportement d'un Pieu Sollicite Horizontalement," *Bull. Liaison Labo. P. et Ch. No. 67*, September/October 1973.

(4) ASTM Standard D4719-87, "Standard Test Method for Pressuremeter Testing in Soils," *Annual Book of ASTM Standards*, Vol. 04.08, American Society for Testing and Materials, Philadelphia, 1968.

(5) Baguelin, F.J., "Rules of Foundation Design Using Selfboring Pressuremeter Test Results," *Symposium on the Pressuremeter and Its Marine Applications*, Editions Technip, Paris, 1982.

(6) Baguelin, F.J., Bustamante, M., Frank, R.A., "The Pressuremeter for Foundations: French Experience," *Use of In Situ Tests in Geotechnical Engineering*, ASCE Geotechnical Special Publication No. 6, June 1986.

(7) Baguelin, F., Frank, R., and Jezequel, J.F., "Parameters for Friction Piles in Marine Soils," *Second Int. Conf. in Numerical Methods for Offshore Piling*, Austin, April 1982.

(8) Baguelin, F. and Jezequel, J.F., "Etude Experimentale du Comportement de Pieux Sollicites Horizontalement," *Bll. Liaison Labo. P. et Ch. No. 62*, November/December 1972.

(9) Baguelin, F. and Jezequel, J.F., "Le Pressiometre Autoforeur," *Annales de L'I.T.B.T.P.*, Paris, Serie Sols et Fondations, No. 97, Juillet-Aout, 1973.

(10) Baguelin, F., Jezequel, J.F., and Shields, D.H., *The Pressuremeter and Foundation Engineering*, Trans Tech Publications, Clausthal-Zellerfeld, W. Germany, 1978.

(11) Bierschwale, M.W., Coyle, H.M., and Bartoskewitz, R.E., "Field Tests and New Design Procedure for Laterally Loaded Drilled Shafts in Clay," *Report TTI 211-3F*, Texas Transportation Institute, Texas A&M University, January 1981.

(12) Bigot, G. Bourges, F., and Frank, R., "Etude Experimentale d'un Pieu Soumis aux Poussees Laterales des Sols," *Revue Francaise de Geotechnique*, No. 18, February 1982.

(13) Briaud, J.L., "The Pressuremeter: Application to Pavement Design," Ph.D. dissertation, Civil Engineering Department, University of Ottawa, 1979.

(14) Briaud, J.L., "Pressuremeter and Deep Foundation Design," *The Pressuremeter and Its Marine Applications: 2nd Int. Symp.*, ASTM STPS50, Texas A&M University, April 1986.

(15) Briaud, J.L., "Pressuremeter and Foundation Design," *Use of In Situ Tests in Geotechnical Engineering*, ASCE Geotechnical Publication No. 6, Virginia Polytechnic Institute, June 1986.

(16) Briaud, J.L., Braswell, T.E., and Tucker, L.M., "Case History of Two Laterally Loaded Piles at Lock & Dam 26 Replacement Site," *Research Report 4690-2*, Civil Engineering, Texas A&M University, June 1984.

(17) Briaud, J.L., Cosentino, P.J., and Terry, T.A., "Pressuremeter Moduli for Airport Pavement Design and Evaluation," *Research Report 7035-2F* to Pailen-Johnson Associates and the Federal Aviation Administration, Civil Engineering Department, Texas A&M University, August 1987.

(18) Briaud Engineers, "Pressuremeter, Cone Penetrometer Testing for SH146 Bridge over the Houston Ship Channel," Report to the Texas State Department of Highways and Public Transportation, May 1986.

(19) Briaud Engineers, "Foundation Investigations Using Pressuremeter Testing at Chocolate Bayou and Texas City Amoco Plants," *Report to Kenneth E. Tand and Associates, Inc.*, January 1984.

(20) Briaud Engineers, "Pressuremeter Test and Pile Capacity at Lock & Dam 2, Red River, Alexandria, Louisiana, *Report to Corps of Engineers*, Vicksburg District, June 1984.

(21) Briaud Engineers, "Lackland Air Force Base Vertical and Lateral Drilled Shaft Load Test: Pressuremeter Testing," *Report to the U.S. Army Engineers Waterway Experiment Station*, September 1982.

(22) Briaud, J.L., and Gambin, M., "Suggested Practice for Drilling Boreholes for Pressuremeter Testing," ASTM, *Geotechnical Testing Journal*, Vol. 7, No. 1, March 1984.

(23) Briaud, J.L., Huff, L.G., Tucker, L.M., and Coyle, H.M., "Evaluation of In Situ Test Methods for Vertically Loaded H Piles at Lock & Dam 26 Replacement Site," *Research Report 4690-1*, Civil Engineering, Texas A&M University, July 1984.

(24) Briaud, J.L., Makarim, C.A., Little, R., and Tucker, L.M., "Development of a Pressuremeter Method for Predicting the Behavior of Single Piles in Clay Subjected to Cyclic Lateral Loads," *Research Report 5112*, Civil Engineering Department, Texas A&M University, November 1985.

(25) Briaud, J.L., Noubani, A., Kilgore, J., and Tucker, L.M., "Correlation between Pressuremeter Data and Other Parameters," *Research Report*, Civil Engineering Department, Texas A&M University, 1985.

(26) Briaud, J.L., Pacal, A.J., and Shively, A.W., "Powerline Foundation Design Using the Pressuremeter," *International Conference on Case Histories in Geotechnical Engineering*, St. Louis, 1984.

(27) Briaud, J.L., and Riner, K. "A Study of Cyclic Pressuremeter Testing for Offshore Applications," *Research Report 4839* to the Fukada Geological Institute, Civil Engineering Department, Texas A&M University, 1984.

(28) Briaud, J.L. and Shields, D.H., "Use of a Pressuremeter Test to Predict the Modulus and Strength of Pavement Layers," *Transportation Research Record No. 810*, 1981.

(29) Briaud, J.L., Smith, T.D., and Meyer, B.J., "Pressuremeter Gives Elementary Model for Laterally Loaded Piles," *Int. Symp. on In Situ Testing of Soil and Rock*, Paris, May 1983.

(30) Briaud, J.L., Tand, K.E., and Funegard, E.G., "Pressuremeter and Shallow Foundations on Stiff Clay," *Spread Foundations*, Transportation Research Board Annual Meeting, Washington, January 1986.

(31) Briaud, J.L. and Tucker, L.M., "Pressuremeter and Foundation Design," Short Course notes, Vol. 1, Civil Engineering Department, Texas A&M Univesity, 1985.

(32) Briaud, J.L. and Tucker, L.M., "Pressuremeter and Shallow Foundations on Sand," *Settlement of Shallow Foundations on Sand*, Session at the ASCE Convention, Seattle, April 1986.

(33) Briaud, J.L. and Tucker, L.M., "Measured and Predicted Axial Response of 98 Piles," *Journal of Geotechnial Engineering*, ASCE, September 1988.

(34) Briaud, J.L., Tucker, L.M., Anderson, J.S., Perdomo, D., and Coyle, H.M., "Development of an Improved Pile Design Procedure for Single Piles in Clays and Sands," *Research Report 4981-3F* to the Mississippi State Highway Department, Civil Engineering, Texas A&M University, August 1986.

(35) Briaud, J.L., Tucker, L.M., Lytton, R.L., and Coyle, H.M., "Behavior of Piles in Cohesionless Soils," *Reserch Report 4777*, Civil Engineering Department, Texas A&M University, September 1983.

(36) Briaud, J.L., Tucker, L.M., and Makarim, C.A., "Pressuremeter Standard and Pressuremeter Parameters," *The Pressuremeter and Its Marine Applications: 2nd Int. Symp.*, ASTM STP 950, Texas A&M University, 1986.

(37) Burgess, N. and Eisenstein, Z., "Determination of Deformation Characteristics of Soils and Rocks in Western Canada by the Pressuremeter," *28th Canadian Geotechnical Conf.*, Montreal, 1975.

(38) Bustamante, M. and Gianeselli, L., "Prevision de la Capacite Portante des Pieux Isoles, sous Charge Verticale: Regles Pressiometriques et Penetrometriques," *Bull. Liaison Labo. P. et Ch. 113*, May-June 1981.

(39) Cassan, M., "Correlation Entre Essais In Situ en Mechanique des Sols, *Internal Report*, Fondasol, Avignon, 1972.

(40) Dauvisis, J.P. and Menard, L., "Etude Experimentale du Tassement et de la Force Portante de Fondations Superficielles," *Sols-Soils*, Vol. 3, No. 10, 1964.

(41) Davidson, R.R. and Bodine, D.G., "Analysis and Verification of Louisiana Pile Foundation Design Based on Pressuremeter Results," *The Pressuremeter and Its Marine Applications: 2nd Int. Symp.*, ASTM, STP 950, 1986.

(42) Davidson, R.R. and Perez, J.Y., "Pressuremeter Research: I-90 Project," Woodward-Clyde Consultants, *Research Report*, February 1980.

(43) Deschenes, J.H., "Bearing Capacity of Footings Close to Slopes of Cohesionless Soil," Ph.D. dissertation, Civil Engineering, University of Ottawa, 1978.

(44) GAI Consultants, Inc., "Laterally Loaded Drilled Pier Research: Vol. 1: Design Methodology, Volume 2: Research Documentation," *Research Report EPRI EL-2197*, January 1982.

(45) Gan, K.C. and Briaud, J.L., "Use of the Stepped Blade in Foundation Design and Comparison with the Pressuremeter," *Reserch Report 7032 to Iowa State University and the Federal Highway Administration*, Civil Engineering, Texas A&M University, July 1987.

(46) Greenland, "Economic Loading Tests with the Menard Pressuremeter," *Proceedings of Symp. on the Economic Use of Soil Testing*, Birmingham, 1964.

(47) Hansbo, S., "Prediction of Load vs. Settlement Curves for Friction Piles," Contribution to *Symposium on the Pressuremeter and Its Marine Applications*, Editions Technip, Paris, 1982.

(48) Hartman, J.P., "Finite Element Parametric Study of Vertical Strain Influence Factor and the Pressuremeter Test to Estimate the Settlement of Footings in Sand," Ph.D. dissertation, Civil Engineering Department, University of Florida, 1974.

(49) Higgins, C., "Pressuremeter Correlation Study," *Highway Research Record*, Highway Research Board, No. 284, 1969.

(50) Holloway, G.L., Coyle, H.M., Bartoskewitz, R.E., and Sarver, W.G., "Field Test and Preliminary Design Method of Laterally Loaded Drilled Shafts in Clay," *Report TTI 211-2*, Texas Transportation Institute, Texas A&M University, September 1978.

(51) Hughes, J.M.O., Wroth, C.P., and Windle, D., "Pressuremeter Tests in Sand," *Geotechnique*, Vol. 27, No. 4, 1977.

(52) Jeyapalan, J.K., Boehm, R., "Proceedings for Predicting Settlement in Sands," *Settlement of Shallow Foundations on Cohesionless Soils: Design and Performance*, ASCE Geotechnical Special Publication No. 5, April 1986.

(53) Jezequel, J.F., Lemasson, H., and Touze, J., "Le Pressiometre Louis Menard: Quelques Problemes de Mise en oeuvre et leur Influence Sur les Valeurs Pressiometriques," *Bulletin de Liaison des Laboratoires Routiers des Ponts et Chaussees*, No. 32, 1968.

(54) Johnson, L.D., "Correlation of Soil Parameters from In Situ and Laboratory Tests for Building 333," *ASCE Specialty Conference, Use of In Situ Testing in Geotechnical Engineering*, Blacksburg, Virginia, 1986.

(55) Kahle, J.G., "Predicting Settlement in Piedmont Residual Soil with the Pressuremeter Test," *Transportation Research Board Meeting*, Washington, January 1983.

(56) Kasch, V.R., Coyle, H.M., Bartoskewitz, R.E., and Sarver, W.G., "Lateral Load Test of a Drilled Shaft in Clay," *Report TTI 211-1*, Texas Transportation Institute, Texas A&M University, November 1977.

(57) Komornik, A., Wiseman, G., and Frydman, S., "A Study of In Situ Testing with the Pressuremeter," *Conf. on In Situ Investigations on Soils and Rocks*, Institution of Civil Engineers, London, 1970.

(58) Konstantinidis, Byron, Schneider, J.P., Van Reissen, Gary, "Structural Settlements of a Major Power Plant," *Settlement of Shallow Foundations on Cohesionless Soils: Design and Performance*, ASCE Geotechnical Special Publication No. 5, New York, April 1986.

(59) Laboratoire des Ponts et Chaussees, "Internal Documents on Lateral Pile Load Tests," Paris, 1982.

(60) Ladd, C.C., Foot, R., Ishihara, K., Schlosser, F., and Poulos, H.G., "Stress-Deformation and Strength Characteristics," State of the Art Report, *9th Int. Conf. on Soil Mech. and Found. Engrg.*, Vol. 2, Tokyo, 1977.

(61) LCPC-SETRA, *Regles de Justification des Fondations sur Pieux a Partir des Resultats des Essais Pressiometriques*," Laboratoire Central des Ponts et Chaussees - Service d'Etudes Techniques des Routes et Autoroutes, Paris, October 1985.

(62) LeBlanc, J., "Menard Pressuremeter Testing," *Symposium on the Pressuremeter and Its Marine Applications*, Editions Technip, Paris, 1982.

(63) Leichner, W., "Die Bautechnische Baugrund Beurteilung Mittels Horizontaler Belastungsversuche im Bohrloch nach dem Kogler-Verfahren," *Der Bauingenieur*, Heft 12, 1966.

(64) Le Mauff, H. and Peignaud, M., "Solicitations Horizontales de Dispositifs Legers d'Amarrage," *Bull. Liaison Labo. P. et Ch. No. 64*, March-April, 1973.

(65) Little, R.L., Tucker, L.M., and Briaud, J.L., "User's Manual for PYPMT," Civil Engineering, Texas A&M University, 1986.

(66) Lukas, R.G., "Settlement Prediction Using the Pressuremeter," *The Pressuremeter and Its Marine Applications: 2nd Int. Symp.*, ASTM STP 950, Texas A&M University, 1986.

(67) Lukas, G.L., LeCler de Bussy, B., "Pressuremeter and Laboratory Test Correlations for Clays," *Journal of the Geotechnical Engineering Division*, ASCE, Vol. 102, No. GT9, September 1976.

(68) Marsland, A. and Randolph, M.F., "Comparison of the Results from Pressuremeter Tests and Large In Situ Plate Tests in London Clay," *Geotechnique 27 (2)*, 1977.

(69) Matlock, H., "Correlations for Design of Laterally Loaded Piles in Soft Clay," *Offshore Technology Conference*, Paper 1204, Houston, 1970.

(70) Matlock, H., Ripperger, E.A., and Fitzgibbon, D.P., "Static and Cyclic Lateral Loading of an Instrumented Piles," *A Report to Shell Oil Company*, Houston, July 1956.

(71) Matlock, H. and Tucker, R.L., "Lateral Load Tests of an Instrumented Pile at Sabine, Texas," *A Report to Shell Development Company*, Houston, September 1961.

(72) Meigh, A. and Greenland, S., "In Situ Testing of Soft Rocks," *6th Int. Conf. on Soil Mech. and Found. Engrg.*, Vol. 1, Montreal, 1965.

(73) Menard, L., "Calcul de la Force Portante des Fondations sur la Base des Resultats des Essais Pressiometriques," *Sols-Soils*, Vol. 2, Nos. 5 and 6, June 1963a.

(74) Menard, L., "Calcul de la Force Portante des Fondations sur la Base des Resultats des Essais Pressiometriques, Seconde Parie: Resultats Experimentaux et Conclusions," *Sols-Soils*, No. 6, September 1963b.

(75) Menard, L., "The Menard Pressuremeter: Interpretation and Application of the Pressuremeter Test Results to Foundations Design," *Sols-Soils No. 26*, 1975.

(76) Menard, L. and Bourdon, G., "Calcul des Rideaux de Soutenement: Methode Nouvelle Prenant en Compte les Conditions Reeles d'Encastrement," *Sols-Soils No. 12*, 1965.

(77) Menard, L., Bourdon, G., and Gambin, M., "Methode Generale de Calcul d'un Rideau ou Pieu Sollicite Horizontalement en Fonction des Resultats Pressiometriques," *Sols-Soils No. 22/23*, 1969.

(78) Menard, L., Bourdon, G., and Houy, A., "Etude Experimentale de l'Encastrement d'un Rideau en Fonction des Caracteristiques Pressiometriques du Sol de Fondation," *Sols-Soils No. 9*, 1964.

(79) Menard, L. and Rousseau, J., "L'Evaluation des Tassements-Tendances Nouvelles," *Sols-Soils*, Vol. 1, No. 1, June 1962.

(80) Merritt, B.K., Davidson, B.R., and Baker, G.L., "Menard Pressuremeter Experience in Beaumont Clay," Texas Section Meeting, ASCE, Austin, Spring 1979.

(81) Meyerhof, G.G., "The Bearing Capacity of Foundations under Eccentric and Inclined Loads," *3rd Int. Conf. on Soil Mech. and Found. Engrg.*, Vol. 1, Zurich, 1953.

(82) Meyerhof, G.G., "The Bearing Capacity of Foundations on Slopes," *4th Int. Conf. on Soil Mech. and Found. Engrg.*, Vol. 1, London, 1957.

(83) O'Neill, M.W. and Dunnavant, T.W., "A Study of the Effect of Scale, Velocity, and Cyclic Degradability on Laterallyt Loaded Single Piles in Overconsolidated Clay," *Research Report No. UHCE 84-7*, Civil Engineering, University of Houston, October 1984.

(84) O'Neill, M.W., Hawkins, R.A., and Mahar, L.T., "Field Study of Pile Group Action," *Research Report No. FHWA/RD-81*, Civil Engineering, University of Houston, October 1980.

(85) O'Neill, M.W. and Reese, L.C., "Behavior of Axially Loaded Drilled Shafts in Beaumont Clay," *Research Report 89-8N*, Center for Highway Research, University of Texas, 1970.

(86) O'Neill, M.W. and Sheikh, S.A., "Geotechnical Behavior of Underreams in Pleistocene Clay," *Proceedings of the Session on drilled Piers and Caissons II*, ASCE Convention, Denver, May 1985.

(87) Peck, R.B. and Bazaraa, A.R., "Discussion of Settlement of Spread Footings on Sand," by D'Appolonia et al., *Journal of Soil Mechanics and Foundation Division*, ASCE, May 1969.

(88) Randolph, M.F. and Wroth, C.P., "Analysis of Deformation of Vertically Loaded Piles," *ASCE Geotechnical Engineering Journal*, Vol. 104, GT12, December 1978.

(89) Reese, L.C., "Laterally Loaded Piles: Program Documentation," ASCE, *Journal of Geotechnical Engineering Division*, Vol. 103, GT4, April 1977.

(90) Reese, L.C., Cox, W.R., and Koop, F., "Analysis of Laterally Loaded Pile Tests in Sand at Mustang Island," *A Report to Shell Development Company*, Houston, November 1967.

(91) Roy, M., Juneau, R., LaRochelle, P., and Tavenas, F., "In Situ Measurements of the Properties of Sensitive Clays by Pressuremeter Test," *Spec. Conf. on In Situ Measurement of Soil Properties*, ASCE, Vol. 1, Raleigh, 1975.

(92) Shields, D.H. and Bauer, G.E., "Determination of the Modulus of Deformation of a Sensitive Clay Using Laboratory and In Situ Tests," *ASCE Specialty Conference on In Situ Measurement of Soil Properties*, North Carolina State University, 1975.

(93) Shields, D.H., Scott, J.D., Bauer, G.E., Deschennes, J.-H., and Barszary, A.K., "Bearing Capacity of Foundations Near Slopes," *9th Int. Conf. on Soil Mech. and Found. Engrg.*, Vol. 1, Tokyo, 1977.

(94) Smith, R.E. and Lytton, R.L., "Operating Characteristics of and User Satisfaction with Commercially Available NDT Equipment," *64th Annual TRB*, Washington, D.C., 1985.

(95) Smith, T.D., "Pressuremeter Design Method for Single Piles Subjected to Static Lateral Load," Ph.D. dissertation, Civil Engineering Department, Texas A&M University, 1983.

(96) Soil Mechanics, Inc., "Lateral Pile Load Tests at Exxon Baytown Olefins Plant," *A Report to Exxon Chemical Americas*, Bryan, Texas, January 1982.

(97) Tand, K.E., Funnegard, E.G., and Briaud, J.L., "Bearing Capacity of Footings on Clay: CPT Method," *ASCE Specialty Conference, Use of In Situ Tests in Geotechnical Engineering*, Blacksburg, Virginia, 1986.

(98) Tavenas, F., Blanchette, G., Leroueil, S., Roy, M., and La Rochelle, P., "Difficulties in the In Situ Determinatio of K_0 in Soft Sensitive Clays," *Specialty Conference on In Situ Measurement Soil Properties*, ASCE, Vol. 1, Raleigh, 1975.

(99) Terzaghi, K., "Anchored Bulkheads," *ASCE Transactions*, Paper No. 2720, Vol. 119, 1954.

(100) Tucker, L.M. and Briaud, J.L., "User's Manual for SHALPMT," Civil Engineering, Texas A&M University, 1986.

(101) Tucker, L.M. and Briaud, J.L., User's Manual for PILPMT," Civil Engineering, Texas A&M University, 1986.

(102) Tucker, L.M. and Briaud, J.L., "User's Manual for PRESRED," Civil Engineering, Texas A&M University, 1986.

(103) Tucker, L.M. and Briaud, J.L., "Analysis of Pile Load Test Program at the Lock and Dam No. 26 Replacement Project," *Summary Report*, Civil Engineering, Texas A&M University, November 1987.

(104) Welch, R.C. and Reese, L.C., "Lateral Load Behavior of Drilled Shafts," *Research Report 89-10*, Center for Highway Research, The University of Texas at Austin, May 1972.

(105) Woodward-Clyde Consultants, "Foundation Investigation and Test Program, Lock & Dam No. 16, Mississippi, Alton, Illinois, *Report to the St. Louis District, U.S. Corps of Engineers*, 1979.

(106) Woodward-Clyde Consultants, "Study to Investigate the Effects of Skin Friction on the Performance of Drilled Shafts in Cohesive Soils," *Report to the U.S. Army Waterways Experiment Station*, August 1981.

(107) Wroth, C.P., "British Experience with the Selfboring Pressuremeter," *Symposium on the Pressuremeter and Its Marine Applications,* Institut Francais du Petrole, Paris, April 1982.